NUREG/CR-6719
BNL-NUREG-52619

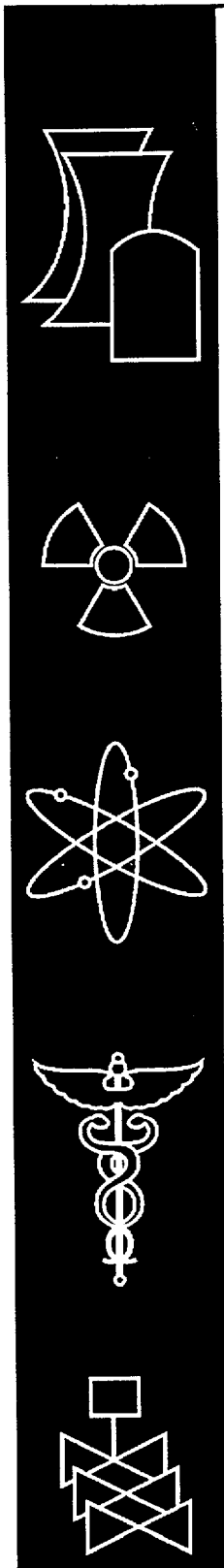

Assessment of the Relevance of Displacement Based Design Methods/Criteria to Nuclear Plant Structures

Brookhaven National Laboratory

U.S. Nuclear Regulatory Commission
Office of Nuclear Regulatory Research
Washington, DC 20555-0001

AVAILABILITY OF REFERENCE MATERIALS IN NRC PUBLICATIONS

NRC Reference Material

As of November 1999, you may electronically access NUREG-series publications and other NRC records at NRC's Public Electronic Reading Room at www.nrc.gov/NRC/ADAMS/index.html.
Publicly released records include, to name a few, NUREG-series publications; *Federal Register* notices; applicant, licensee, and vendor documents and correspondence; NRC correspondence and internal memoranda; bulletins and information notices; inspection and investigative reports; licensee event reports; and Commission papers and their attachments.

NRC publications in the NUREG series, NRC regulations, and *Title 10, Energy*, in the Code of *Federal Regulations* may also be purchased from one of these two sources.

1. The Superintendent of Documents
   U.S. Government Printing Office
   Mail Stop SSOP
   Washington, DC 20402–0001
   Internet: bookstore.gpo.gov
   Telephone: 202-512-1800
   Fax: 202-512-2250
2. The National Technical Information Service
   Springfield, VA 22161–0002
   www.ntis.gov
   1–800–553–6847 or, locally, 703–605–6000

A single copy of each NRC draft report for comment is available free, to the extent of supply, upon written request as follows:

Address: Office of the Chief Information Officer,
Reproduction and Distribution
Services Section
U.S. Nuclear Regulatory Commission
Washington, DC 20555-0001
E-mail: DISTRIBUTION@nrc.gov
Facsimile: 301–415–2289

Some publications in the NUREG series that are posted at NRC's Web site address www.nrc.gov/NRC/NUREGS/indexnum.html are updated periodically and may differ from the last printed version. Although references to material found on a Web site bear the date the material was accessed, the material available on the date cited may subsequently be removed from the site.

Non-NRC Reference Material

Documents available from public and special technical libraries include all open literature items, such as books, journal articles, and transactions, *Federal Register* notices, Federal and State legislation, and congressional reports. Such documents as theses, dissertations, foreign reports and translations, and non-NRC conference proceedings may be purchased from their sponsoring organization.

Copies of industry codes and standards used in a substantive manner in the NRC regulatory process are maintained at—

The NRC Technical Library
Two White Flint North
11545 Rockville Pike
Rockville, MD 20852–2738

These standards are available in the library for reference use by the public. Codes and standards are usually copyrighted and may be purchased from the originating organization or, if they are American National Standards, from—

American National Standards Institute
11 West 42nd Street
New York, NY 10036–8002
www.ansi.org
212–642–4900

Legally binding regulatory requirements are stated only in laws; NRC regulations; licenses, including technical specifications; or orders, not in NUREG-series publications. The views expressed in contractor-prepared publications in this series are not necessarily those of the NRC.

The NUREG series comprises (1) technical and administrative reports and books prepared by the staff (NUREG–XXXX) or agency contractors (NUREG/CR–XXXX), (2) proceedings of conferences (NUREG/CP–XXXX), (3) reports resulting from international agreements (NUREG/IA–XXXX), (4) brochures (NUREG/BR–XXXX), and (5) compilations of legal decisions and orders of the Commission and Atomic and Safety Licensing Boards and of Directors' decisions under Section 2.206 of NRC's regulations (NUREG–0750).

NUREG/CR-6719
BNL-NUREG-52619

Assessment of the Relevance of Displacement Based Design Methods/Criteria to Nuclear Plant Structures

Manuscript Completed: February 2001
Date Published: July 2001

Prepared by
Y. K. Wang, C. A. Miller, C. H. Hofmayer

Brookhaven National Laboratory
Upton, NY 11973-5000

J. F. Costello, NRC Project Manager

Prepared for
Division of Engineering Technology
Office of Nuclear Regulatory Research
U.S. Nuclear Regulatory Commission
Washington, DC 20555-0001
NRC Job Code W6691

NUREG/CR-6719, has been reproduced from the best available copy.

ABSTRACT

The objective of the work described in this report is to evaluate the extent to which displacement based methods may be useful to evaluate the seismic response of nuclear power station structures. A literature review of displacement based seismic design methods was completed during the first phase of the project. As a result of this review it was decided to investigate the displacement based method outlined in FEMA 273 by applying it to two structures.

The first structure considered was a four story reinforced concrete building with shear walls. FEMA 273 pushover analysis methods were compared with nonlinear time history analysis and response spectrum analysis including ductility factors. The comparisons show that the FEMA analysis results are comparable to those achieved with the current force based methods.

The second structure analyzed was the Diablo Canyon nuclear power station turbine building. The main portion of this building is a reinforced concrete shear wall building that contains the turbine. The turbine is mounted on a pedestal which is a reinforced concrete frame structure. It is separately founded from the building and separated from the building by gaps at the operating floor. These gaps close under large earthquakes resulting in geometric nonlinearities. The results predicted with the FEMA analysis are found to compare poorly with nonlinear time history analyses.

CONTENTS

CONTENTS (continued)

Page

List of Figures

List of Tables

CONTENTS (continued)

Page

EXECUTIVE SUMMARY

The recent trend in earthquake engineering has been to perform seismic evaluations based on deformation rather than stress limits. Deformation based analytical methods are better suited to account for the increased seismic capacity of a structure when the structure is ductile. This program was undertaken to investigate the extent to which such methods may be useful for the evaluation of nuclear power stations.

A literature review was undertaken during the initial phase of the program and the results of that review are reported in the Appendix. A slow trend toward the utilization of displacement based methods for design was noted. However, there is a more rapid trend toward the use of displacement based methods for seismic evaluation of existing facilities. FEMA 273 has been developed and is being used as the basic criteria for the design of modifications to enhance the seismic capability of existing non-nuclear facilities. The review concluded that displacement based methods, such as given in FEMA 273, may be useful for seismic margin studies of existing nuclear power stations. They would not be useful for the design of new stations since nuclear power stations are designed to remain elastic during a seismic event.

The methods of FEMA 273 are used to evaluate two example structures during the second phase of the study. The procedures recommended in FEMA 273 are summarized in Section 2 of this report. A nonlinear static pushover analysis is performed on the structure accounting for both material and geometric nonlinearities. Loads are applied to the structure and distributed over the structure as expected for the seismic induced inertial loads. These are increased until the displacement of a control point (usually selected at the roof) reaches the peak displacement expected during the seismic event. The expected displacement is computed as the elastic displacement (from the design response spectrum) modified by factors accounting for nonlinear effects in the structure. The deformations of the structure (as found from the nonlinear pushover analysis) at this expected displacement are then compared with allowable displacements (such as story drifts or inelastic rotations).

The first example structure is a four-story shear wall building. This is a conventional structure with vertical loads carried through a reinforced concrete frame system and lateral seismic loads carried though a symmetric shear wall system. The frame contributes little to the lateral strength and stiffness of the structure. Three analyses are performed to evaluate the response of the structure to an El Centro like earthquake. A nonlinear time history analysis is performed using the IDARC computer code. The peak displacement of the roof is found to be 4.75 inches (12.1 cm). The maximum drifts are found to be 0.54 %, 0.98 %, 0.98 %, and 0.97 % for the first through fourth floors, respectively. The FEMA 273 displacement based method is then performed and the roof displacement is found to be 4.36 inches (11.1 cm) with the story drifts equal to 0.61 %, 0.79 %, 0.82 %, and 0.81 % for the first through fourth floors respectively. It can be seen that the roof displacement predictions agree quite well. There is a somewhat larger difference in the individual story drifts. These differences are likely due to the fact that the applied static load in the pushover analysis does not exactly represent the distribution of inertial loads during the nonlinear time history analysis. FEMA 273 limits the drift in a shear wall to 0.75 %. Therefore, the FEMA analysis would predict the capacity of the building to be equal to 92 % of the El Centro earthquake. A response spectrum analysis is also performed for the building. A ductility factor is used to reduce seismic loads as recommended in the Uniform Building Code (UBC). A ductility factor equal to 4.4 is required to result in the same seismic capacity as that found from the FEMA approach. The UBC allows a ductility factor equal to 5. It can be seen that the FEMA 273 approach gives results that are close to those found with either the nonlinear time history analysis or with a response spectrum analysis combined with the use of ductility factors.

The turbine building at the Diablo Canyon nuclear power station is used for the second example. The main portion of this building is a reinforced concrete shear wall building containing the turbine. The

turbine is mounted on a pedestal, which is a reinforced concrete frame structure. The foundation of the pedestal is independent from the building's foundation, and a gap separates the pedestal from the building at the operating floor elevation. The gap is expected to close during large earthquakes. Since the turbine represents over 60 % of the total mass in the building, the dynamic characteristics of the building change significantly when the gaps close. Seismic margin studies had been performed for this building during plant licensing. Nonlinear time history analyses were performed using twenty five seismic input motions developing a probabilistic description of the building's response. The models used for these analysis included both material nonlinear effects and geometric nonlinearities resulting from the gaps between the building and turbine pedestal. These same models are used in this study to evaluate the building's response based on the FEMA 273 methodology. The median response spectrum of the twenty five input motions used in the seismic margin studies is used to define the seismic motion and median structural properties are used. The pushover load deflection curve indicates that the building stiffness increases when the gaps closed. This is different than found for material nonlinear effects which cause continual softening of the structure as the load is increased. These predictions are then compared with those made from the time history analyses. The predicted values are found to be significantly different from the time history analysis results. It is concluded the FEMA methodology is not appropriate for structures that have load – deflection characteristics containing significant portions where hardening occurs as the load is increased.

The conclusions of this study indicate that the FEMA 273 methodology (or some equivalent displacement based method) may be appropriate for seismic margin studies of structures that exhibit a decrease in stiffness as the load is increased. The primary advantage of the displacement based methods is that they are simpler and are less costly to apply than the more rigorous nonlinear time history analyses. They currently offer no advantage for nuclear plant design projects since current NRC criteria require that the buildings remain elastic.

Based on the conclusions of this study, the following recommendations are given:

- There is no need to revise the Standard Review Plan for seismic design to address displacement based methods.

- The NRC should consider developing guidance for the use of the displacement based approach for seismic margin/fragility analysis.

- Additional studies would need to be performed for nuclear power plant structures with both material and geometric nonlinearities to further define the scope of the problems that can be treated with the displacement based methods before it would be possible to establish sufficient guidance for their use.

- If displacement based methods are to be applied on a wide scale to nuclear facilities, efforts must be undertaken to develop appropriate "C" coefficients and drift limits that are consistent with the importance of the structure.

ACKNOWLEDGMENTS

The Office of Nuclear Regulatory Research of the U. S. Nuclear Regulatory Commission sponsored the research program described in this report. The authors would like to express their gratitude to Dr. James F. Costello, NRC Project Manager, for the technical and administrative support that he has provided in performing the study. The work on the initial phase of the project was peer reviewed by Dr. Robert P. Kennedy, Dr. Mete A. Sozen, and Dr. Anestis S. Veletsos. The final phase of the project was peer reviewed by Dr. Kennedy and Dr. Sozen. The authors would like to recognize the valuable insights provided during these reviews.

The work on the initial phase of this project was performed by Dr. Young J. Park who died suddenly during the course of this project. Dr. Park was an exceptional engineer who had keen insights and enormous capabilities in the areas of nonlinear dynamic analysis and seismic probabilistic risk assessment. He will be sorely missed by his colleagues and the entire earthquake engineering community.

Thanks are also given to the various authors and organizations that provided authorizations to reprint certain tables and figures which were essential to convey the current technology available to perform displacement based analyses.

The authors also express special thanks to Ms. Susan J. Signorelli for her secretarial help throughout this project and in the preparation of this report.

1. INTRODUCTION

The NRC is in the process of updating its requirements for earthquake engineering design of nuclear power plants. The regulation governing seismic criteria and design, Appendix A to 10 CFR Part 100, was revised in December 1996. Regulatory guides and associated Standard Review Plan Sections treating the identification of seismic sources and determination of the Safe Shutdown Earthquake Ground Motion were published in March 1997 along with a revised Regulatory Guide on Seismic Instrumentation and new Regulatory Guides on OBE exceedence criteria on post-earthquake shutdown and re-start.

Revisions to the Regulatory Guides and Standard Review Plan Sections devoted to earthquake engineering practice are currently in process. The intent is to reflect changes in engineering practice that have evolved in the twenty years that have passed since those criteria were originally published. Additionally, field observations of the effects of the Northridge (1994) and Kobe (1995) earthquakes have inspired some reassessment in the technical community about certain aspects of design practice. In particular, questions have arisen about the effectiveness of basing earthquake resistant designs on resistance to seismic forces and, then evaluating tolerability of the expected displacements. Therefore, this research effort was undertaken to examine the implications for NRC's seismic practice of the move, in the earthquake engineering community, toward using expected displacement rather than force (or stress) as the basis for assessing design adequacy.

As part of the initial phase of this study, a literature survey was conducted on the recent changes in seismic design codes and standards, on-going activities of code-writing organizations and published documents by researchers on the displacement-based design methods. Appendix A to this report provides summaries of the reviewed documents, together with a brief overview of the current seismic design practice and design criteria for nuclear power plant facilities.

Based on the survey of the related areas, it was observed that the transition to displacement based seismic design is a rather slow process due to inertia invariably encountered in the engineering community. Changes in one element of a design tend to be counterbalanced by changes in another element. Uniform nationwide acceptance is expected to come slowly. Thus, it did not appear that there would be a major "ground swell" of demand to change NRC criteria for new plants.

In the area of rehabilitation of existing buildings, however, it was noted that a need for change has been accepted. Researchers and practitioners tend to experiment with their new ideas in the areas of repair or rehabilitation. Thus, it was concluded that if the nuclear industry proposed to utilize some of the recent developments, it would at first be most likely applied to issues related to seismic reevaluation or seismic margin/PRA studies.

The response of structures to seismic induced loadings has been traditionally performed using elastic methods. This approach was a natural outgrowth of the use of elastic analysis methods to evaluate structural performance under working loads. The acceptance criteria for load combinations on structures, including seismic effects, have been based on ultimate strength provisions. Seismic loads have often been reduced in this process by dividing the loads by ductility factors to account for the fact that ductile structures can withstand dynamic loads larger than the elastic limit load.

This reliance on elastic analytical methods has been changing over the past few years as a result of the growing interest in reducing the potential effects of earthquakes on the nation's building inventory. Under the National Earthquake Hazards Reduction Program (NEHRP), all federal agencies are required to evaluate the seismic capacities of their building inventory, to develop retrofits that reduce the seismic risk, and to prioritize the repairs based on cost benefit criteria. In this program, it soon became apparent that budgetary constraints place great importance on the last of these tasks. Useful cost benefit criteria

require that the seismic response used to evaluate the buildings be as realistic as possible. Elastic analysis methods (even with the use of ductility factors) are not adequate for this purpose. Rather the analytical methods must focus on inelastic methods which rationally account for the effect of ductile behavior on the seismic capability of the building. FEMA 273 [1] sets the basic criteria to be used in implementing NEHRP. Inelastic analysis methods are proposed which focus on predicting the maximum seismic displacement rather than the seismic load that a structure can withstand. It is expected that these requirements will transform the profession so that inelastic deformation seismic analyses are used rather than elastic load based methods. The purpose of this study is to explore the extent to which this change in methodology should be of interest to the USNRC.

Nonlinear analyses of nuclear power station structures have been used for margin studies where it is desired to account for ductility effects in a rigorous manner. Seismic margin studies relate demand loads to a prediction of ultimate capacity. The ultimate capacity for ductile structures subjected to dynamic loading is tied to a deformation criteria, such as a number of yield deflections, for estimating failure. Elastic analysis is not suited to this task as it focuses on load and says nothing about structural behavior post yield. A nonlinear dynamic analysis is required, but is difficult and time consuming to perform. Hence attempts have been made to apply factors (ductility) to elastic analysis to account for acceptable structural response into the post yield range.

The FEMA 273 methodology is an alternate approach that accounts for performance into the post yield range. It requires the performance of a nonlinear static analysis of the structure with the loading monotonically increased (pushover analysis). Criteria are then given for the maximum displacement that the structure must withstand; this displacement is related to the level of the earthquake and the dynamic characteristics of the structure. The distribution of loads and displacements throughout the elements of the structure at this displacement are then investigated by comparing the element deformations with acceptance limits. The acceptance limits are set to values typically suitable for margin studies.

The objective of this BNL study is to explore the extent to which FEMA 273 methodology could be useful for reviewing nuclear power stations. It has the very desirable characteristic in that the same analysis can be used for evaluating the facility at the design level earthquake and at larger magnitude earthquakes associated with margin studies. It is also directly applicable to a graded criteria where more important facilities would be subjected to more stringent acceptance limits than less important facilities.

Two structures have been chosen as the analysis models for this BNL study. The first structure is a four story frame structure with shear walls providing the primary lateral load system, referred herein as the shear wall model. The second structure is the turbine building of the Diablo Canyon nuclear power plant. Both models are analyzed using the displacement based (pushover) analysis and nonlinear dynamic analysis. In addition, for the shear wall model an elastic analysis with ductility factors applied was also performed. The objective of this work is to compare the results between the analyses, and to develop insights regarding the work that would be needed before the displacement based analysis methodology could be considered applicable to facilities licensed by the NRC.

In this report, the nonlinear static analysis procedure of FEMA 273 is first explained in Section 2. It is followed by application of the procedure to two models: the shear wall model in Section 3 and the turbine building model in Section 4. Section 5 summarizes the overall conclusions and recommendations resulting from this study.

2 FEMA 273 NONLINEAR STATIC ANALYSIS PROCEDURE

2.1 General Discussion of the Procedure

FEMA 273, Section 3.3.3.1, defines the Nonlinear Static Procedure as follows:

"Under the Nonlinear Static Procedure (NSP), a model directly incorporating inelastic material response is displaced to a target displacement, and the resulting internal deformations and forces are determined. The nonlinear load-deformation characteristics of individual components and elements of the building are modeled directly. The mathematical model of the building is subjected to monotonically increasing lateral forces or displacements until either a target displacement is exceeded or the building collapses. The target displacement is intended to represent the maximum displacement likely to be experienced during the design earthquake. The target displacement may be calculated by any procedure that accounts for the effects of nonlinear response on displacement amplitude."

One acceptable procedure based on the Displacement Coefficient Method is described in Section 3.3.3.3. of FEMA 273.

2.2 Load Patterns

The lateral forces placed on the building during the static analysis are distributed over the building in a manner that is consistent with the expected dynamic response of the building. This usually requires that a response spectrum analysis of the building be performed prior to the non-linear static analysis.

FEMA 273, Section 3.3.3.2, Subsection C specifies the lateral load patterns for the pushover analysis as follows:

"Lateral loads shall be applied to the building in profiles that approximately bound the likely distribution of inertia forces in an earthquake. For a three-dimensional analysis, the horizontal distribution should simulate the distribution of inertia forces in the plane of each floor diaphragm. For both two- and three-dimensional analyses, at least two vertical distributions of lateral load shall be considered. The first pattern, often termed the uniform pattern, shall be based on lateral forces that are proportional to the total mass at each floor level. The second pattern, termed modal pattern should be selected from one of the following options:

- A lateral load pattern represented by values of C_{vx} given in Equation 3-8, which may be used if more than 75% of the total mass participates in the fundamental mode in the direction under consideration; or
- A lateral load pattern proportional to the story inertia forces consistent with the story shear distribution calculated by combination of modal responses using (1) response spectrum analysis of the building including a sufficient number of modes to capture 90% of the total mass, and (2) the appropriate ground motion spectrum."

Equation 3-8 of FEMA 273 is:

$$C_{vx} = \frac{w_x h_x^k}{\sum_{i=1}^{n} w_i h_i^k}$$

C_{vx} = Vertical distribution factor

w_i = Portion of the total building weight W located on or assigned to floor level i
w_x = Portion of the total building weight W located on or assigned to floor level x
h_i = Height from the base to floor level i
h_x = Height from the base to floor level x

Where

$k = 1.0$ for $T \leq 0.5$ seconds
$k = 2.0$ for $T \geq 2.5$ seconds

T = Fundamental period (in seconds) of the building in the direction under consideration

For intermediate values of T, linear interpolation should be used to estimate values of k.

2.3 Determination of the Effective Fundamental Period

The fundamental period of a building generally increases as the response increases and non-linear effects become more important. An "effective" period of T_e is used in FEMA 273 to account for this degradation in stiffness.

According to FEMA 273, the effective fundamental period of the building T_e in the direction under consideration should be calculated using the force-displacement relationship of the Nonlinear Static Procedure. The nonlinear force displacement relationship between the base shear and the target node displacement obtained from the pushover analysis is replaced with a bilinear relationship (dotted lines shown in Fig. 2-1). The intersection of these two linear segments is called the yield strength V_y, and the first segment of the bilinear curve is restricted to intersect the nonlinear curve at a base shear equal to $0.6V_y$. The bilinear curves can be constructed using the following iterative process:

1) Construct a straight line (L_2 in Fig. 2-1) that represents the larger displacement portion of the nonlinear pushover curve
2) Guess a value of V_y
3) Construct the lower portion of the bilinear curve (L_1 in Fig. 2-1) by passing a straight line between the origin and the point on the nonlinear curve at $0.6V_y$.
4) Guess an improved value of V_y and repeat step (3) - (4) until the intersection of L_1 and L_2 is at $0.6V_y$

Once the iteration is complete, the slope of the line L_1 is the effective lateral stiffness K_e of the structure. The effective fundamental period T_e can be obtained as:

$$T_e = T_i \sqrt{\frac{K_i}{K_e}}$$

Where
T_i = The period of the fundamental mode of the building (in seconds)
K_i = Elastic lateral stiffness of the building in the direction under consideration
K_e = Effective lateral stiffness of the building in the direction under consideration

2.4 Determination of the Target Displacement

The "target displacement" used in FEMA 273 is the expected maximum displacement (usually measured at the roof) which occurs during the design earthquake. This is determined as the spectral displacement at the effective period of the building modified by a series of coefficients accounting for non-linear effects.

One accepted procedure by FEMA 273 for evaluating the target displacement (δ_t) is given by Equation 3-11 of FEMA 273 as shown below:

$$\delta_t = C_0 C_1 C_2 C_3 S_a (T_e/2\pi)^2 g \qquad \text{Equation 3-11 of FEMA 273}$$

Where S_a is the response spectrum acceleration in units of g at the effective fundamental period T_e and damping ratio of the building in the direction under consideration. C_0 to C_3 are coefficients discussed below. Thus, the $S_a (T_e/2\pi)^2 g$ term is the spectral displacement at the effective fundamental period.

The term, $S_a (T_e/2\pi)^2 g$, represents the displacement of the target node when subjected to the criteria earthquake, if the structure is modeled as being linearly elastic. The coefficients C_0, C_1, C_2, and C_3 modify this displacement to account for nonlinear and inelastic effects. They are described in the following:

- Coefficient C_0

  The spectral displacement at the effective period represents the expected displacement if the building responded as a single degree of freedom system and was elastic. The coefficient C_0 is introduced to modify this expected displacement to account for the fact that the building may respond as a multi-degree of freedom system.

  C_0 is a modification factor to relate spectral displacement and likely building roof displacement. FEMA 273 provides procedures for the estimation of C_0 values, including direct use of a pre-calculated Table (Table 3-2 of FEMA 273) based on the number of the stories of the building. A copy of the Table is included in this report as Table 2-1.

- Coefficient C_1

  C_1 is a modification factor to relate expected maximum inelastic displacements to the displacements calculated for linear elastic response. Its value is dependent on the values of T and T_0 and is equal to 1.5 for $T < 0.1$ seconds, 1 for $T \geq T_0$, and interpolated between the two for values of T between 0.1 and T_0.

  The parameter T_0 in the definition of coefficient C_1 is the characteristic period of the site specific response spectrum. It is defined as

  $$T_0 = S_{x1}/S_{xs}$$

  Where S_{xs} is the design short-period spectral response acceleration parameter. It shall be taken as the response acceleration obtained from the site-specific spectrum at a period of 0.2 seconds, except that it should be taken as not less than 90% of the peak response acceleration at any period.

  S_{x1} is the design spectral response acceleration at a period of one second but is restricted to satisfy the following criteria. At all periods (T) the value of S_a determined from $S_a = S_{x1}/T$ must not be less than 90% of the value of S_a determined from the response spectrum.

- Coefficient C_2

  C_2 is a modification factor to represent the effect of hysteresis shape on the maximum displacement response. Table 2-2 specifies various values for C_2. This table is the same as Table 3-1 of FEMA 273.

- Coefficient C_3

  C_3 is a modification factor to represent increased displacements due to dynamic P-Δ effects. For buildings with positive post-yield stiffness, C_3 shall be set equal to 1.0. For buildings with negative post-yield stiffness, the value of C_3 shall be calculated using Equation 3-13 of FEMA 273. Values for C_3 shall not exceed the values set forth in Section 3.3.1.3 of FEMA 273.

2.5 Summary of the Analysis Steps

The FEMA 273 procedure for nonlinear static analysis can be summarized as the following eleven steps:

1) Perform the pushover analysis of the structure subjected to a lateral loading based on the uniform pattern.

2) Draw the load deformation curve based on the base shear and the roof displacement result.

3) Measure the initial stiffness K_i and the effective stiffness K_e from the curve.

4) Calculate the effective fundamental period T_e.

5) Determine the modification factors, C_0, C_1, C_2, C_3.

6) Read the spectral acceleration value S_a off the response spectrum curve at the period of T_e.

7) Calculate the target displacement δ_t.

8) Locate the δ_t on the load deformation curve and find the corresponding load step.

9) Calculate the floor drift ratios at that particular load step.

10) Repeat the process, from step 1 to step 9, for the modal pattern loading case.

11) Compare the larger of the max. floor drift ratio results of the two cases with the FEMA allowable.

3 SHEAR WALL MODEL

In this section, the model of the shear wall structure is described in Section 3.1 followed by a discussion of the non linear time history analysis in Section 3.2, the response spectrum analysis in Section 3.3, and the FEMA analyses in Section 3.4. A comparison between the results of the three analysis methods are presented in Section 3.5.

3.1 Description of the Model and Loading

The shear wall model is a four story reinforced concrete building with shear walls. The typical floor framing plan of the building is shown in Fig. 3-1. The building is 197 feet (60 m) long in the North-South direction and 95.75 feet (29.18 m) wide in the East-West direction, and it is symmetric in both directions. Since the building is symmetric and the input loading is applied in the North-South direction, a simplified 2D model which represents half of the building in the East-West direction has been generated and used in the analyses. This building was previously used as a sample problem for the IDARC program [2].

IDARC is a Fortran program developed and maintained by the National Center for Earthquake Engineering Research (NCEER) at the State University of New York at Buffalo. The program was designed to perform Inelastic Damage Analysis for Reinforced Concrete structures, thus it was named IDARC. Since the code has been used to perform nonlinear static (pushover) analysis for commercial buildings, it was selected for this study to perform both the time history analyses and the FEMA analyses.

The 2D model is based on the combined stiffness of the three frames marked as N1, N2, and N3 in Fig. 3-1. Frame N1 contains 22 columns, frame N2 contains 6 columns and frame N3 consists of 2 shear walls. The lateral load resisting capacity of the building in the North-South direction comes mainly from the shear walls. The total height of the building is 48 feet (14.6 m) as each floor has the same height of 12 feet (3.66 m).

All of the components of the building; columns, beams, and shear walls are modeled as reinforced concrete elements in the IDARC model. The bases of all of the columns and shear walls are assumed fixed in all degrees of freedom. The weight of the building is assumed evenly distributed to the joints of the beams and columns as nodal weights. Table 3-1 shows the values of these nodal weights. A stick model with four nodal masses was generated to represent the mathematical model of the building (Fig. 3-2). The mass of one half of the building is lumped at these four nodes with each node representing one floor of the building.

The stress-strain curve of the concrete material is shown in Fig. 3-3. Its properties are:

- Unconfined compressive strength of the concrete – f'c = 3 ksi (20.7 N/mm^2);
- Tensile strength of the concrete – ft = 0.36 ksi (2.48 N/mm^2);
- Elastic Young's Modulus of the concrete – Ec = 3,122 ksi (21.5 kN/mm^2);
- Strain at maximum strength of the concrete – ε_o = 0.002 in/in;
- Ultimate strain of the concrete – ε_u = 0.004 in/in

The stress-strain curve of the reinforcement steel is shown in Fig. 3-4. The steel properties are:

- Yield strength of the steel – fy = 60 ksi (414 N/mm^2);
- Ultimate strength of the steel – fu = 84 ksi (579 N/mm^2);
- Young's Modulus of the steel – Es = 29,000 ksi (200 kN/mm^2);
- Hardening modulus of the steel – E_t = 203.5 ksi (1.4 kN/mm^2);
- Yield strain of the steel – ε_y = 0.00207 in/in;
- Strain at start of hardening of the steel – ε_h = 0.03 in/in

The El Centro 1940 N-S earthquake was assumed as the site specific ground motion for this study. A record of 20 seconds duration digitized on a 0.02 second time interval was used in the time history analysis. The peak acceleration of the ground motion is 0.348g. Fig. 3-5 shows this time history record. A response spectrum of 5% damping has been generated from this time history record and used in the response spectrum analysis. Fig. 3-6 shows the response spectrum curve (acceleration vs. period) and Table 3-2 tabulates the digitized values of the spectral accelerations at selected frequencies and periods.

3.2 Nonlinear Time History Analysis

In order to evaluate the efficiency and accuracy of the FEMA process, a nonlinear time history analysis was performed on the shear wall model to provide a comparison basis. As discussed above, the ground excitation input used in the nonlinear time history analysis was the El Centro 1940 NS earthquake, a record of 20 seconds with an interval of 0.02 seconds (Fig. 3-5). The viscous damping of 5% used in the response spectrum analysis was modeled as mass proportional damping in the time history analysis. An integration time interval of 0.005 seconds was used to ensure that the responses of high frequency modes were not missed from the result.

The result shows that the maximum displacement at the roof is 4.75 inches (12.1 cm). The floor displacement time histories of the analysis are shown in Fig. 3-7. A comparison of the results of the time history analysis with the results from the FEMA process is discussed later in Section 3.4.

A series of runs were executed to calculate the magnitude of the El Centro Earthquake that would cause the maximum floor drift ratio to reach 0.75%, the FEMA 273 allowable drift ratio. This is because the time history analysis is nonlinear, thus interpolation is not applicable. From the previous time history analysis, it is observed that the potential magnitude of the El Centro earthquake to reach the allowable drift ratio would be about 75%. After seven tries, the closest answer to the target is 71.55% (0.249g), at which the maximum floor drift ratio is 0.69%. Table 3-3 shows the result of these runs. It can be seen from the Table, that with a slight change of the magnitude of the earthquake (i.e., 0.0005g, from 71.55% to 71.69%), the floor drift ratio jumps up from 0.69% to 0.83%.

3.3 Response Spectrum Analysis

A modal analysis of the building is performed using IDARC. The modal characteristics found from IDARC are used to perform a response spectrum analysis by hand calculation.

Data for the hand calculation are obtained from a modal analysis using IDARC. The dynamic characteristics of the model are listed in Table 3-4, the mode shapes are shown in Fig. 3-8, the mass normalized modal matrix, Φ, and the modal participation vector, Γ, are listed below.

$$\Phi = \begin{bmatrix} 0.345 & -0.238 & 0.165 & -0.091 \\ 0.235 & 0.093 & -0.231 & 0.228 \\ 0.128 & 0.262 & -0.048 & -0.287 \\ 0.042 & 0.186 & 0.26 & 0.145 \end{bmatrix}$$

$$\begin{Bmatrix} \Gamma_1 \\ \Gamma_2 \\ \Gamma_3 \\ \Gamma_4 \end{Bmatrix} = \begin{Bmatrix} 4.1133 \\ 2.4544 \\ 1.2164 \\ 0.3809 \end{Bmatrix}$$

The modal generalized coordinates can be calculated from the modal participation factors and spectral accelerations as follows:

$$\ddot{y}_1 = \Gamma_1 S_{a1} = 4.1133 \text{ x } 0.827g = 3.4g$$

$$\ddot{y}_2 = \Gamma_2 S_{a2} = 2.4544 \text{ x } 0.743g = 1.82g$$

$$\ddot{y}_3 = \Gamma_3 S_{a3} = 1.2164 \text{ x } 0.495g = 0.6g$$

$$\ddot{y}_4 = \Gamma_4 S_{a4} = 0.3809 \text{ x } 0.35g = 0.133g$$

The modal spectral accelerations S_{a1}, S_{a2}, S_{a3}, and S_{a4} are obtained from the input spectrum curve (Table 3-2) at the periods corresponding to each of the modes, respectively.

The floor acceleration response of each mode can be obtained by multiplying the modal matrix and the modal acceleration responses (generalized coordinates). The total acceleration response of each floor is obtained by combining the four modal responses using the SRSS combination method.

$$\ddot{v}_4 = \sqrt{(0.345x3.4g)^2 + (-0.238x1.82g)^2 + (0.165x0.6g)^2 + (-0.091x0.133g)^2} = 1.255g$$

$$\ddot{v}_3 = \sqrt{(0.235x3.4g)^2 + (0.093x1.82g)^2 + (-0.231x0.6g)^2 + (0.228x0.133g)^2} = 0.83g$$

$$\ddot{v}_2 = \sqrt{(0.128x3.4g)^2 + (0.262x1.82g)^2 + (-0.048x0.6g)^2 + (-0.287x0.133g)^2} = 0.648g$$

$$\ddot{v}_1 = \sqrt{(0.042x3.4g)^2 + (0.186x1.82g)^2 + (0.26x0.6g)^2 + (0.145x0.133g)^2} = 0.4g$$

The inertia force of each floor is the product of the floor acceleration with its floor mass

$F_4 = m_4 \ddot{v}_4 = 1692 \text{ x } 1.255 = 2124$ kips (9,448 kN)

$F_3 = m_3 \ddot{v}_3 = 2051 \text{ x } 0.83 = 1701$ kips (7,566 kN)

$F_2 = m_2 \ddot{v}_2 = 2051 \times 0.648 = 1329$ kips (5,912 kN)

$F_1 = m_1 \ddot{v}_1 = 2863 \times 0.4 = 1146$ kips (5,098 kN)

The total base shear of the model is the sum of these floor shear forces

$T = 2124 + 1701 + 1329 + 1146$
$= 6301$ kips (28,028 kN)

This result is used in Section 3.5 to compare with the FEMA analysis results.

3.4 Analysis of the Shear Wall Model by FEMA 273

To demonstrate the FEMA 273 procedure, two analyses based on different input loading were completed. One loading was with the uniform load pattern and the other was with the modal load pattern. The step by step calculations following the FEMA 273 procedure for these two cases are described below.

3.4.1 Uniform Loading Case

In the Uniform Loading Case the distribution of the lateral input loading applied to each floor of the model is proportional to the mass of that floor divided by the total mass of the structure. Fig. 3-9A shows the distribution ratio of this uniform-pattern loading applied to the model. A pushover analysis was then performed by applying the loading of this pattern step by step, starting from zero, with predefined increments. During the analysis the displacements of the roof at various loading levels were recorded along with the total shear force at the building base. Then these force displacement data were used to generate the required load deformation curve to start the FEMA 273 procedure. Fig. 3-9B shows the load deformation curve. The backbone curve is generated out to a displacement of 6 inches (15.2 cm) as that is the maximum displacement of interest. The FEMA allowable drift is 0.75 % which corresponds to a total roof displacement equal to 4.3 inches (10.9 cm). It is not likely that displacements larger than 6 inches (15.2 cm)would be of interest.

- Determination of the Effective Fundamental Period - T_e

  In order to accurately get the values of the curve points for calculation, a digitized table of these points was established as Table 3-5. The initial stiffness, K_i , the slope of the curve in the elastic range, can be determined by dividing a selected shear force less than the yield strength with its corresponding roof displacement. In this case the pairs on the seventh row of Table 3-5 were picked and K_i is calculated as

  $$K_i = 149.91/0.071 = 2111.4 \text{ kips/inch } (2{,}568 \text{ kN/m})$$

  In determining the effective lateral stiffness some trial and error effort were required, since the value for V_y is not known until the K_e line is drawn (see Fig. 3-9B). After several tries and adjustments, the best estimated value of V_y is 1520 kips (6,761 kN). Therefore 0.6 V_y is equal 912 kips (4,057 kN). From Table 3-5 (between step 43 and step 44) the corresponding displacement is 0.45 inches (1.14 cm). Thus the effective stiffness K_e is

  $$K_e = 912 / 0.45 = 2027 \text{ kips/inch } (2{,}465 \text{ kN/m})$$

A plot of the resulting bilinear backbone curve is shown on Fig. 3-9B.

From the modal analysis discussed in Subsection 3.3 (Table 3-4), the period of the first mode is

$$T_i = 0.55 \text{ seconds}$$

Therefore the effective fundamental period, Te, can be calculated as

$$\begin{aligned} Te &= T_i \sqrt{\frac{Ki}{Ke}} \\ &= 0.55\ [2111.4/2027]^{1/2} \\ &= 0.561 \text{ sec} \end{aligned}$$

- Coefficient C_0

The sample model is a four story building. From Table 2-1 the value of C_0 can be obtained by averaging C_0 values of three stories and five stories as

$$C_0 = 1.35$$

- The Characteristic Period of the Site Specific Response Spectrum- T_0

According to FEMA 273 the characteristic period of the site specific response spectrum is defined by the following equation (refer to Subsection 2.4 for details)

$$T_0 = S_{x1}/S_{xs}$$

Where S_{xs} is the design short-period spectral response acceleration parameter; its value is the larger of S_a at t = 0.2 seconds or $0.9S_{amax}$. From Table 3.2, the S_a at t = 0.2 seconds is 0.645g and the S_{amax} is 0.915g, thus

$$S_{xs} = 0.9 * 0.915 = 0.8235g$$

A trial value of S_{x1} is taken as the spectral response acceleration at one second (S_{x1}= 0.484g). The curve for $S_a = S_{x1}/T$ is then overlaid on the spectrum in Fig. 3-10. It can be seen that the value of S_a evaluated from S_{x1}/T is always greater than 90% of the value of S_a found from the spectrum. The initial trial value of S_{x1}= 0.484g is therefore adequate. Subsequently, the value of T_0 can be obtained as

$$T_0 = 0.484/0.8235 = 0.588 \text{ sec}$$

- Coefficient C_1

C_1 is a modification factor to relate expected maximum inelastic displacement to displacements calculated for linear elastic response. Its value is dependent on the comparison between T and T_0. For this case T = 0.55 sec < T_0 = 0.588 sec, therefore

$$C_1 = 1.04$$

This is obtained by interpolating between $C_1 = 1.5$ for $T < 0.1$ sec and $C_1 = 1$ for $T > T_0$ as recommended in FEMA 273.

- Coefficient C_2

  For this case T is 0.55 sec and it is smaller than T_0, therefore interpolating between the values from Table 2-2 for the Collapse Prevention Performance Level

  $$C_2 = 1.22$$

- Coefficient C_3

  For this case the post-yield stiffness is positive, therefore

  $$C_3 = 1.0$$

- Spectral Acceleration - S_a

  The response spectrum of the El Centro earthquake was generated with 5% damping and is shown in Fig. 3-6. At the effective fundamental period of 0.561 seconds,

  $$S_a = 0.83 \text{ g}$$

With all the parameters determined, the target displacement at the Collapse Prevention performance level can be obtained as follows:

$$\begin{aligned}\delta_t &= C_0 C_1 C_2 C_3 S_a (T_e/2\pi)^2 g \\ &= 1.35 * 1.04 * 1.22 * 1.0 * 0.83 * (0.561/6.28)^2 * 386.4 \\ &= 4.38 \text{ inches } (11.1 \text{ cm})\end{aligned}$$

For a shear resisting structure, FEMA 273 allows a floor drift ratio equal to 0.75% for the Collapse Prevention Performance Level (Table 5-18 of Ref. 1.)

As discussed above, a pushover analysis was carried out with the uniform pattern loading applied to the model laterally. The floor drift results of the analysis are tabulated in Table 3-6. Table 3-6 contains results of four floors and each floor result occupies two columns; one for the drift and one for the drift ratio. The drift is the difference between the displacements at the top and the bottom of the floor and the drift ratio is the drift divided by the height of the floor. There are total of 124 load steps in the Table.

Table 3-7 tabulates the floor drift and drift ratio for each floor corresponding to the roof displacement of 4.38 inches (11.1 cm) for the Uniform Pattern loading case (the Modal Pattern loading and nonlinear time history analysis results are also shown in this table and will be discussed later). It is observed that among the four floors, the first floor has the maximum drift ratio from Table 3-6. The load step at which the maximum drift of the first floor reaches the FEMA allowable of 0.75% is between load step 118 (0.732%) and load step 119 (0.773%). The exact location of the allowable between these steps can be calculated by a linear interpolation as:

$$(0.75-0.732)/(0.773-0.732) = 0.44 \text{ from load step } 118$$

The target displacement corresponding to this loading can be found from Table 3-5 which shows the roof displacements at load steps 118 and 119 are 4.031 inches (10.2 cm) and 4.211 inches (10.7 cm), respectively. Therefore knowing that δ_t is a factor of 0.44 away from step 118 toward step 119, its value can be obtained as 4.031+0.44(4.211-4.031)= 4.11 inches (10.4 cm).

Applying δ_t and the C coefficients calculated previously to Eq 3-11, the value of S_a can be back calculated as

$$\delta_t = C_0 C_1 C_2 C_3 S_a (T_e/2\pi)^2 g$$
$$4.11 = 1.35 * 1.04 * 1.22 * 1.0 * S_a * (0.561/6.28)^2 * 386.4$$
$$S_a = 0.78\ g$$

This means it would require an earthquake like El Centro, with its 5% damped response spectrum having a spectral acceleration of 0.78 g at the period of 0.561 seconds, to fail this model. Actually only 94% of the El Centro Eq. is enough to fail the model, because at the period of 0.561 seconds, El Centro's S_a is 0.83g.

$$0.78 / 0.83 = 0.94$$

Or put in another way, an earthquake equivalent to the El Centro earthquake with a peak ground acceleration of 0.327 g would be capable of failing the model based on the following calculation:

$$0.94 * 0.348\ g = 0.327\ g$$

3.4.2 Modal Loading Case

In the modal loading case, the distribution of the lateral loading at each floor level is consistent with the distribution of the inertia force of that floor obtained from a response spectrum analysis of the building. The response spectrum analysis should include a sufficient number of modes to capture 90% of the total mass of the building and the input should be an appropriate ground motion spectrum.

- Determination of the Floor Load Distribution Factors

  From the response spectrum analysis of the shear wall model (Section 3.2.2), the inertia forces of the floors, from floor 1 through 4, are 1,146 kips 5,098 kN), 1,329 kips (5,912 kN), 1,701 kips (7,566 kN) and 2,124 kips (9,448 kN), respectively, and the total base shear is 6,301 kips 28,028 kN).

  The distribution factor for each floor is the ratio of the floor shear force to the base shear of the building, thus factors f_1, f_2, f_3 and f_4 can be obtained as follows:

$$f_4 = \frac{F_4}{T} = \frac{2124}{6301} = 0.34$$

$$f_3 = \frac{F_3}{T} = \frac{1701}{6301} = 0.27$$

$$f_2 = \frac{F_2}{T} = \frac{1329}{6301} = 0.21$$

$$f_1 = \frac{F_1}{T} = \frac{1146}{6301} = 0.18$$

With determination of the load distribution, a pushover analysis using this loading pattern (see Fig. 3-11A) was performed and a load deformation curve result was obtained. The load deformation curve shows the relationship of the base shear force vs. the roof displacement of the building (Fig. 3-11B). The digitized data of the curve is tabulated in Table 3-8 and will be used for the calculation of the effective fundamental period of the model.

- Determination of the Effective Fundamental Period - T_e

Following the same process as in the Uniform Loading Case, T_e can be obtained by first determining the initial stiffness K_i, followed by the effective lateral stiffness K_e. K_i can be obtained from the load deformation curve in the elastic range. In this case, the base shear at the roof displacement of 0.053 inches (1.3 mm) (Load Step 4 in Table 3-8) was picked for calculating K_i

K_i = 83.5/0.053 = 1575 kips/inch (1,915 kN/m)

After completing a trial and error process on the load deformation curve (Fig. 3-11B), the yield strength V_y was estimated as 1,310 kips (5,827 kN) and 0.6 V_y as 786 kips (3,496 kN). From Table 3-8, the displacement at load of 786 kips (3,496 kN) can be interpolated as 0.519 inches (13.2 mm) between Load Steps 38 and 39, thus the lateral stiffness K_e equals to 1310 / 0.519 = 1,514 kips/inch (1,841 kN/m). Consequently, the effective fundamental period, T_e , can be calculated with T_i = 0.55 seconds as

$$\begin{aligned} Te &= Ti \sqrt{\frac{Ki}{Ke}} \\ &= 0.55\ [\ 1575 / 1514]^{1/2} \\ &= 0.56 \text{ sec} \end{aligned}$$

- Coefficient C_0

The modification factor to relate spectral displacement and likely building roof displacement, remains the same as in the Uniform Loading Case as

$C_0 = 1.35$

- The Characteristic Period of the Site Specific Response Spectrum - T_0

  In this case, T_0 is the same value as the one used in the Uniform Loading Case, since T_0 is related to the input spectrum not to the input loading pattern

  $$T_0 = 0.588 \text{ sec}$$

- Coefficient C_1

  The modification factor to relate expected maximum inelastic displacement to displacements is the same as for the uniform load

  $$C_1 = 1.04$$

- Coefficient C_2

  The modification factor to represent the effect of hysteresis shape on the maximum displacement response is the same as for the uniform load case

  $C_2 = 1.22$ for the Collapse Prevention Performance Level

- Coefficient C_3

  C_3 is a modification factor to represent increased displacements due to dynamic P-Δ effects. In this case $C_3 = 1.0$, since the post-yield stiffness is positive

- Spectral Acceleration - S_a

  From the digitized data of the response spectrum curve (Table 3-2), the spectral acceleration response at the period of 0.56 seconds can be linearly interpolated between 0.667 sec. and 0.625 sec. as 0.83g. Thus, the target displacement at the Collapse Prevention performance level is

  $$\delta_t = C_0 C_1 C_2 C_3 S_a (T_e/2\pi)^2 g$$
  $$= 1.35 * 1.04 * 1.22 * 1.0 * 0.83 * (0.56/6.28)^2 * 386.4$$
  $$= 4.36 \text{ inches } (11.1 \text{ cm})$$

As discussed above, a pushover analysis was carried out with modal pattern loading applied to the model laterally. The floor drift results of the analysis are tabulated in Table 3-9. Table 3-9 has a total of eight columns for four floors with each floor containing two columns for the drift and the drift ratio. There are 119 load steps in this case.

From Table 3-7, it is observed that among the four floors the third floor has the maximum drift ratio. Thus, by searching through the drift ratio column under third floor of Table 3-9, the drift ratio which fits the 0.75% allowable is found to be between step 97 (0.726%) and step 98 (0.76%). The exact location can be determined by a linear interpolation as

$$(0.75-0.726)/(0.76-0.726) = 0.71 \text{ from the step 97}$$

The target displacement corresponding to this loading can be found by applying the same procedure used in the uniform loading case: The roof displacements at load steps 97 and 98 in Table 3-8 are 3.865 inches (9.8 cm) and 4.05 inches (10.3 cm), respectively. Knowing that δ_t is a factor of 0.71 from load step 97 toward step 98, its value can be obtained as 3.865+0.71(4.05-3.865) = 4.0 inches (10.2 cm).

Applying δ_t and the C coefficients calculated previously to Eq. 3-11, the value of S_a can be back calculated as follows:

$$\delta_t = C_0 C_1 C_2 C_3 S_a (T_e/2\pi)^2 g$$
$$4.0 = 1.35 * 1.04 * 1.22 * 1.0 * S_a * (0.56/6.28)^2 * 386.4$$
$$S_a = 0.76g$$

This means it would require an earthquake like El Centro, with its 5% damped response spectrum having a spectral acceleration of 0.76g at the period of 0.56 seconds, to fail this model.

Actually only 92% of the El Centro Eq. is enough to fail the model, because at the period of 0.56 seconds, El Centro's S_a is 0.83g.

$$0.76 / 0.83 = 0.92$$

Or, alternatively, an earthquake equivalent to the El Centro Eq. with a peak ground acceleration of 0.319g would be capable of failing the model based on the following calculation

$$0.92 * 0.348g = 0.319g$$

3.5 Comparison Between Methods

Table 3-7 compares the time history analysis results to those obtained using the pushover analyses. Since the modal pattern results in the larger maximum floor drift, it is controlling and used to compare with the time history results. The displacement based method predicts a roof displacement of 4.36" (11.1 cm) or 8 % lower than the time history analysis. This result is quite good. For the floor drifts, the Modal Pattern loading case shows the same trend as the time history analysis; the floor drift gets larger as the height increases, and the third floor has the largest drift.

It is also interesting to compare the predicted seismic capacity of the building using both the time history and displacement based methods. The capacity is based on an allowable drift of 0.75% as specified in FEMA 273. The seismic capacity of the building was found from the time history analysis to be defined with an El Centro response spectra anchored at 0.25g ZPA (see Section 3.2). This compares with a displacement based predicted seismic capacity of 0.32g ZPA as found in Section 3.4.

As discussed in Section 3.3, a response spectrum analysis was performed on the structure so that the results of a force based analysis could be compared with the deformation centered approach represented by the pushover analyses. The response spectrum method is, of course, a linear elastic method. In some cases the loads are reduced by "ductility factors" reflecting the fact that structures can withstand seismic loads greater than those required to reach the elastic limit provided some inelastic deformations are permissible. The response spectrum analysis was used to evaluate the ductility factors required to produce results similar to those obtained with the pushover and nonlinear time history analyses. These ductility factors were then compared with those in use to evaluate whether the newer deformation based analyses give similar results to those found with the older force based analyses.

The pushover analysis discussed in Section 3.4 indicated that the building could withstand 0.92 times El Centro. If earthquakes of this size were used in the response spectrum analysis, the base shear would be 0.92 * 6301 = 5,797 kips (25,777 kN). The capacity of the walls is set at V_y = 1,310 kips (5,827 kN). The response spectrum analysis discussed in Section 3.4 would predict the same capacity as the pushover analysis if the ductility factor of 5797 / 1310 = 4.4 were used. The Uniform Building Code allows an R factor (accounting for ductility, overstrength, and load redistribution effects) equal to 5 for a shear wall structure so that the pushover analysis gives slightly more conservative results for this case.

It is also interesting to compare the results for a case applicable to nuclear structures where lower ductility factors are permitted. DOE Standard 1020 would permit a ductility factor equal to 1.5 (for shear walls subjected to shear failures). This is probably a reasonable value to use for NPP facilities. If a ductility factor of 1.5 is used the allowable base shear is:

$$V_b = 1.5 * 1310 = 1{,}965 \text{ kips } (8{,}741 \text{ kN})$$

The allowable earthquake is therefore 1965 / 6301 = 0.31 times El Centro

Shear wall drift is usually limited to 0.4 % in nuclear structures. The FEMA modal solution shows that this drift is reached at load step 69 (see Table 3-9). The results in Table 3-8 indicate that the roof displacement at this load step is equal to 1.427 inches (3.62 cm). The value of Sa corresponding to this target displacement is found from

$$\delta_t = C_0 C_1 C_2 C_3 S_a (T_e/2\pi)^2 g$$
$$1.427 = 1.35 * 1.04 * 1.22 * 1.0 * S_a * (0.56/6.28)^2 * 386.4$$
$$S_a = 0.27 \text{ g}$$

This means it would require an earthquake like El Centro, with its 5% damped response spectrum having a spectral acceleration of 0.27 g at the period of 0.56 seconds, to fail this model. Actually only 33 % of the El Centro Eq. is enough to fail the model, because at the period of 0.56 seconds, El Centro's S_a is 0.83g.

$$0.27 / 0.83 = 0.33$$

This agrees very well with the 31 % found above using more conventional methods of analyzing nuclear facilities. It does, however, imply that to get equivalent results the allowable ductility factors listed in FEMA 273 should be reduced when applying the methodology to nuclear facilities.

4 DIABLO CANYON TURBINE BUILDING

The Diablo Canyon turbine building is selected for the second case study comparing results obtained using the non linear time history and displacement based methods. This is selected because it is a nuclear power plant structure for which complete non linear time history analyses are available. These analyses are available for two different seismic input levels such as would be required for a seismic margin study. It is also of interest since the nonlinear effects include both material nonlinearity and geometric nonlinearity (gaps).

A probabilistic evaluation of the Diablo Canyon turbine building was performed (Ref. 4) during the plant licensing reviews. The objective of that evaluation was to determine the probability of failure for several levels of severe earthquake inputs. The study developed a simple model of the building that characterized its performance through displacements that were likely to cause collapse. Nonlinear load – deflection curves were defined for each element of the model.

A suite of 25 seismic motions, defined with response spectra, was then selected from actual earthquake records recorded at sites that have similar geologic formations as found at the Diablo Canyon site. These records were scaled to obtain any required magnitude of input motions.

Nonlinear dynamic response analyses were then performed to evaluate the peak model displacements for each of the 25 seismic input motions scaled to a common average spectral acceleration (averaged over the 3 cps to 8.5 cps frequency range). A statistical analysis was performed on the 25 predicted displacements to obtain median and standard deviation estimates of the displacements. A comparison of this displacement data with likely element failure displacements resulted in a prediction of the probability of failure for each earthquake level.

A displacement-based analysis (FEMA 273) is performed for this structure and the results compared with those obtained from the time history methodology used in Ref. 4. Median model characteristics are used and the input seismic motion is defined with the median response spectra for the 25 input motions used in the Ref. 4 study. These predictions are then compared with the median results obtained from the force base probabilistic analyses.

A summary of the Ref. 4 study is first discussed followed with a detailed description of the displacement based analysis. The results from each of the analyses are then compared.

4.1 Non Linear Time History Analysis

The Diablo Canyon turbine building is a reinforced concrete shear wall building below the elevation of the operating floor with a steel superstructure over the operating floor. The building is about 139 feet (42.4 m) wide by 267 feet (81.4 m) long. The turbine is located at the elevation of the operating floor and founded on a pedestal, which is separated from the operating floor by a gap of 3.375 inches (8.57 cm). The operating floor is 55 feet (16.8 m) above the foundation.

Since almost all of the mass is contained within the concrete portion of the building (the operating floor and below), the steel superstructure portion of the building is not included in the model. A sketch of the model used in the force based analyses is shown on Fig. 4-1 (Fig. 2-3 of Ref. 4). The walls (19 and 31) are shown horizontal for clarity. Each node is defined with a single degree of freedom (displacement in the short direction of the building) and the seismic input is placed in this direction. Note that the shear wall models consist of shear and flexural elements. It was found that the shear flexibility is much larger

than the flexural flexibility. Gap elements separate the turbine (node 12) from the operating floor (nodes 10 and 11).

The nodal coordinates are shown on Table 4-1 (Table 2-1 of Ref. 4) and the nodal masses are shown on Table 4-2 (Table 2-2 of Ref. 4). Note that the mass of the turbine (node 12) represents 62 % of the total mass. Therefore the turbine mass has a major influence on the building response when the gaps are closed and has no influence when the gaps are open. The shear walls are modeled with bilinear load – deflection curves with the elastic stiffness shown on Table 4-3 (Table 2-4 of Ref. 4). These data show that the response is controlled by the shear behavior of the walls with the flexural deformations only playing a minor role. The wall capacities controlling the transition from the elastic portion of the curve are shown on Table 4-4 (Table 2-3 of Ref. 4). It can be seen that the shear capacities control so that the flexural elements will not exceed yield. The slope of the plastic portion of the curve is taken to be 3 % of the elastic portion of the load – deflection curve. The load – deflection curve for each element of the diaphragm is shown on Fig. 4-2 (Fig. 2-10 of Ref. 4). The turbine pedestal is modeled with an elasto-perfectly plastic load deflection curve having an initial stiffness of 2.88×10^5 k /ft (4.203×10^6 kN/m) up to a load of 67,000 kips (298,031 kN)

A modal analysis was performed indicating the following modes:

- 3.1 cps involving the turbine pedestal
- 4.0 cps involving the operating floor
- 8.6 cps involving the wall at line 31
- 9.5 cps involving the wall at line 19

The dynamic analyses were performed using 25 time histories scaled so that the average (over the 3 cps to 8.5 cps frequency range) spectral accelerations were 3 g's and 6 g's. Spectral characteristics of this suite of earthquakes are shown on Fig. 4-3 (Fig. 3-27 of Ref. 4). Each of the accelerograms was used as input and peak displacements determined. The results for the 25 cases with the 3 g input are shown on Table 4-5 (from Table 5-1 of Ref. 4). The results for the 25 cases with the 6 g input are shown on Table 4-6 (from Table 5-2 of Ref. 4). The median and standard deviation for these 25 cases were calculated as part of this study and included as part of Tables 4-5 and 4-6.

4.2 Displacement Based Analyses (FEMA 273)

Two models, designated A and B, are used for the displacement based analyses. Model A is identical to the one described above. Model B is shown on Fig. 4-4. The two elements of the operating floor diaphragm for Model A are combined into a single element for Model B with two rigid links used to connect the center of the operating floor to the gap elements around the turbine.

The first step in the FEMA 273 analyses is to construct a backbone curve (load deflection curve) continuing up to deflections expected during the seismic event. The load is applied as an inertial load distributed based on the expected response mode. As discussed in Section 2.2, FEMA 273 requires that two load distributions be considered: one where the loads are placed in proportion to the mass distribution, and the second where the load is placed in proportion to the load obtained from a response spectrum analysis.

The loading for the first case is placed on each node in proportion to the nodal masses shown on Table 4-2. A response spectrum analysis is performed with the ANSYS code [3] using the median spectrum on Fig. 4-3 as input to obtain the load distribution for the modal loading case. Of course the same results are obtained for models A and B discussed above since the gaps do not close for the response

spectrum analysis. The frequencies and mode shapes found for this analysis are identical to those found in Ref. 4. The distribution of load for the uniform and modal load distributions are shown on Table 4-7.

It can be seen that a major portion of the load comes through the turbine since its mass is such a large percentage of the total building mass. As a result one can expect major changes in the response of the remainder of the structure when the gaps close and the turbine loads are transferred to the building.

Static analyses are performed using the ANSYS computer code. Loads are applied in the +y direction. The resulting load – deflection backbone curve for the uniform load case with Model A is shown on Fig. 4-5. The load shown on the figure is the total shear load applied to the model. The Model A backbone curve for the modal load case is shown on Fig. 4-6. These load – deflection data are tabulated on Tables 4-8 and 4-9 for the uniform and modal load cases, respectively. It can be seen that the modal load case is critical since it shows larger displacements than the uniform load case. For example, the node 12 displacements for the two cases at a total load of 150,000 kips (667,233 kN) are 4.02 feet (1.23 m) and 6.85 feet (2.09 m), respectively. The displacement-based solutions are therefore carried out for the modal load distribution. The resulting load – deflection backbone curve for the modal load case with Model B is shown on Fig. 4-7. A tabular listing of the backbone curve results is given on Table 4-10. It can be seen that the displacements are smaller for this model than for Model A.

It is interesting to review the behavior of the model as the load is increased. The results for the modal load distribution on Model A are used (backbone curve on Fig. 4-6 and tabular listing of curve on Table 4-9). A review of the building model indicates that the shear walls are very stiff as compared with the diaphragms (about 500,000 k / ft [7.297×10^6 kN/m] for wall 19 versus 25,000 k / ft [3.648×10^5 kN/m] for the diaphragm). The diaphragm yields at a load of 1210 kips (5,382 kN) which occurs at a displacement of 0.048 feet (1.46 cm). The turbine pedestal has a stiffness of 288,000 k / ft (4.203×10^6 kN/m)and a yield load of 67,000 kips (298,031 kN). The yield displacement of the pedestal is therefore 0.23 feet (7.0 cm). The data of Table 4-9 indicates that the response is linear up to a shear load of 28,000 kips (124,550 kN) at which time the yield displacements (0.048 feet [1.46 cm]) of the diaphragms are exceeded. At a load of about 57,000 kips (253,549 kN) the difference between the displacements of nodes 10 and 12 equals the gap (0.28 feet [8.57 cm]) indicating the gap is closed and node 10 is being supported from the turbine pedestal. As the load is increased, the gap remains closed and the building is partially supported by the pedestal. This continues until a load of about 100,000 kips (444,822 kN) at which time the pedestal yields. The pedestal then separates from node 10. The gap between nodes 11 and 12 closes at a load of about 113,000 kips (502,649 kN). The turbine is then partially supported from the building for larger loads. Since the turbine is so massive relative to the building (62 % of the total mass is in the turbine), the dynamic characteristics of the building change significantly as the load path is changed from the building supported from the pedestal to the pedestal supported from the building.

The next step in the displacement-based analysis is to evaluate the target displacement. Node 10, located at the center of the diaphragm, is selected as the target node for Model A since it has the larger displacement of the two diaphragm nodes, and node 8 is selected as the target node for Model B. Several dynamic characteristics of the building and response spectrum are required to evaluate the target displacement:

- T_o is the period associated with the transition from the constant acceleration to constant velocity portion of the response spectrum. The value of T_o is taken as 0.34 seconds based on the shape of the response spectrum shown on Fig. 4.3.

- T_i is the fundamental period of the building. The fundamental mode associated with the diaphragm response has a frequency of 4 cps so the T_i is equal to 0.25 seconds.

- T_e is defined as an effective period accounting for the degradation in building stiffness as the deflections increase. The effective period is obtained by scaling the fundamental period in proportion to the square root of the initial stiffness (K_i) to the effective stiffness (K_e). The initial stiffness is 508,595 k / ft (7.422×10^6 kN/m). The effective stiffness is the slope of the first portion of the bilinear representation of the pushover curve. FEMA 273 suggests that this slope be established between the origin and a point on the pushover curve at 60 % of the yield load. The bilinear curve constructed satisfying this criteria is shown on Fig. 4-6 and results in an effective stiffness equal to 137,436 k / ft (2.006×10^6 kN/m). The value of T_e is

$$T_e = T_i \, [K_i / K_e]^{0.5} = 0.48 \text{ seconds}$$

The stiffness of Model B is found in the same manner and is shown on Fig, 4-7, and degrades from an initial value of 508,595 k / ft (7.422×10^6 kN/m) to 147,183 k / ft (2.148×10^6 kN/m) so that the value of T_e is:

$$T_e = T_i \, [K_i / K_e]^{0.5} = 0.46 \text{ seconds}$$

- S_a is the spectral acceleration at the effective period. Therefore $S_a = 2.39$ g for Model A and 2.45 g for Model B. Results are first developed for the 3 g input and then for the 6 g input.

The target displacement is calculated as:

$$\delta = C_0 \, C_1 \, C_2 \, C_3 \, S_a \, (T_e / 2\pi)^2 \, g$$

The constants C_0, C_1, and C_2 are the same for both Models A and B. The value of C_0 is taken from Table 3-2 of FEMA 273 to be 1.0 for a one-story building. The value of C_1 is taken as unity since $T_e > T_o$ for both models. The value of C_3 is taken as 1 since $P - \Delta$ effects are not significant.

The constant C_2 reflects the effect of hyteresis loop shape and depends on the type of framing, the period of the building, and the performance level of the building. The values of the constant are found to be 1.31 for both models. The values of the target displacement (δ) for the 3 g input are then found to be 0.59 feet (18 cm) and 0.55 feet (16.8 cm) for Models A and B, respectively. These values are doubled for the 6 g input. The resultant displacements are then located on the tabular listing for the backbone curves and corresponding displacements found for other nodes in the models. The resultant displacements are shown on Table 4-11.

4.3 Comparison of Time History and Displacement Based Results

The displacement results obtained with the displacement-based method and the time history methods are compared in this section. The time history methods developed log normal distributions for the displacements. The error between the two is normalized with respect to the log standard deviation and is defined as:

$$E = \text{ABS} \, [\ln (D_{fema} / D_m)] / \beta_D$$

Where,

D_{fema} = displacement based prediction
D_m = median of time history prediction
β_D = log standard deviation for time history analysis

The results of the time history analyses given in Tables 4-5 and 4-6 are combined with the results of the displacement based analyses given in Table 4-11 to calculate the differences between the two sets of results with a summary given in Tables 4-12 and 4-13 for the 3 g and 6 g cases respectively.

It can be seen that the agreements between the time history and displacement results are not very good and that the displacement-based method generally over-predicts the response. The predictions between the two methods are closer for the response at the top of the shear walls than for the diaphragms or for the turbine pedestal. For the 3 g input motion, the Model A predictions of the shear wall displacements are better than the Model B predictions, but the reverse is true for the diaphragm and pedestal displacements. The Model B predictions are better than the Model A predictions for the 6g input except for the turbine deflection.

It does not appear that a simple adjustment in the constants (C_0 through C_3) will improve the results. There are probably four reasons for the large differences:

- The dynamic characteristics of the building change dramatically when the gaps close since the turbine is so massive. The basic idea behind the displacement-based approach is that an "equivalent" static analysis can be performed to represent the dynamic response. It is unlikely that a single static model could adequately model the response of a system that changes so dramatically as the gaps close and open.

- The load path changes from the pedestal supporting the building to the building supporting the pedestal as the diaphragm and then pedestal reach their respective yield loads. It is also unlikely that this could be modeled with a single equivalent static model.

- The displacement-based methodology was developed for cases where the building has softening stiffness characteristics. Some aspects of the turbine building problem have the opposite characteristic. After the diaphragm yields it is partially supported from the pedestal. This support results in a nonlinear increase in building stiffness.

- The turbine and shearwall structure behave as uncoupled systems during a large part of the response. The displacement based method attempts to model this with a single degree of freedom system which cannot capture the dynamic characteristics of both in a single model.

5 CONCLUSIONS AND RECOMMENDATIONS

This report considers the extent to which a displacement based seismic analysis such as prescribed in FEMA 273 may have applicability to nuclear power plant facilities. The FEMA approach is based on the development of a force-displacement curve for the structure of interest by performing a pushover analysis (placing a static load on a nonlinear model of the structure) with the loads monotonically increased until the peak displacement reaches that expected during the criteria earthquake. The member displacements at this peak displacement (found from the pushover analysis) are then compared with allowable limits (also given in FEMA 273) to determine whether the structure can withstand the criteria earthquake.

Current seismic analysis methods are force based in that member forces rather than displacements are compared with acceptance limits. The specific methods used to perform these analyses for those problems where inelastic action is anticipated, and acceptable, are either a nonlinear time history analysis or an elastic analysis with member seismic loads reduced by ductility factors to account for inelastic action. Analyses presented in this report compare results from displacement based analyses with those obtained from each of the other methods.

The following conclusions are found from these comparisons:

1. The displacement based method gives results comparable to the nonlinear time history analysis for the shear wall building where there are only material nonlinearities.

2. The use of ductility factors with a linear response spectrum analysis gives results which are comparable to those obtained from either the nonlinear time history analysis or the displacement based method.

3. The displacement based method does not give results which are comparable to the nonlinear time history analysis for the Diablo Canyon turbine building where both material and geometric nonlinearities (gaps) are included. This conclusion is probably due to the strong effect of the gaps on the system response.

Based on these conclusions, the following recommendations are given:

1. The displacement based approach is not applicable for the design of nuclear power facilities since the acceptance criteria are force based and all responses are required to remain in the linear elastic range. While the displacement based approach could be used in this area, it offers no advantages over the force based methodologies currently in use for evaluating design adequacy. Therefore, there is no need to revise the Standard Review Plan for seismic design to address displacement based methods.

2. Seismic margin studies for nuclear facilities are based on displacement acceptance criteria (usually inelastic deformation limits corresponding to a given probability of failure). The displacement based analysis is directly applicable to those problems where only material nonlinearities occur. The displacement based methods offer two advantages over the nonlinear time history analysis. First, the displacement based approach or pushover analysis is much simpler and less time consuming to use than the time history analysis. This simplification is likely to reduce the potential for erroneous results and to increase the number of engineers that have the background required to perform the analysis. Second, the method greatly reduces the effort required to produce structural fragility curves from that which is required using time history analyses. A single static nonlinear analysis is required

to produce the pushover curve. Solutions for different probabilities of failure are then obtained by evaluating the criteria earthquake required for the structural displacement to reach the acceptance criteria associated with the probability of failure. Many non linear time history analyses would be required to generate the fragility curve. Therefore, the NRC should consider developing guidance for the use of the displacement based approach for seismic margin/fragility analysis.

3. Additional studies would need to be performed for nuclear power plant structures with both material and geometric nonlinearities to further define the scope of the problems that can be treated with the displacement based methods before it would be possible to establish sufficient guidance for their use.

4. If displacement based methods of FEMA 273 are to be applied on a wide scale to nuclear facilities, efforts must be undertaken to develop appropriate "C" coefficients and drift limits that are consistent with the importance of the structure. Alternative forms of displacement based methods are also possible. The primary steps in any displacement based method are to predict the expected displacement of the structure to earthquakes of interest accounting for nonlinear characteristics of the structure, and to evaluate the details of the structure to determine whether sufficient ductility is available to accommodate the displacement pattern with adequate margin. A method, similar to FEMA 273, could be developed specifically for nuclear structures.

6 REFERENCES

[1] BSSA, "NEHRP Guidelines for the Seismic Rehabilitation of Buildings," FEMA-273, October 1997.

[2] IDARC 2D Version 4.0 " A Program for the Inelastic Damage Analysis of Buildings" NCEER-96-0010. SUNY at Buffalo, Jan, 1996

[3] ANSYS Version 5.6

[4] Kennedy, R.P., Wesley, D.A., Tong, W.H., "Probabilistic Evaluation of the Diablo Canyon Turbine Building Seismic Capacity Using Nonlinear Time History Analyses," Report Number 1643.01 prepared for Pacific Gas and Electric Company, San Francisco, California, December 1988.

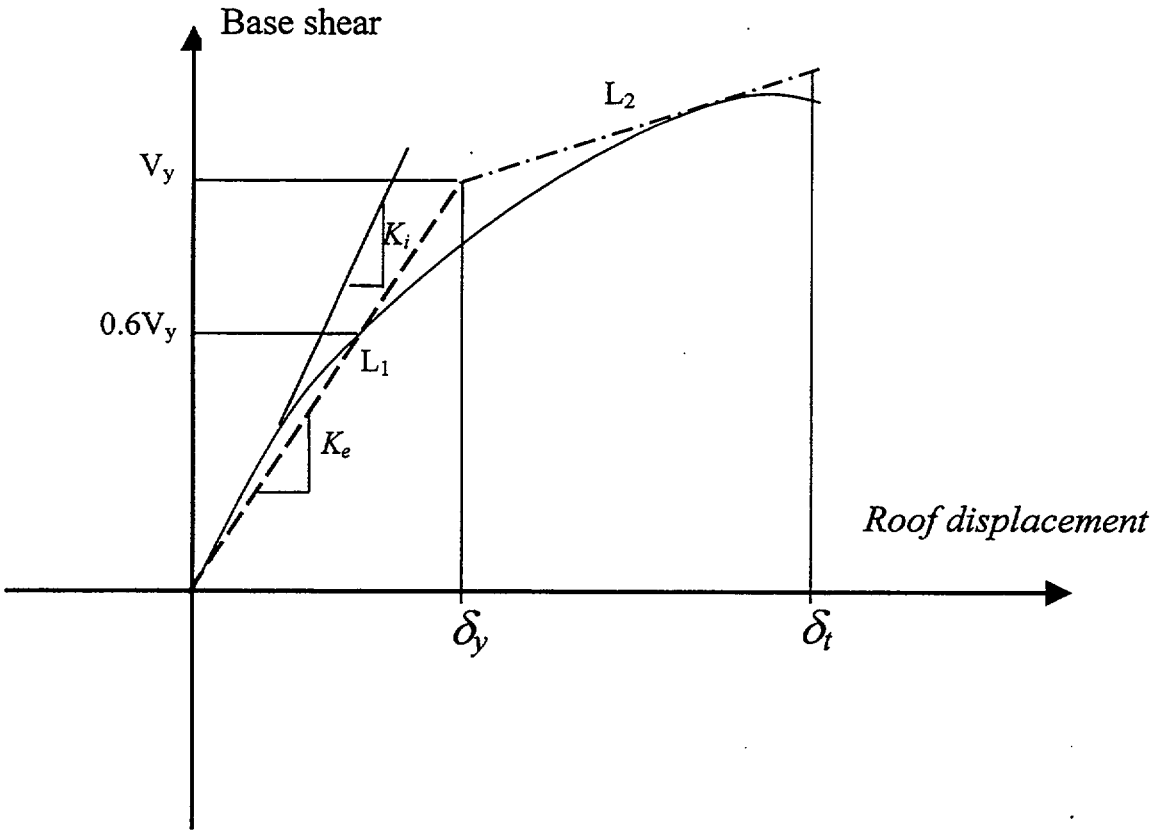

Figure 2-1 – Calculation of the Effective Stiffness, K_e

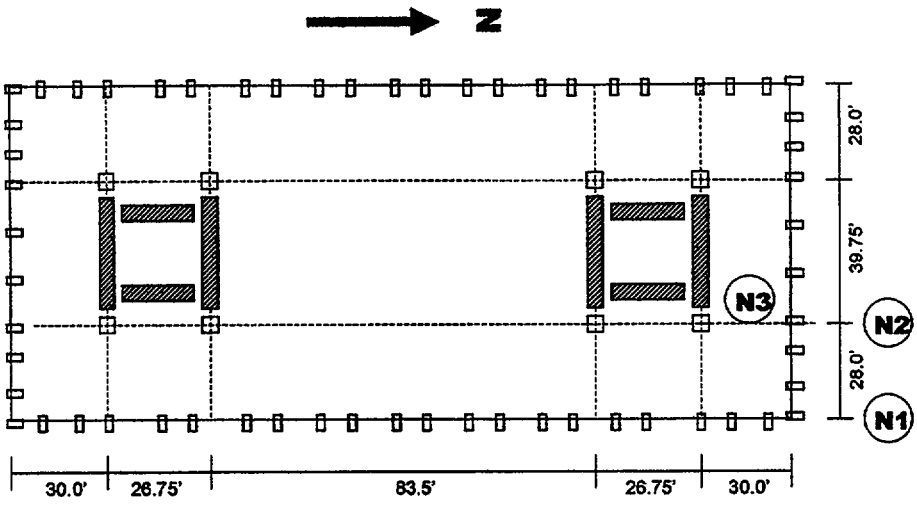

Figure 3-1 - Plan View of the Sample Model [Ref. 1]
(1 ft. = .3048 m)

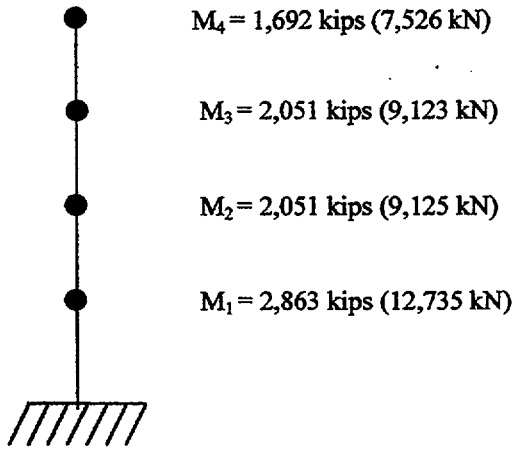

Figure 3-2 - Stick Model of Shear Wall Building

Properties for Model		
f_c'	3 ksi	20.7 N/mm^2
f_t	0.36 ksi	2.48 N/mm^2
E_c	3,122 ksi	21.5 kN/mm^2
ε_o	0.002 in/in	0.002 mm/mm
ε_u	0.004 in/in	0.004 mm/mm

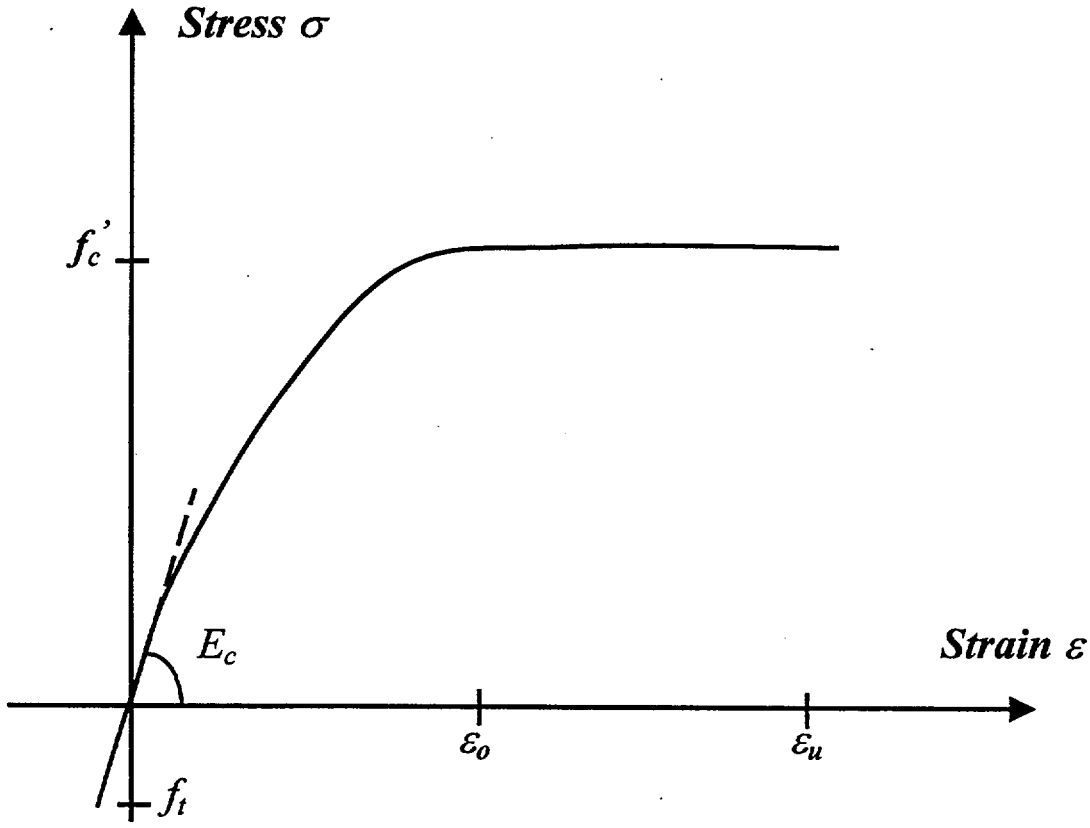

Figure 3-3 – Stress-Strain Curve of the Unconfined Concrete

Properties for Model		
f_u	84 ksi	579 N/mm^2
f_y	60 ksi	414 N/mm^2
E_s	29,000 ksi	200 kN/mm^2
E_t	203.5 ksi	1.4 kN/mm^2
ε_y	0.002 in/in	0.002 mm/mm
ε_h	0.03 in/in	0.03 mm/mm

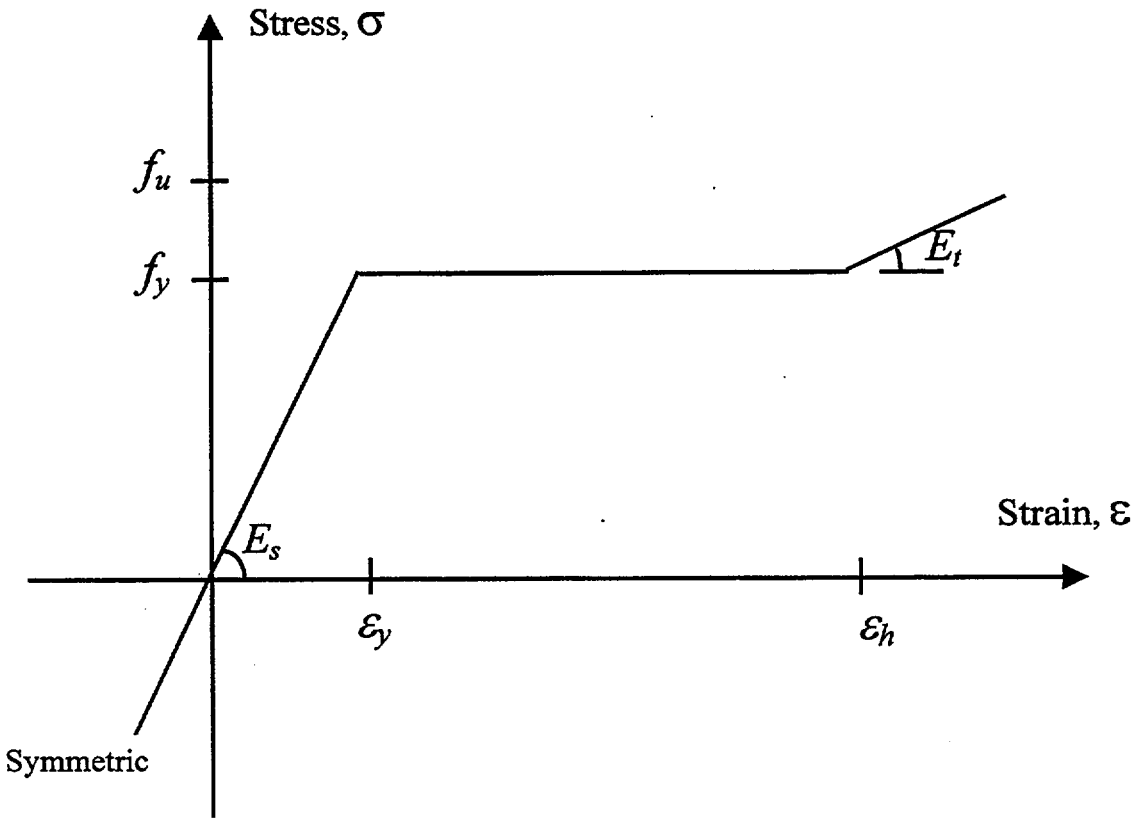

Figure 3-4 – Stress- Strain Curve of the Reinforcing Steel

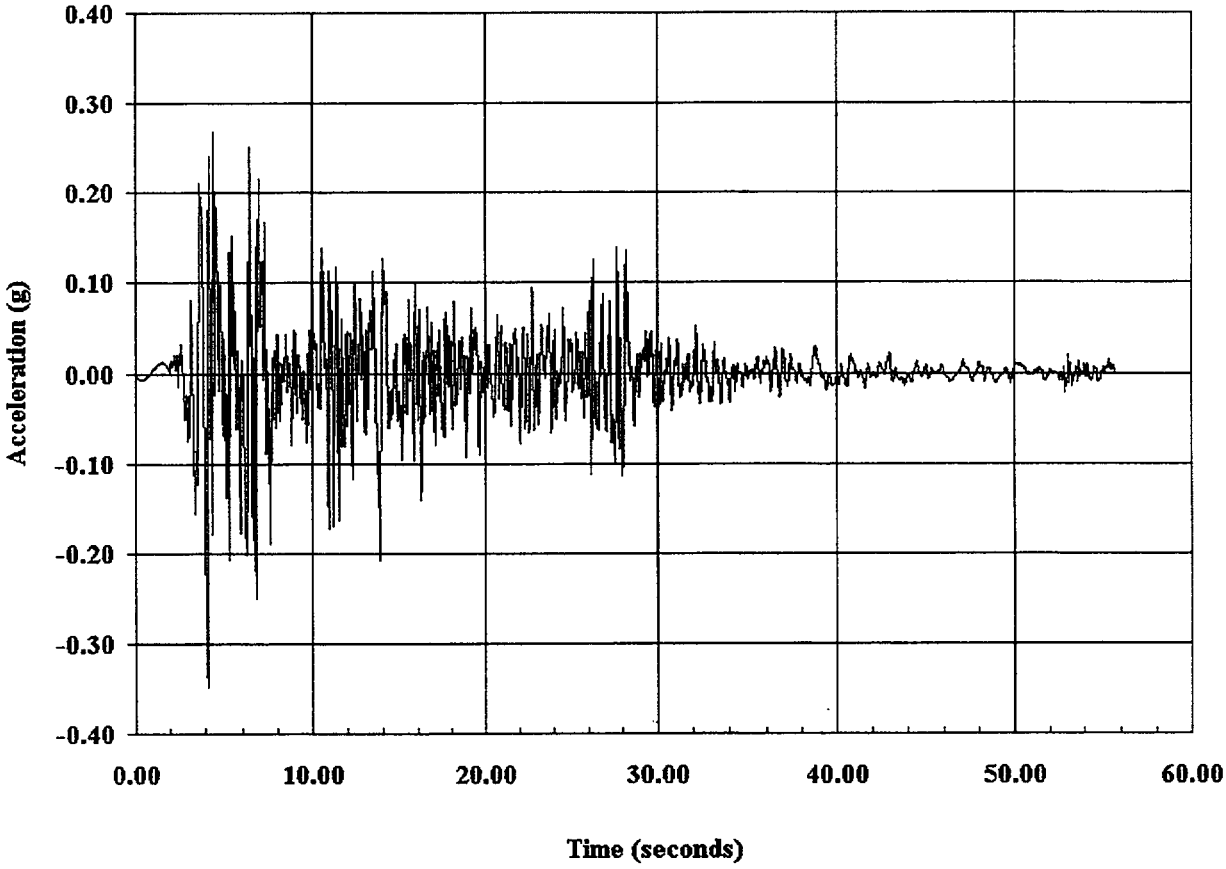

Figure 3-5 – Time History Record of the El Centro Earthquake (1940, NS)

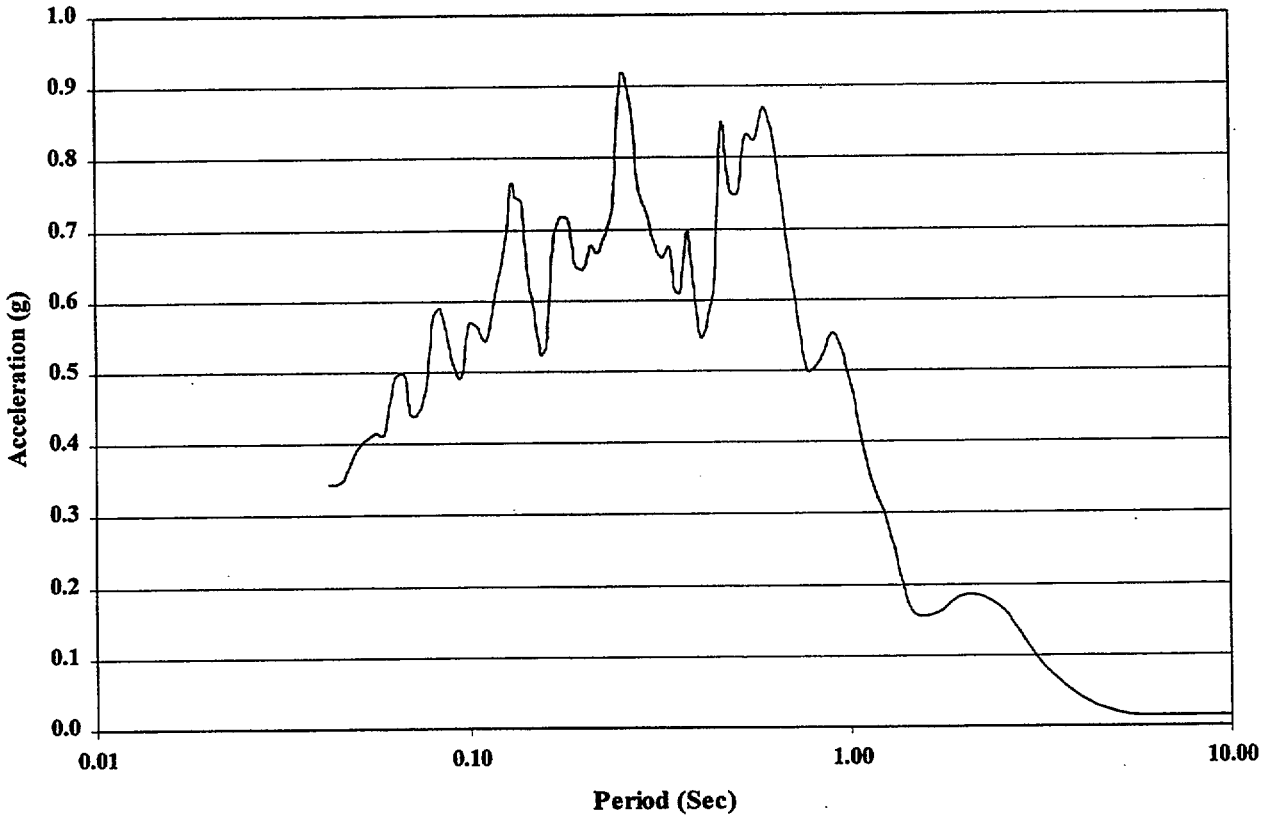

Figure 3-6 – Response Spectrum of the El Centro Earthquake (5% Damping)

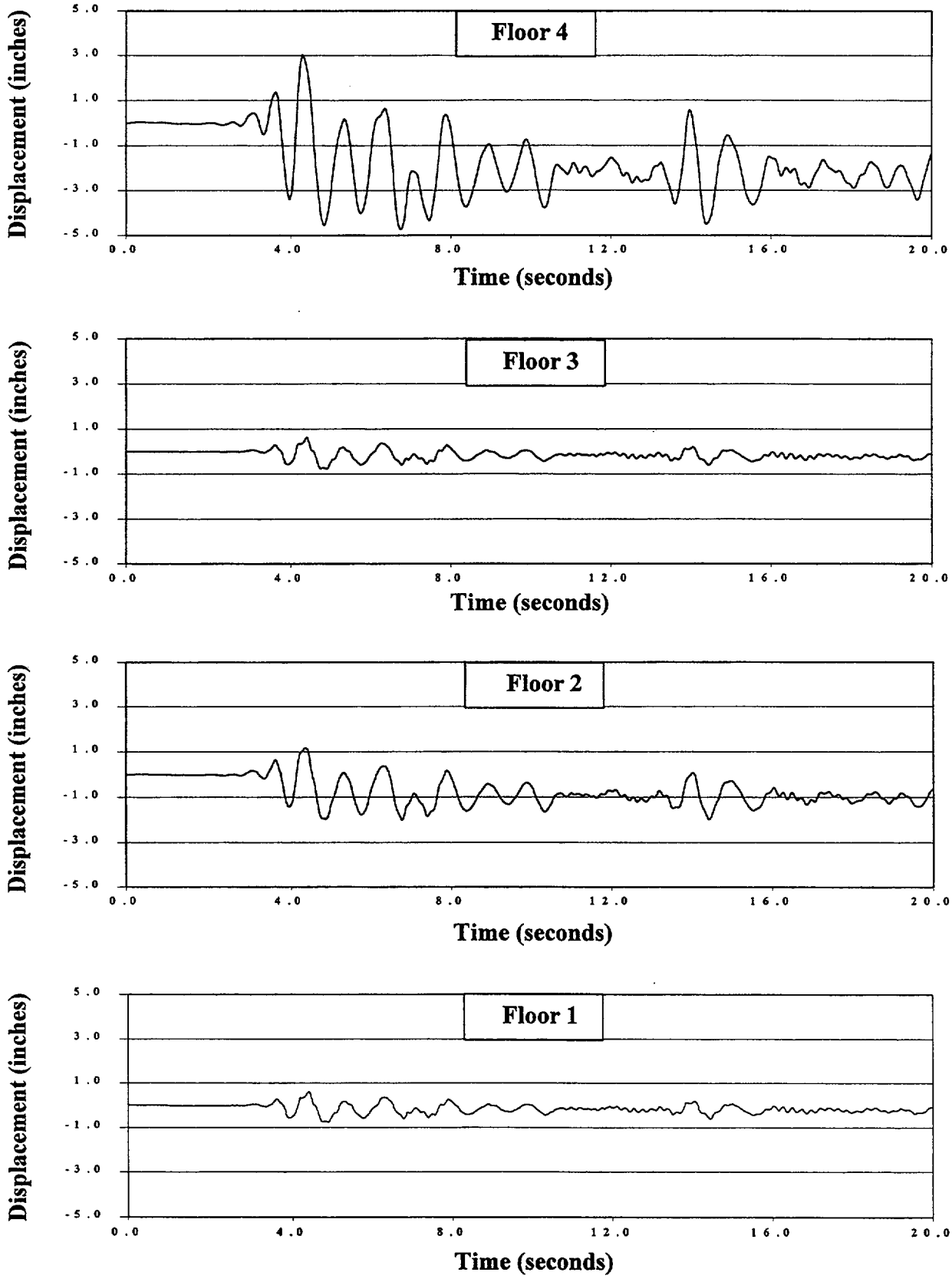

Figure 3-7 – Floor Displacement Time Histories (1 in. = 25.4 mm)

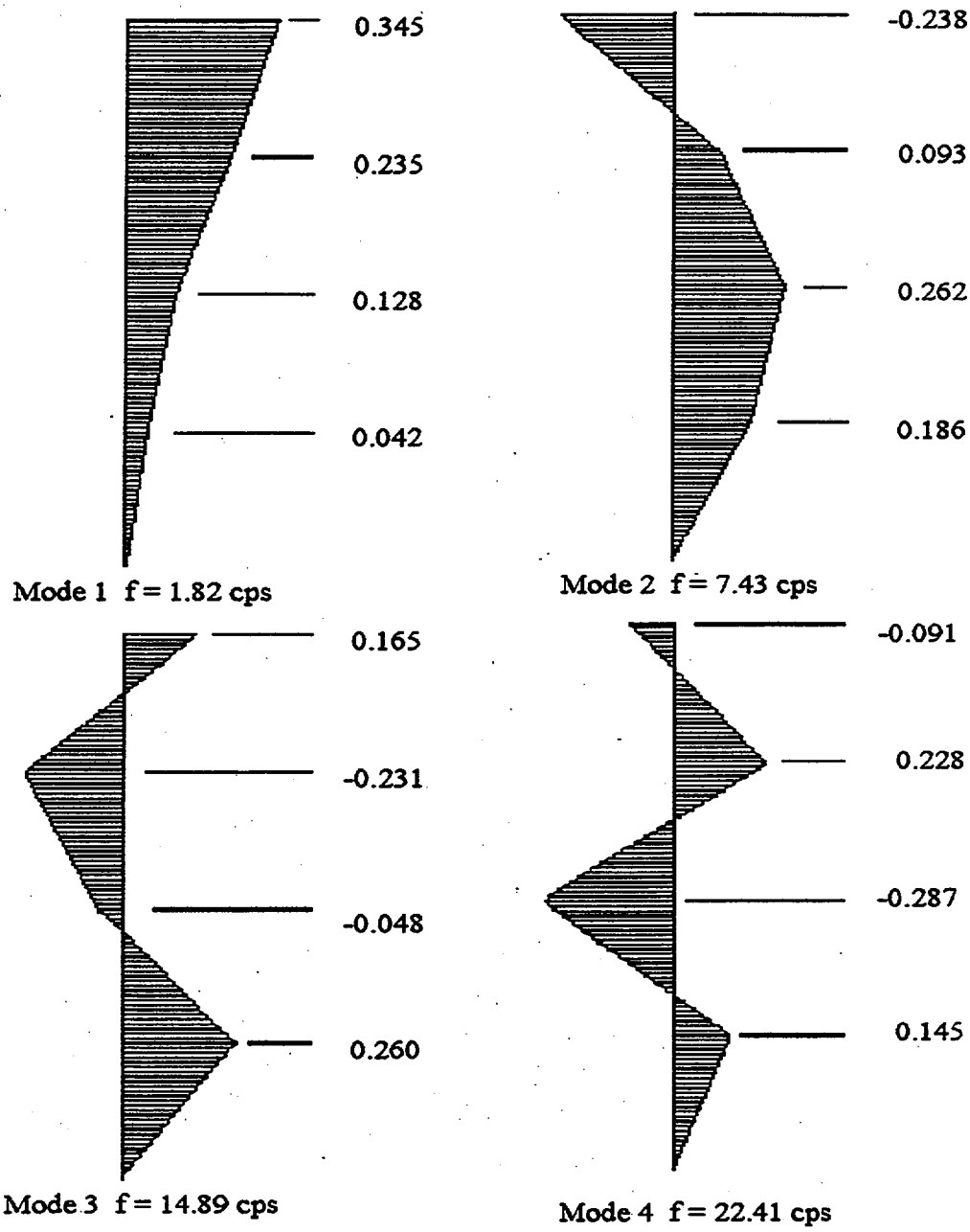

Figure 3-8 – Mode Shapes of the Shear Wall Model

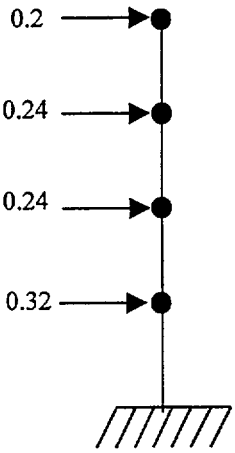

Figure 3-9A – Distribution of Input Loading for the Uniform Loading Case

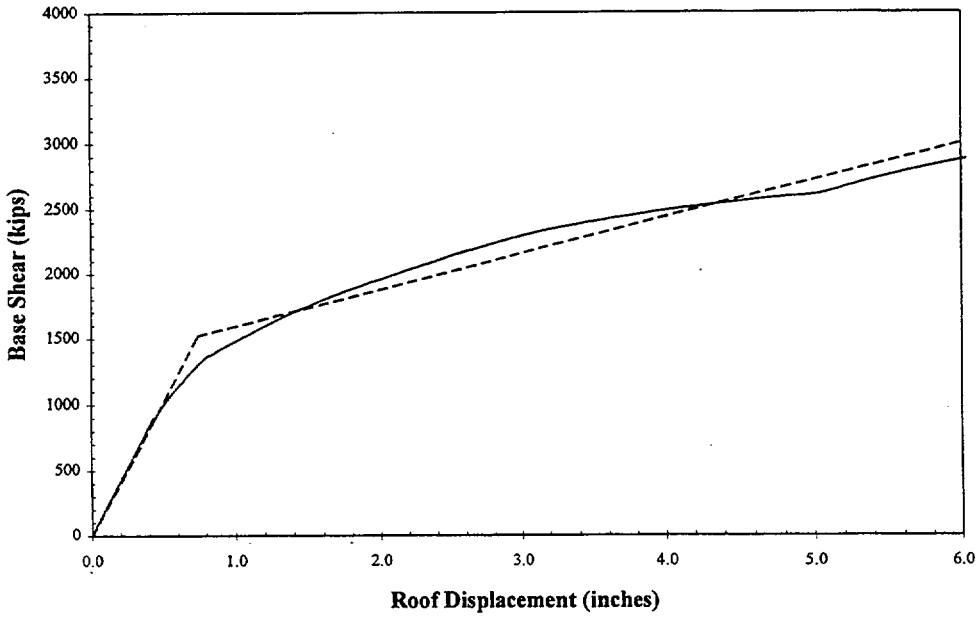

Figure 3-9B – Load Deformation Curve for the Uniform Loading Case
(1 kip = 4.448 kN, 1 in. = 25.4 mm)

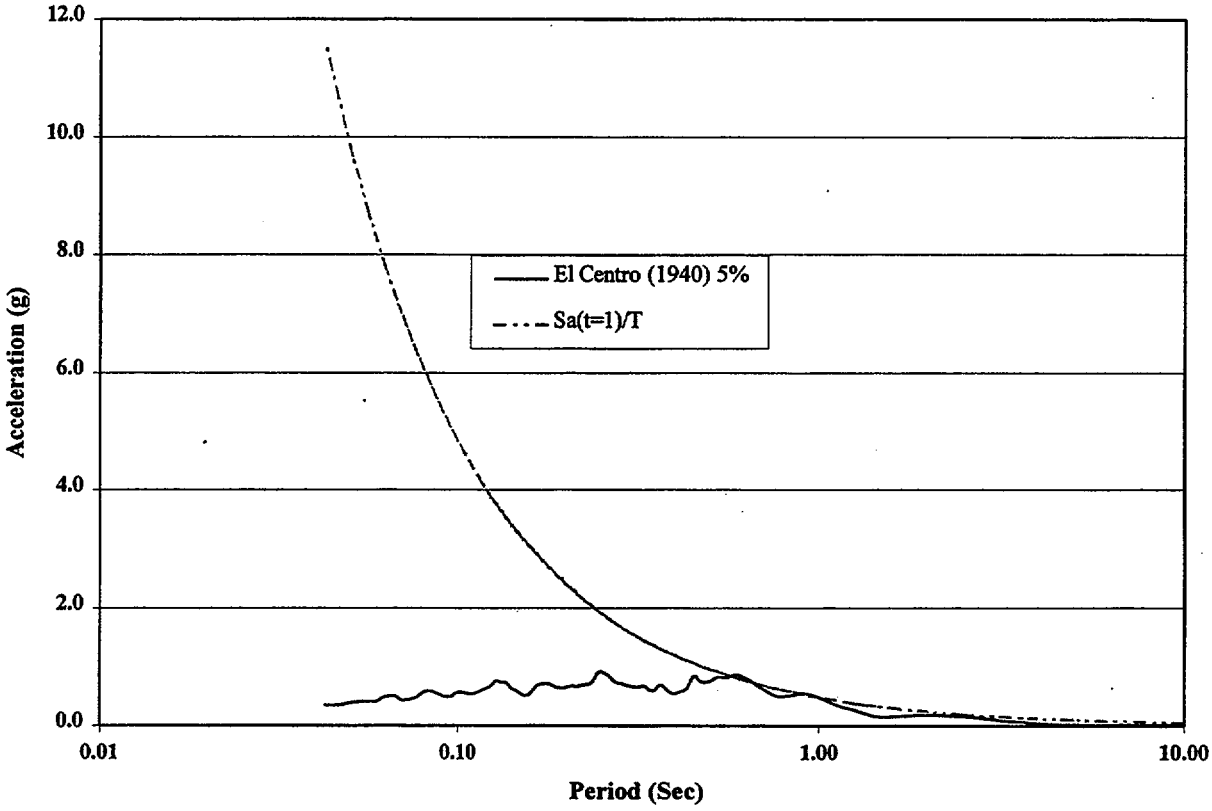

Figure 3-10 – Calculation Curve of S_{x1} for the El Centro Earthquake

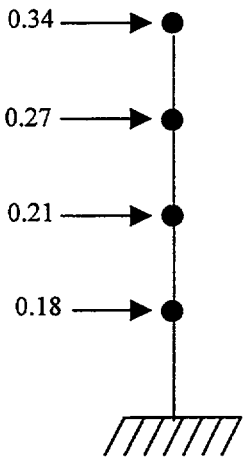

Figure 3-11A Distribution of Input Loading for the Modal Loading Case

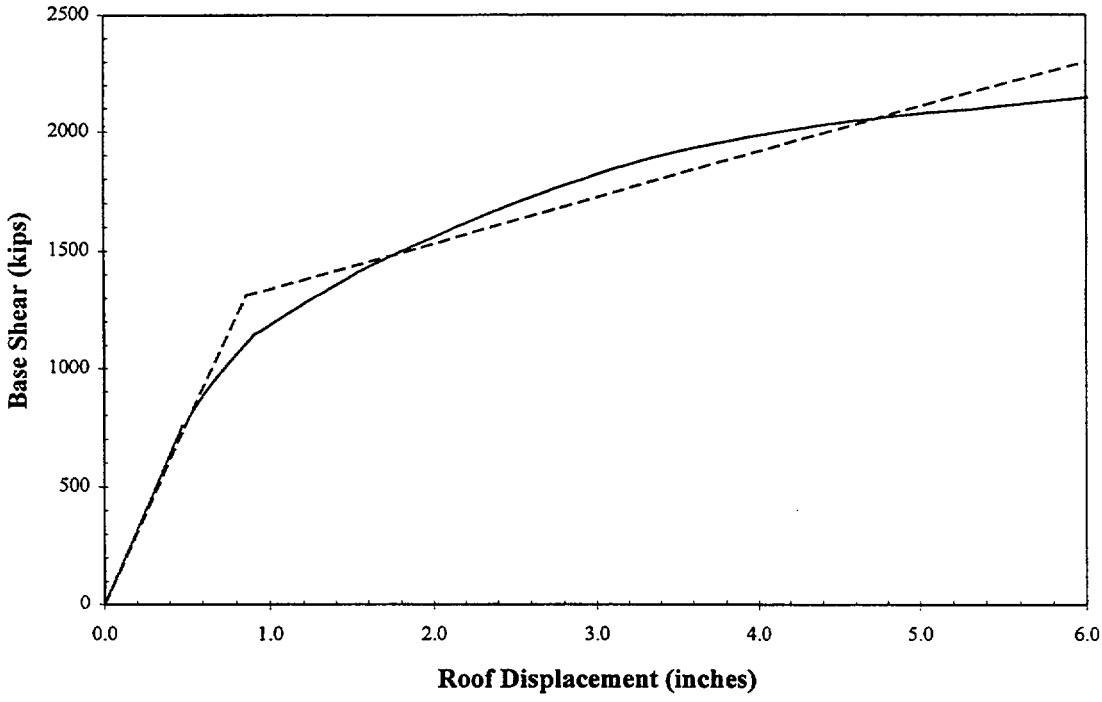

Figure 3-11B – Load Deformation Curve for the Modal Loading Case
(1 kip = 4.448 kN, 1 in. = 25.4 mm)

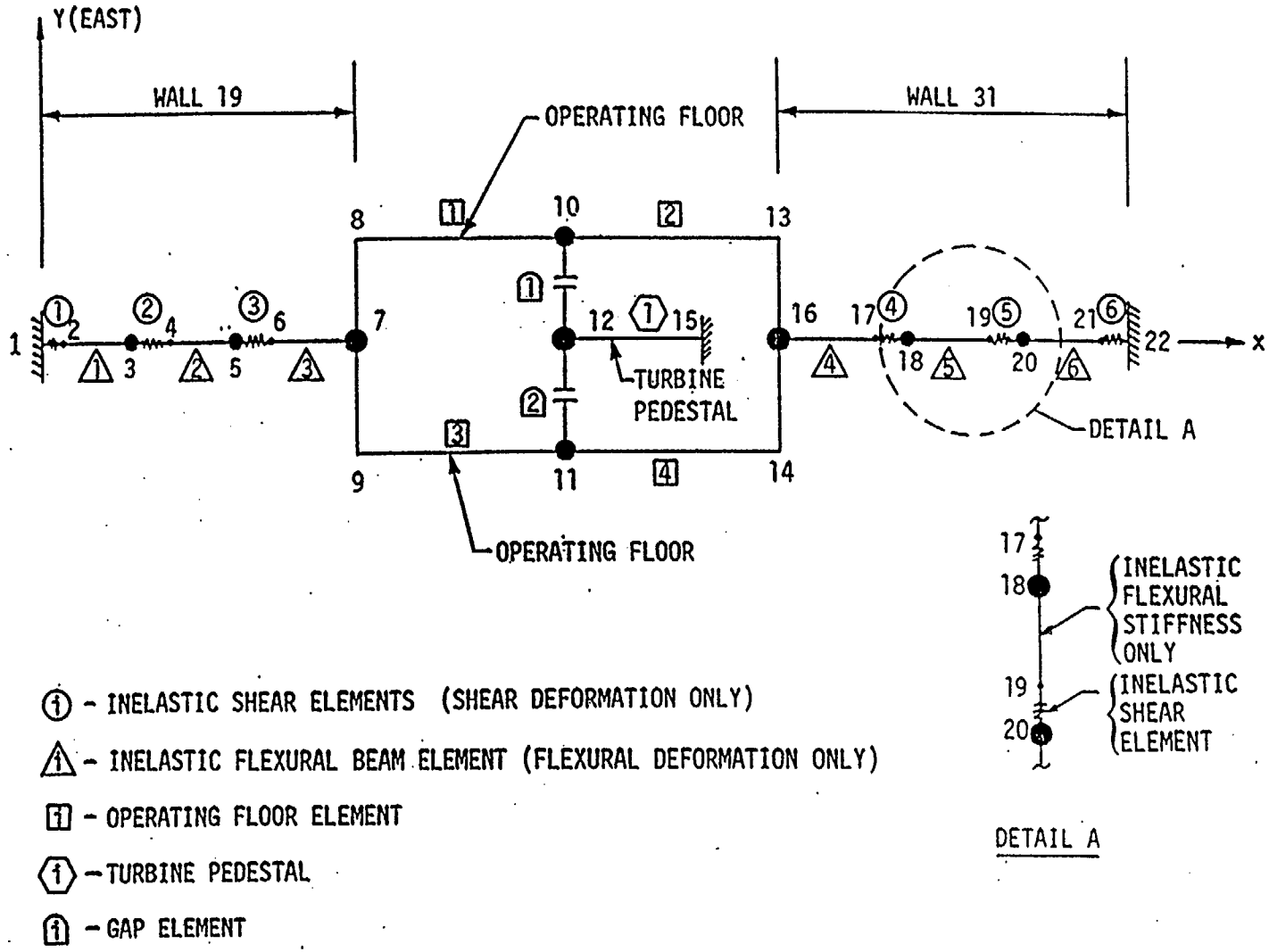

Figure 4-1 - Diablo Canyon Turbine Building Model A (Figure 2-3 of Ref. 4)

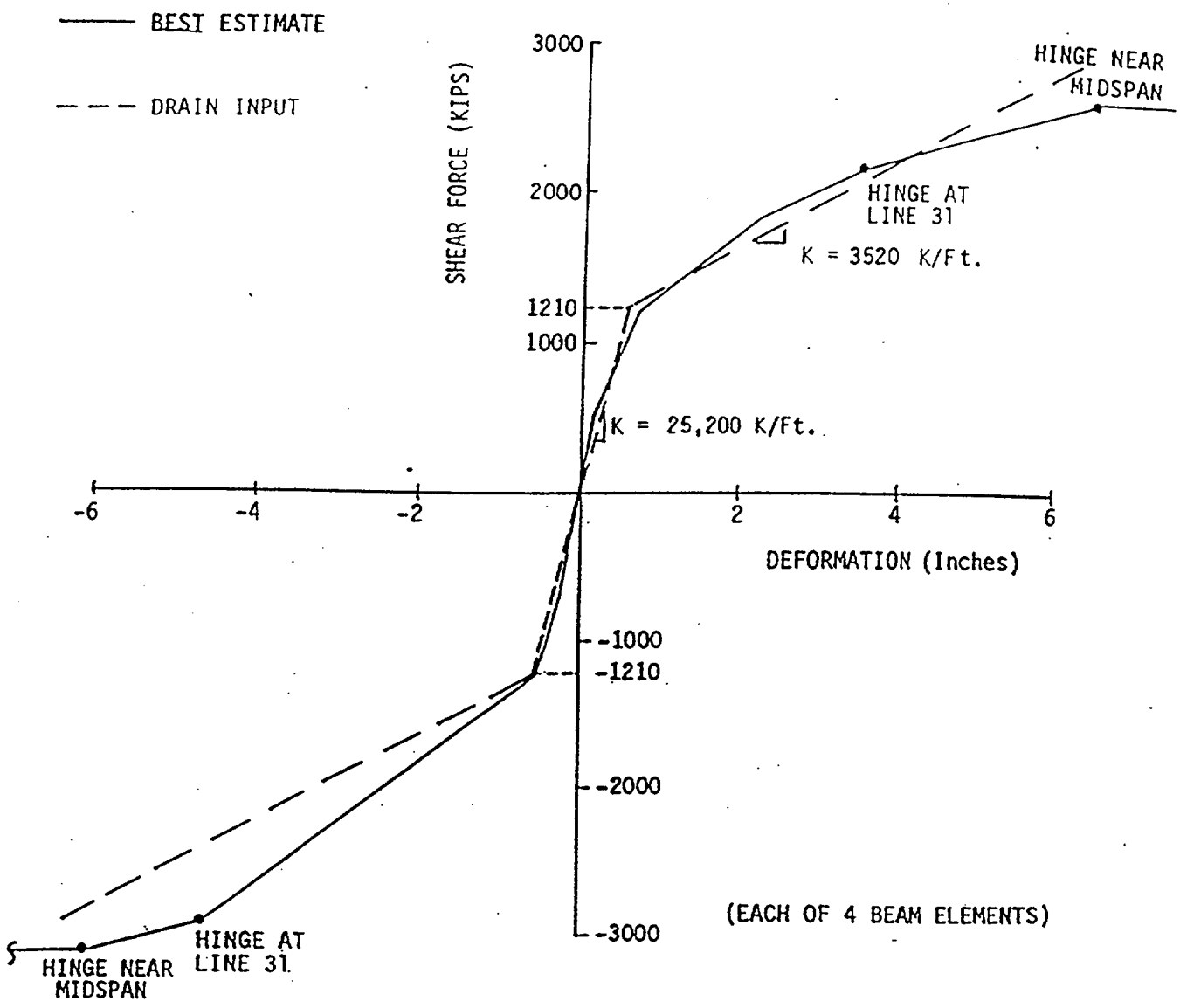

Figure 4-2 - Shear-Deformation Curve for Each Beam-Like Portion of the Operating Diaphram at the Midspan (Fig. 2-10 of Ref. 4)
(1 kip = 4.448 kN, 1 k/ft. = 14.59 kN/m, 1 in. = 25.4 mm)

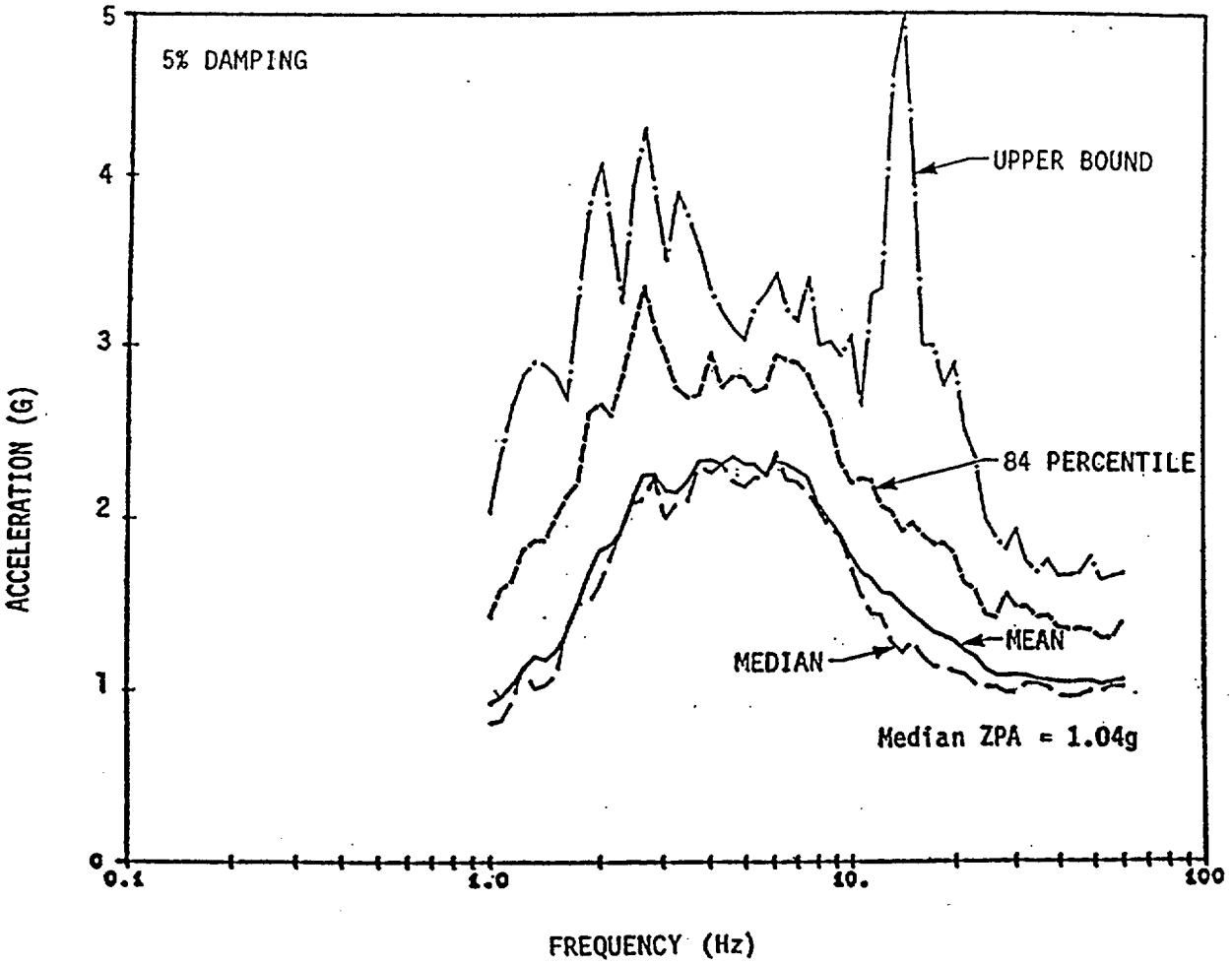

Figure 4-3 - Mean, Median, 84% NEP, and Upper Bound Spectra for Ensemble of 25 Scaled Records ($\bar{S}_a = 2.25g$) (Fig. 3-27 of Ref. 4)

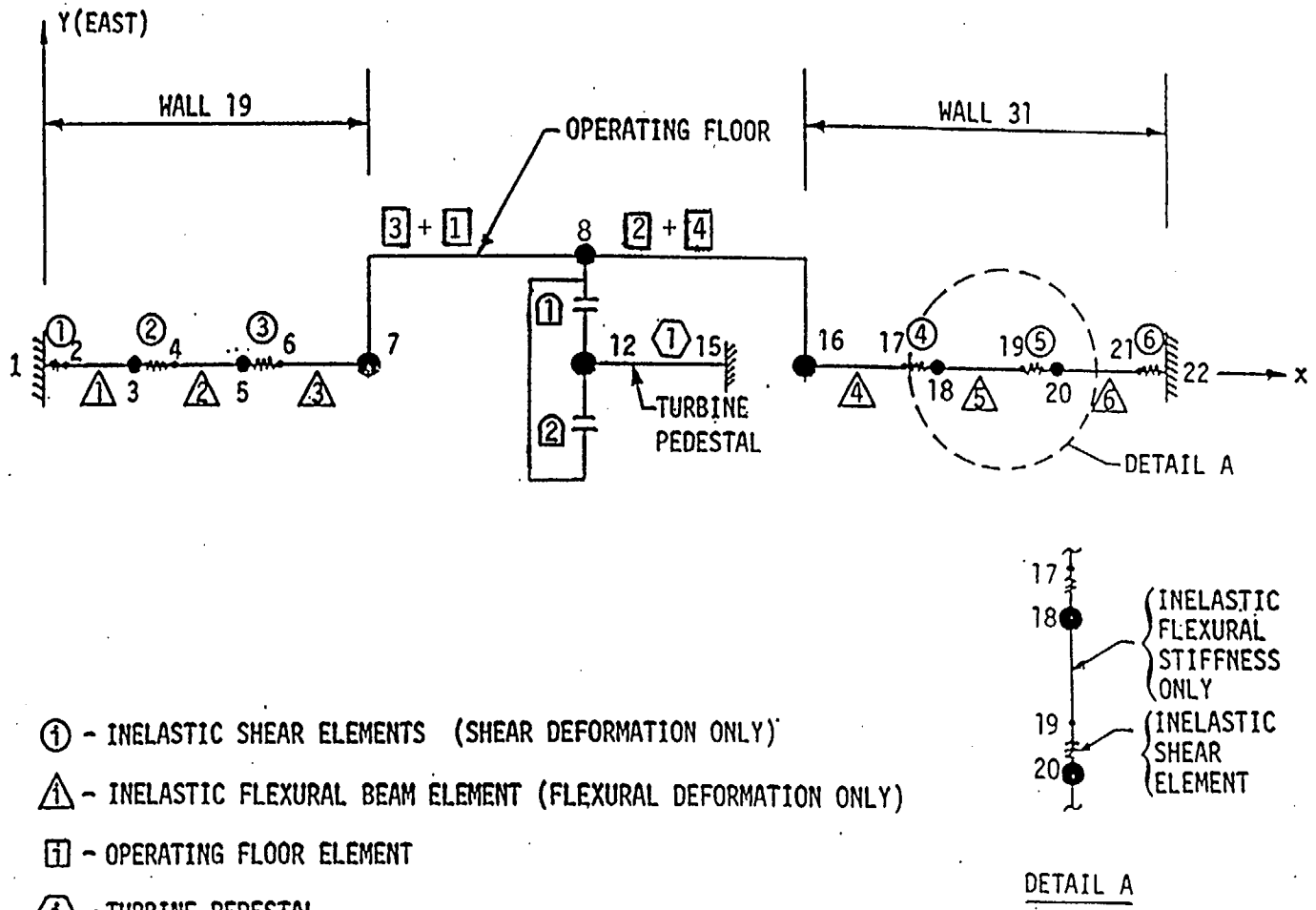

Figure 4-4 - Diablo Canyon Turbine Building Model B

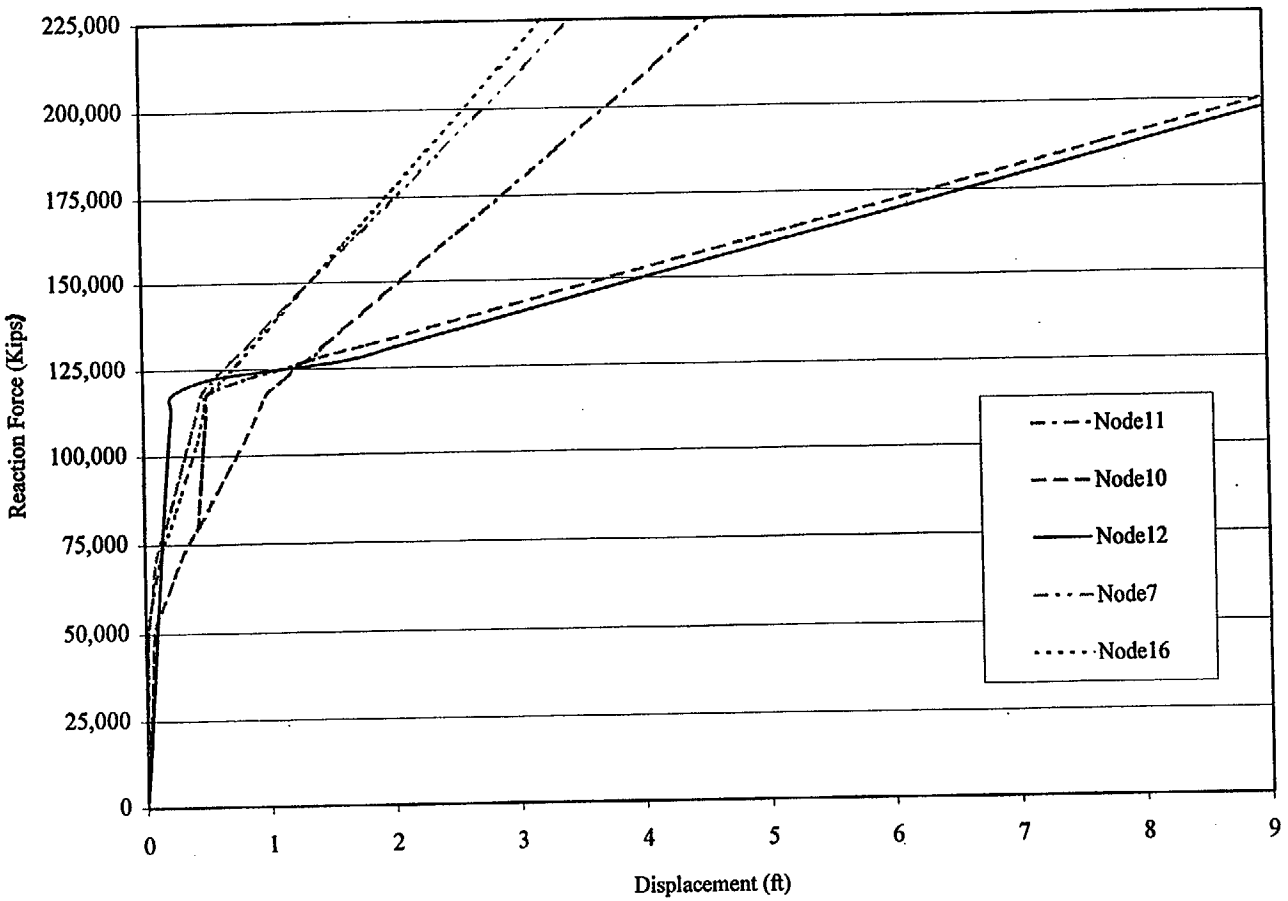

Figure 4-5 - Load Deflection Curves for the Uniform Loading Case for Model A
(1 kip = 4.448 kN, 1 ft. = .3048 m)

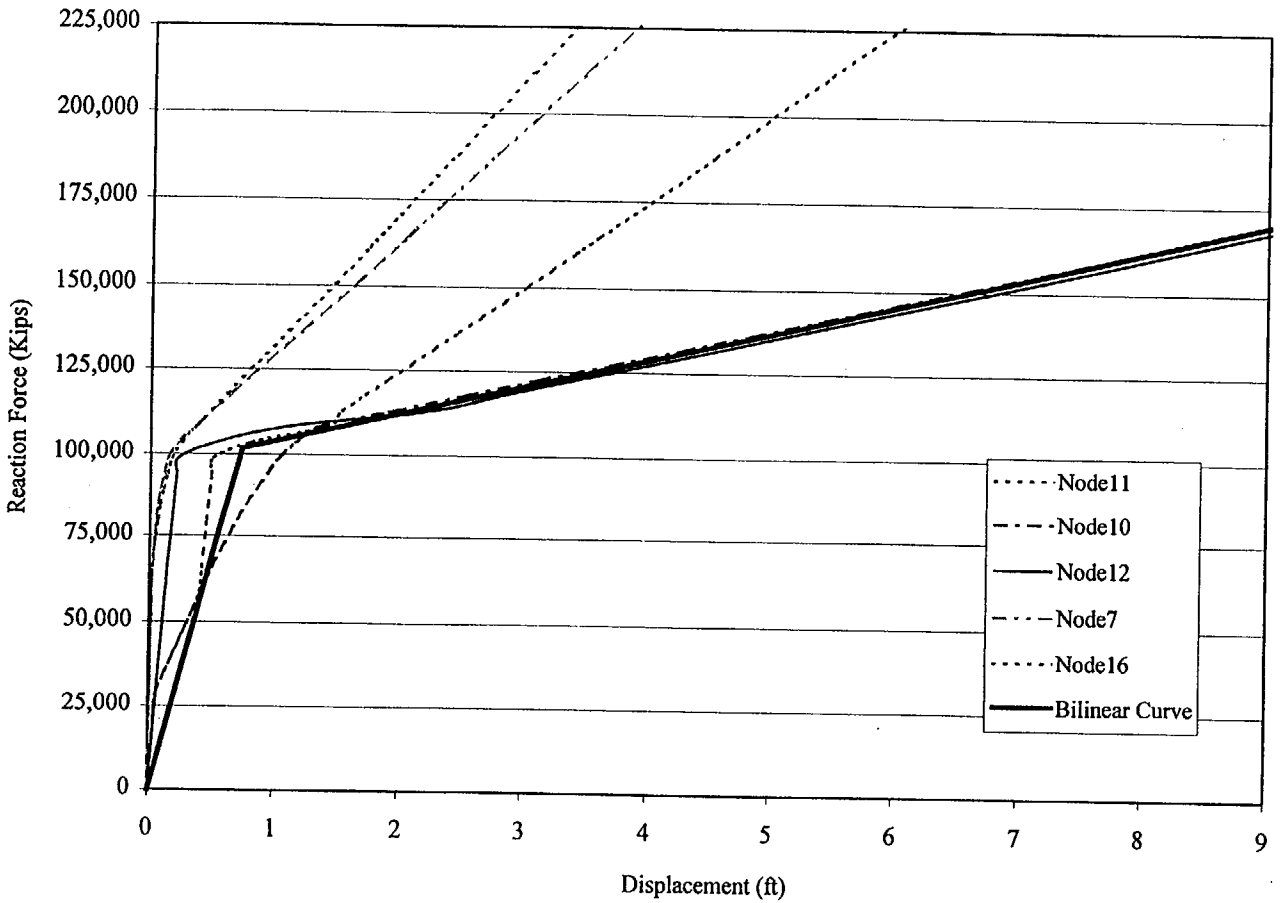

Figure 4-6 - Load Deflection Curves for the Modal Loading Case for Model A
(1 kip = 4.448 kN, 1 ft. = .3048 m)

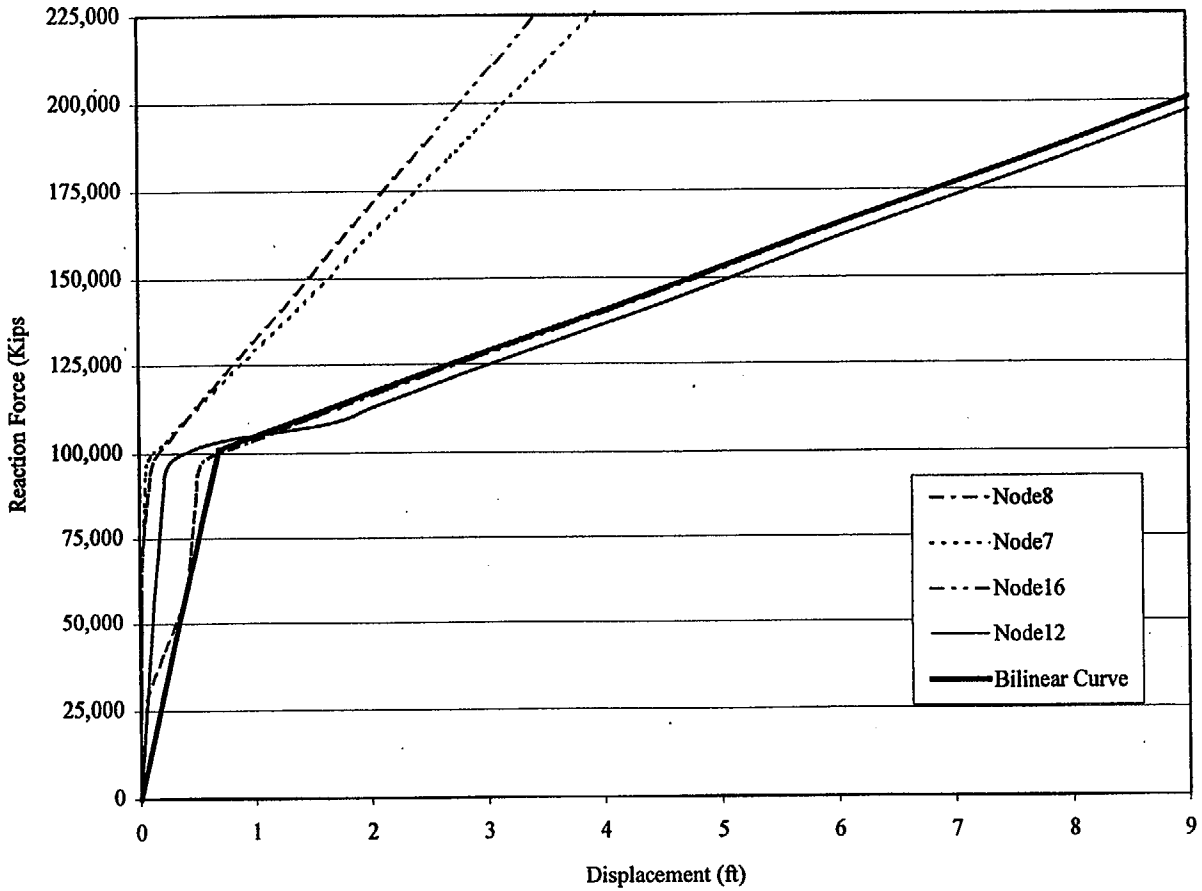

Figure 4-7 - Load Deflection Curves for the Modal Loading Case for Model B
(1 kip = 4.448 kN, 1 ft. = .3048 m)

Table 2-1 - Values for Modification factor C_0
(Table 3-2 of FEMA 273)

Values for Modification Factor C_0

Number of Stories	Modification Factor[1]
1	1.0
2	1.2
3	1.3
5	1.4
10+	1.5

1. Linear interpolation should be used to calculate intermediate values.

Table 2-2 - Values for Modification factor C_2
(Table 3-1 of FEMA 273)

Values for Modification Factor C_2

	T = 0.1 second		$T \geq T_0$ second	
Performance Level	Framing Type 1[1]	Framing Type 2[2]	Framing Type 1[1]	Framing Type 2[2]
Immediate Occupancy	1.0	1.0	1.0	1.0
Life Safety	1.3	1.0	1.1	1.0
Collapse Prevention	1.5	1.0	1.2	1.0

1. Structures in which more than 30% of the story shear at any level is resisted by components or elements whose strength and stiffness may deteriorate during the design earthquake. Such elements and components include: ordinary moment-resisting frames, concentrically-braced frames, frames with partially-restrained connections, tension-only braced frames, unreinforced masonry walls, shear-critical walls and piers, or any combination of the above.
2. All frames not assigned to Framing Type 1.

Table 3-1- Nodal Weights of the Shear Wall Model

Floor #	Frame #	Joint 1	Joint 2	Joint 3	Joint 4	Joint 5	Joint 6	Joint 7	Joint 8	Joint 9	Joint 10	Joint 11	Joint 12	Joint 13	Joint 14	Joint 15	Joint 16	Joint 17	Joint 18	Joint 19	Joint 20	Sub. Total	Floor Weight
4th Floor	1	48.3	36.2	36.2	36.2	36.2	36.2	36.2	36.2	36.2	36.2	36.2	36.2	36.2	36.2	36.2	36.2	36.2	36.2	36.2	48.3	748	
"	2	125	69.4	69.4	139	139	69.4	69.4	125													805	
"	3	139																				139	1692
3rd floor	1	13.3	35	35	35	35	35	35	35	35	35	35	35	35	35	35	35	35	35	35	13.3	657	
"	2	124	115	115	229	229	115	115	124													1165	
"	3	229																				229	2051
2nd Floor	1	13.3	35	35	35	35	35	35	35	35	35	35	35	35	35	35	35	35	35	35	13.3	657	
"	2	124	115	115	229	229	115	115	124													1165	
"	3	229																				229	2051
1st Floor	1	81.7	61.3	61.3	61.3	61.3	61.3	61.3	61.3	61.3	61.3	61.3	61.3	61.3	61.3	61.3	61.3	61.3	61.3	61.3	81.7	1267	
"	2	211	117	117	235	235	117	117	211													1361	
"	3	235																				235	2863

Note: Weights are in kips (1 kip = 4.448 kN)

Table 3-2 - Response Spectral Acceleration Values of El Centro Earthquake (5 % Damping)

Frequency(hz)	Period (sec)	S_a (g's)
0.1	10.000	0.015
0.2	5.000	0.019
0.3	3.333	0.074
0.4	2.500	0.165
0.5	2.000	0.185
0.6	1.667	0.16
0.7	1.429	0.164
0.8	1.250	0.28
0.9	1.111	0.363
1	1.000	0.484
1.1	0.909	0.552
1.2	0.833	0.515
1.3	0.769	0.502
1.4	0.714	0.602
1.5	0.667	0.713
1.6	0.625	0.823
1.7	0.588	0.87
1.8	0.556	0.825
1.9	0.526	0.831
2	0.500	0.75
2.1	0.476	0.756
2.2	0.455	0.847
2.3	0.435	0.632
2.4	0.417	0.572
2.5	0.400	0.548
2.6	0.385	0.623
2.7	0.370	0.698
2.8	0.357	0.61
2.9	0.345	0.615
3	0.333	0.674
3.15	0.317	0.66
3.3	0.303	0.683
3.45	0.290	0.723
3.6	0.278	0.756
3.8	0.263	0.877
4	0.250	0.915
4.2	0.238	0.738
4.4	0.227	0.695
4.6	0.217	0.668
4.8	0.208	0.677
5	0.200	0.645

Table 3-2 - Response Spectral Acceleration Values of El Centro Earthquake (5 % Damping) (Continued)

Frequency(hz)	Period (sec)	S_a (g's)
5.25	0.190	0.65
5.5	0.182	0.714
5.75	0.174	0.717
6	0.167	0.679
6.25	0.160	0.535
6.5	0.154	0.524
6.75	0.148	0.592
7	0.143	0.639
7.25	0.138	0.739
7.5	0.133	0.745
7.75	0.129	0.765
8	0.125	0.685
8.5	0.118	0.608
9	0.111	0.545
9.5	0.105	0.563
10	0.100	0.568
10.5	0.095	0.494
11	0.091	0.51
11.5	0.087	0.555
12	0.083	0.59
12.5	0.080	0.578
13	0.077	0.488
13.5	0.074	0.451
14	0.071	0.438
14.5	0.069	0.441
15	0.067	0.497
16	0.063	0.491
17	0.059	0.413
18	0.056	0.414
20	0.050	0.394
22	0.045	0.348
24	0.042	0.343
Max S_a		0.915

Table 3-3 - Floor Drift Result from Nonlinear Time History Analyses

	Percentage Magnitude of El Centro Earthquake						
% of El Centro	70%	71.26%	71.55%	71.69%	71.84%	73.28%	75%
Peak Acceleration	0.244g	0.248g	0.249g	0.2495g	0.25g	0.255g	0.261g
	Floor Drift Ratio (%)						
4th Floor	0.68	0.69	0.69	0.83	0.86	0.81	0.78
3rd Floor	0.66	0.7	0.67	0.82	0.89	0.83	0.8
2nd Floor	0.59	0.67	0.6	0.65	0.83	0.82	0.74
1st Floor	0.3	0.5	0.49	0.54	0.51	0.51	0.58

Control

Table 3-4 - Dynamic Characteristics of the Shear Wall Model

Mode No	Frequency (Hz)	Period (SEC)	Modal Participation Factor	Modal Weight (weight units)	Relative Modal Weight (%)
1	1.82	0.55	4.1133	6534.20	68.87
2	7.43	0.13	2.4544	2326.58	24.52
3	14.89	0.07	1.2164	571.40	6.02
4	22.41	0.04	0.3809	56.02	0.59

Table 3-5 - Digitized Values of the Load Deflection Curve for the Uniform Loading Case

Step No.	Base Shear Coefficient	Roof Drift Ratio (%)	Base Shear (kips)	Roof Displ. (inches)
1	0.0023	0.0018	21.82	0.010
2	0.0045	0.0035	42.70	0.020
3	0.0068	0.0053	64.52	0.031
4	0.009	0.0071	85.39	0.041
5	0.0113	0.0089	107.22	0.051
6	0.0135	0.0106	128.09	0.061
7	0.0158	0.0124	149.91	0.071
8	0.018	0.0142	170.79	0.082
9	0.0203	0.016	192.61	0.092
10	0.0225	0.0177	213.48	0.102
11	0.0248	0.0195	235.31	0.112
12	0.0271	0.0213	257.13	0.123
13	0.0293	0.023	278.00	0.132
14	0.0316	0.0248	299.83	0.143
15	0.0338	0.0266	320.70	0.153
16	0.0361	0.0284	342.52	0.164
17	0.0383	0.0301	363.40	0.173
18	0.0406	0.0319	385.22	0.184
19	0.0428	0.0337	406.09	0.194
20	0.0451	0.0354	427.92	0.204
21	0.0474	0.0372	449.74	0.214
22	0.0496	0.039	470.61	0.225
23	0.0519	0.0408	492.44	0.235
24	0.0541	0.0425	513.31	0.245
25	0.0564	0.0443	535.13	0.255
26	0.0586	0.0461	556.01	0.266
27	0.0609	0.0479	577.83	0.276
28	0.0631	0.0496	598.71	0.286
29	0.0654	0.0514	620.53	0.296
30	0.0677	0.0532	642.35	0.306
31	0.0699	0.055	663.23	0.317
32	0.0722	0.0568	685.05	0.327
33	0.0745	0.0586	706.87	0.338
34	0.0768	0.0603	728.69	0.347
35	0.0791	0.0621	750.52	0.358
36	0.0814	0.0639	772.34	0.368
37	0.0836	0.0657	793.21	0.378

Table 3-5 - Digitized Values of the Load Deflection Curve for the Uniform Loading Case (Continued)

Step No.	Base Shear Coefficient	Roof Drift Ratio (%)	Base Shear (kips)	Roof Displ. (inches)
38	0.0859	0.0675	815.04	0.389
39	0.0882	0.0693	836.86	0.399
40	0.0905	0.0711	858.68	0.410
41	0.0928	0.0729	880.50	0.420
42	0.0951	0.0747	902.33	0.430
43	0.0941	0.0765	892.84	0.441
44	0.0964	0.0783	914.66	0.451
45	0.0987	0.0803	936.49	0.463
46	0.1009	0.0825	957.36	0.475
47	0.1031	0.0848	978.23	0.488
48	0.1053	0.0872	999.11	0.502
49	0.1075	0.0897	1019.98	0.517
50	0.1097	0.0923	1040.86	0.532
51	0.1118	0.0949	1060.78	0.547
52	0.114	0.0977	1081.65	0.563
53	0.1161	0.1004	1101.58	0.578
54	0.1182	0.1032	1121.51	0.594
55	0.1204	0.1061	1142.38	0.611
56	0.1225	0.109	1162.30	0.628
57	0.1246	0.1119	1182.23	0.645
58	0.1272	0.1152	1206.90	0.664
59	0.1293	0.1182	1226.82	0.681
60	0.1314	0.1213	1246.75	0.699
61	0.1335	0.1244	1266.67	0.717
62	0.1356	0.1276	1286.60	0.735
63	0.1377	0.1309	1306.53	0.754
64	0.1398	0.1341	1326.45	0.772
65	0.1419	0.1374	1346.38	0.791
66	0.144	0.1408	1366.30	0.811
67	0.1445	0.1442	1371.04	0.831
68	0.1464	0.1494	1389.07	0.861
69	0.1488	0.155	1411.84	0.893
70	0.1508	0.1606	1430.82	0.925
71	0.1529	0.1661	1450.75	0.957
72	0.155	0.1718	1470.67	0.990
73	0.157	0.1776	1489.65	1.023
74	0.1592	0.1835	1510.52	1.057

Table 3-5 - Digitized Values of the Load Deflection Curve for the Uniform Loading Case (Continued)

Step No.	Base Shear Coefficient	Roof Drift Ratio (%)	Base Shear (kips)	Roof Displ. (inches)
75	0.1613	0.1894	1530.45	1.091
76	0.1634	0.1953	1550.37	1.125
77	0.1655	0.2015	1570.30	1.161
78	0.1676	0.2077	1590.22	1.196
79	0.1697	0.214	1610.15	1.233
80	0.1719	0.2205	1631.02	1.270
81	0.174	0.227	1650.95	1.308
82	0.1761	0.2337	1670.87	1.346
83	0.1783	0.2407	1691.75	1.386
84	0.1803	0.2477	1710.72	1.427
85	0.1825	0.2548	1731.60	1.468
86	0.1845	0.2621	1750.57	1.510
87	0.1867	0.2695	1771.45	1.552
88	0.1888	0.2771	1791.37	1.596
89	0.1909	0.2847	1811.30	1.640
90	0.193	0.2927	1831.22	1.686
91	0.1952	0.3012	1852.10	1.735
92	0.1974	0.3103	1872.97	1.787
93	0.1996	0.3195	1893.84	1.840
94	0.2021	0.3299	1917.57	1.900
95	0.2044	0.3402	1939.39	1.960
96	0.2068	0.3506	1962.16	2.019
97	0.2091	0.3611	1983.98	2.080
98	0.2114	0.3718	2005.81	2.142
99	0.2139	0.383	2029.53	2.206
100	0.2163	0.3942	2052.30	2.271
101	0.2187	0.4055	2075.07	2.336
102	0.2211	0.4171	2097.84	2.402
103	0.2245	0.4312	2130.10	2.484
104	0.2271	0.4438	2154.77	2.556
105	0.2296	0.4565	2178.49	2.629
106	0.232	0.4691	2201.26	2.702
107	0.2344	0.482	2224.03	2.776
108	0.2368	0.4957	2246.81	2.855
109	0.2393	0.5101	2270.53	2.938
110	0.2417	0.5246	2293.30	3.022
111	0.244	0.5397	2315.12	3.109

Table 3-5 - Digitized Values of the Load Deflection Curve for the Uniform Loading Case (Continued)

Step No.	Base Shear Coefficient	Roof Drift Ratio (%)	Base Shear (kips)	Roof Displ. (inches)
112	0.2466	0.5567	2339.79	3.207
113	0.249	0.5752	2362.56	3.313
114	0.2518	0.5971	2389.13	3.439
115	0.2544	0.6213	2413.80	3.579
116	0.2571	0.6458	2439.42	3.720
117	0.2597	0.6719	2464.09	3.870
118	0.2624	0.6998	2489.70	4.031
119	0.2649	0.731	2513.42	4.211
120	0.2676	0.7646	2539.04	4.404
121	0.2703	0.8006	2564.66	4.611
122	0.273	0.838	2590.28	4.827
123	0.2756	0.8785	2614.95	5.060
124	0.3125	1.1872	2965.06	6.838

Note: 1 kip = 4.448 kN, 1 in.= 25.4 mm

Table 3-6 - Floor Drifts for the Uniform Loading Case

	First Floor		Second Floor		Third Floor		Fourth Floor	
Step No.	Floor Drift (inches)	Drift Ratio (%)	Floor Drift (inches)	Drift Ratio (%)	Floor Drift (inches)	Drift Ratio (%)	Floor Drift (inches)	Drift Ratio (%)
1	0.002	0.001	0.003	0.002	0.003	0.002	0.003	0.002
2	0.003	0.002	0.005	0.004	0.006	0.004	0.006	0.004
3	0.005	0.003	0.008	0.005	0.009	0.006	0.009	0.006
4	0.006	0.004	0.011	0.007	0.012	0.008	0.012	0.008
5	0.008	0.005	0.013	0.009	0.015	0.011	0.015	0.010
6	0.009	0.006	0.016	0.011	0.018	0.013	0.018	0.013
7	0.011	0.007	0.018	0.013	0.021	0.015	0.021	0.015
8	0.012	0.008	0.021	0.015	0.024	0.017	0.024	0.017
9	0.014	0.009	0.024	0.016	0.027	0.019	0.027	0.019
10	0.015	0.011	0.026	0.018	0.031	0.021	0.030	0.021
11	0.017	0.012	0.029	0.020	0.034	0.023	0.033	0.023
12	0.018	0.013	0.032	0.022	0.037	0.025	0.036	0.025
13	0.020	0.014	0.034	0.024	0.040	0.028	0.039	0.027
14	0.021	0.015	0.037	0.026	0.043	0.030	0.042	0.029
15	0.023	0.016	0.039	0.027	0.046	0.032	0.045	0.031
16	0.024	0.017	0.042	0.029	0.049	0.034	0.048	0.033
17	0.026	0.018	0.045	0.031	0.052	0.036	0.051	0.036
18	0.027	0.019	0.047	0.033	0.055	0.038	0.054	0.038
19	0.029	0.020	0.050	0.035	0.058	0.040	0.057	0.040
20	0.030	0.021	0.053	0.037	0.061	0.042	0.060	0.042
21	0.032	0.022	0.055	0.038	0.064	0.045	0.063	0.044
22	0.033	0.023	0.058	0.040	0.067	0.047	0.066	0.046
23	0.035	0.024	0.060	0.042	0.070	0.049	0.069	0.048
24	0.036	0.025	0.063	0.044	0.073	0.051	0.072	0.050
25	0.038	0.026	0.066	0.046	0.076	0.053	0.075	0.052
26	0.039	0.027	0.068	0.047	0.079	0.055	0.078	0.054
27	0.041	0.028	0.071	0.049	0.083	0.057	0.081	0.056
28	0.042	0.029	0.074	0.051	0.086	0.059	0.084	0.059
29	0.044	0.031	0.076	0.053	0.089	0.062	0.087	0.061
30	0.045	0.032	0.079	0.055	0.092	0.064	0.090	0.063
31	0.047	0.033	0.082	0.057	0.095	0.066	0.093	0.065
32	0.049	0.034	0.084	0.059	0.098	0.068	0.096	0.067
33	0.050	0.035	0.087	0.060	0.101	0.070	0.099	0.069
34	0.052	0.036	0.090	0.062	0.104	0.072	0.102	0.071
35	0.053	0.037	0.092	0.064	0.107	0.074	0.106	0.073
36	0.055	0.038	0.095	0.066	0.110	0.077	0.109	0.075

Table 3-6 - Floor Drifts for the Uniform Loading Case
(Continued)

	First Floor		Second Floor		Third Floor		Fourth Floor	
Step No.	Floor Drift (inches)	Drift Ratio (%)	Floor Drift (inches)	Drift Ratio (%)	Floor Drift (inches)	Drift Ratio (%)	Floor Drift (inches)	Drift Ratio (%)
37	0.056	0.039	0.098	0.068	0.113	0.079	0.112	0.077
38	0.058	0.040	0.100	0.070	0.116	0.081	0.115	0.080
39	0.059	0.041	0.103	0.071	0.119	0.083	0.118	0.082
40	0.061	0.042	0.106	0.073	0.123	0.085	0.121	0.084
41	0.062	0.043	0.108	0.075	0.126	0.087	0.124	0.086
42	0.064	0.044	0.111	0.077	0.129	0.089	0.127	0.088
43	0.065	0.045	0.114	0.079	0.132	0.092	0.130	0.090
44	0.067	0.047	0.116	0.081	0.135	0.094	0.133	0.092
45	0.069	0.048	0.119	0.083	0.138	0.096	0.136	0.095
46	0.071	0.049	0.123	0.085	0.142	0.099	0.140	0.097
47	0.074	0.051	0.126	0.087	0.146	0.101	0.143	0.100
48	0.076	0.053	0.130	0.090	0.149	0.104	0.147	0.102
49	0.079	0.055	0.133	0.093	0.153	0.107	0.151	0.105
50	0.082	0.057	0.137	0.095	0.158	0.109	0.155	0.108
51	0.085	0.059	0.141	0.098	0.162	0.112	0.159	0.110
52	0.088	0.061	0.145	0.101	0.166	0.115	0.163	0.113
53	0.092	0.064	0.149	0.104	0.170	0.118	0.167	0.116
54	0.095	0.066	0.154	0.107	0.175	0.121	0.171	0.119
55	0.098	0.068	0.158	0.110	0.179	0.125	0.176	0.122
56	0.102	0.071	0.162	0.113	0.184	0.128	0.180	0.125
57	0.105	0.073	0.167	0.116	0.188	0.131	0.184	0.128
58	0.110	0.076	0.171	0.119	0.193	0.134	0.189	0.131
59	0.114	0.079	0.176	0.122	0.198	0.137	0.193	0.134
60	0.118	0.082	0.180	0.125	0.202	0.141	0.198	0.137
61	0.123	0.085	0.185	0.128	0.207	0.144	0.202	0.140
62	0.127	0.088	0.189	0.132	0.212	0.147	0.207	0.144
63	0.132	0.091	0.194	0.135	0.217	0.151	0.211	0.147
64	0.136	0.094	0.199	0.138	0.222	0.154	0.216	0.150
65	0.141	0.098	0.204	0.141	0.227	0.157	0.221	0.153
66	0.145	0.101	0.209	0.145	0.232	0.161	0.226	0.157
67	0.150	0.104	0.214	0.148	0.237	0.164	0.230	0.160
68	0.157	0.109	0.222	0.154	0.244	0.170	0.238	0.165
69	0.165	0.115	0.230	0.160	0.252	0.175	0.245	0.170
70	0.173	0.120	0.238	0.166	0.260	0.181	0.253	0.175
71	0.181	0.126	0.247	0.171	0.268	0.186	0.260	0.181
72	0.190	0.132	0.256	0.178	0.277	0.192	0.268	0.186

Table 3-6 - Floor Drifts for the Uniform Loading Case
(Continued)

	First Floor		Second Floor		Third Floor		Fourth Floor	
Step No.	Floor Drift (inches)	Drift Ratio (%)	Floor Drift (inches)	Drift Ratio (%)	Floor Drift (inches)	Drift Ratio (%)	Floor Drift (inches)	Drift Ratio (%)
73	0.198	0.137	0.264	0.184	0.285	0.198	0.276	0.192
74	0.206	0.143	0.273	0.190	0.294	0.204	0.284	0.197
75	0.215	0.149	0.282	0.196	0.302	0.210	0.292	0.203
76	0.223	0.155	0.291	0.202	0.311	0.216	0.300	0.208
77	0.232	0.161	0.301	0.209	0.320	0.222	0.309	0.214
78	0.241	0.167	0.310	0.215	0.329	0.228	0.317	0.220
79	0.249	0.173	0.319	0.222	0.338	0.235	0.326	0.226
80	0.258	0.179	0.329	0.229	0.347	0.241	0.335	0.233
81	0.267	0.186	0.339	0.236	0.357	0.248	0.344	0.239
82	0.277	0.192	0.349	0.243	0.367	0.255	0.353	0.245
83	0.287	0.199	0.360	0.250	0.377	0.262	0.363	0.252
84	0.296	0.206	0.371	0.257	0.387	0.269	0.373	0.259
85	0.306	0.213	0.381	0.265	0.398	0.276	0.383	0.266
86	0.316	0.220	0.392	0.272	0.408	0.283	0.393	0.273
87	0.327	0.227	0.404	0.280	0.419	0.291	0.403	0.280
88	0.337	0.234	0.415	0.288	0.430	0.299	0.414	0.287
89	0.348	0.241	0.427	0.296	0.441	0.306	0.424	0.295
90	0.359	0.249	0.439	0.305	0.453	0.314	0.436	0.303
91	0.370	0.257	0.452	0.314	0.465	0.323	0.448	0.311
92	0.383	0.266	0.465	0.323	0.479	0.333	0.460	0.320
93	0.395	0.274	0.479	0.333	0.492	0.342	0.473	0.329
94	0.409	0.284	0.495	0.344	0.508	0.352	0.488	0.339
95	0.423	0.294	0.511	0.355	0.523	0.363	0.503	0.349
96	0.437	0.304	0.527	0.366	0.538	0.374	0.517	0.359
97	0.452	0.314	0.543	0.377	0.553	0.384	0.532	0.370
98	0.466	0.324	0.559	0.388	0.569	0.395	0.548	0.380
99	0.481	0.334	0.576	0.400	0.586	0.407	0.563	0.391
100	0.496	0.345	0.593	0.412	0.602	0.418	0.579	0.402
101	0.512	0.355	0.610	0.424	0.619	0.430	0.595	0.413
102	0.527	0.366	0.627	0.436	0.636	0.442	0.612	0.425
103	0.555	0.385	0.646	0.449	0.654	0.454	0.629	0.437
104	0.577	0.401	0.663	0.461	0.671	0.466	0.645	0.448
105	0.599	0.416	0.681	0.473	0.688	0.477	0.662	0.460
106	0.621	0.431	0.698	0.485	0.705	0.489	0.678	0.471
107	0.643	0.447	0.716	0.497	0.722	0.501	0.695	0.483
108	0.667	0.463	0.735	0.510	0.740	0.514	0.713	0.495

Table 3-6 - Floor Drifts for the Uniform Loading Case
(Continued)

	First Floor		Second Floor		Third Floor		Fourth Floor	
Step No.	Floor Drift (inches)	Drift Ratio (%)	Floor Drift (inches)	Drift Ratio (%)	Floor Drift (inches)	Drift Ratio (%)	Floor Drift (inches)	Drift Ratio (%)
109	0.692	0.480	0.754	0.524	0.760	0.527	0.732	0.509
110	0.717	0.498	0.774	0.538	0.779	0.541	0.751	0.522
111	0.743	0.516	0.795	0.552	0.799	0.555	0.771	0.536
112	0.776	0.539	0.817	0.567	0.821	0.570	0.793	0.551
113	0.812	0.564	0.841	0.584	0.845	0.586	0.816	0.567
114	0.855	0.594	0.869	0.603	0.872	0.606	0.843	0.586
115	0.903	0.627	0.900	0.625	0.903	0.627	0.873	0.606
116	0.951	0.660	0.932	0.647	0.934	0.648	0.904	0.628
117	1.001	0.695	0.966	0.671	0.967	0.672	0.937	0.651
118	1.054	0.732	1.002	0.696	1.003	0.696	0.972	0.675
119	1.112	0.773	1.043	0.724	1.043	0.724	1.012	0.703
120	1.175	0.816	1.087	0.755	1.087	0.755	1.056	0.733
121	1.241	0.861	1.135	0.788	1.134	0.787	1.103	0.766
122	1.308	0.908	1.184	0.822	1.183	0.821	1.152	0.800
123	1.379	0.958	1.239	0.860	1.237	0.859	1.206	0.837
124	2.063	1.433	1.610	1.118	1.600	1.111	1.566	1.087

Note: 1 in. = 25.4 mm

Table 3-7 – Floor Drift Comparison Nonlinear Time History Analysis and Two Pushover Analyses

	Nonlinear T.H.		Uniform Pattern		Modal Pattern	
Roof Disp.(in)	4.75		4.38		4.36	
Roof Drift (%)	0.82		0.76		0.76	
	Floor Drift (inches)	Drift Ratio (%)	Floor Drift (inches)	Drift Ratio (%)	Floor Drift (inches)	Drift Ratio (%)
Fourth Floor	1.40	0.97	1.05	0.73	1.15	0.81
Third Floor	1.41	0.98	1.08	0.75	1.18	0.82
Second Floor	1.41	0.98	1.08	0.75	1.14	0.79
First Floor	0.77	0.54	1.17	0.81	0.88	0.61

Notes:
1. Modal Pattern case controls
2. FEMA allowable drift ratio is 0.75%, thus structure cannot withstand El Centro
3. 1 in. = 25.4 mm

Table 3-8 - Digitized Values of the Load Deflection Curve for the Modal Loading Case

Step No.	Base Shear Coefficient	Roof Drift Ratio (%)	Base Shear (kips)	Roof Displ. (inches)
1	0.0022	0.0023	20.87	0.013
2	0.0044	0.0046	41.75	0.026
3	0.0066	0.0069	62.62	0.040
4	0.0088	0.0092	83.50	0.053
5	0.011	0.0115	104.37	0.066
6	0.0132	0.0139	125.24	0.080
7	0.0154	0.0162	146.12	0.093
8	0.0176	0.0185	166.99	0.107
9	0.0198	0.0208	187.87	0.120
10	0.0221	0.0231	209.69	0.133
11	0.0243	0.0254	230.56	0.146
12	0.0265	0.0277	251.44	0.160
13	0.0287	0.03	272.31	0.173
14	0.0309	0.0323	293.19	0.186
15	0.0331	0.0346	314.06	0.199
16	0.0353	0.0369	334.93	0.213
17	0.0375	0.0392	355.81	0.226
18	0.0397	0.0416	376.68	0.240
19	0.0419	0.0439	397.56	0.253
20	0.0441	0.0462	418.43	0.266
21	0.0463	0.0485	439.30	0.279
22	0.0485	0.0508	460.18	0.293
23	0.0507	0.0531	481.05	0.306
24	0.053	0.0554	502.87	0.319
25	0.0552	0.0577	523.75	0.332
26	0.0574	0.0601	544.62	0.346
27	0.0596	0.0624	565.50	0.359
28	0.0619	0.0647	587.32	0.373
29	0.0641	0.0671	608.19	0.386
30	0.0664	0.0694	630.02	0.400
31	0.0686	0.0717	650.89	0.413
32	0.0709	0.0741	672.71	0.427
33	0.0731	0.0764	693.59	0.440
34	0.0754	0.0787	715.41	0.453
35	0.0776	0.0811	736.28	0.467
36	0.0799	0.0834	758.11	0.480
37	0.0791	0.0858	750.52	0.494
38	0.0813	0.0882	771.39	0.508
39	0.0835	0.0909	792.26	0.524
40	0.0857	0.0938	813.14	0.540

Table 3-8 - Digitized Values of the Load Deflection Curve for the Modal Loading Case (Continued)

Step No.	Base Shear Coefficient	Roof Drift Ratio (%)	Base Shear (kips)	Roof Displ. (inches)
41	0.0878	0.0969	833.06	0.558
42	0.0899	0.1001	852.99	0.577
43	0.092	0.1035	872.91	0.596
44	0.0941	0.1069	892.84	0.616
45	0.0961	0.1105	911.82	0.636
46	0.0982	0.1141	931.74	0.657
47	0.1002	0.1178	950.72	0.679
48	0.1023	0.1216	970.64	0.700
49	0.1043	0.1254	989.62	0.722
50	0.1063	0.1292	1008.60	0.744
51	0.1084	0.1332	1028.52	0.767
52	0.1104	0.1373	1047.50	0.791
53	0.1124	0.1413	1066.47	0.814
54	0.1145	0.1455	1086.40	0.838
55	0.1166	0.1497	1106.32	0.862
56	0.1186	0.1541	1125.30	0.888
57	0.1207	0.1584	1145.23	0.912
58	0.1217	0.1629	1154.71	0.938
59	0.1236	0.1697	1172.74	0.977
60	0.1256	0.1768	1191.72	1.018
61	0.1276	0.184	1210.69	1.060
62	0.1296	0.1915	1229.67	1.103
63	0.1316	0.1991	1248.65	1.147
64	0.1336	0.2068	1267.62	1.191
65	0.1357	0.2145	1287.55	1.236
66	0.1377	0.2227	1306.53	1.283
67	0.1397	0.2309	1325.50	1.330
68	0.1418	0.2392	1345.43	1.378
69	0.1438	0.2478	1364.40	1.427
70	0.1458	0.2567	1383.38	1.479
71	0.1483	0.2662	1407.10	1.533
72	0.1503	0.2755	1426.08	1.587
73	0.1523	0.285	1445.05	1.642
74	0.1542	0.2948	1463.08	1.698
75	0.1564	0.3053	1483.95	1.759
76	0.1585	0.3165	1503.88	1.823
77	0.1606	0.328	1523.80	1.889
78	0.1628	0.34	1544.68	1.958
79	0.1651	0.353	1566.50	2.033
80	0.1675	0.3662	1589.27	2.109
81	0.1698	0.3795	1611.10	2.186

Table 3-8 - Digitized Values of the Load Deflection Curve for the Modal Loading Case (Continued)

Step No.	Base Shear Coefficient	Roof Drift Ratio (%)	Base Shear (kips)	Roof Displ. (inches)
82	0.1721	0.3931	1632.92	2.264
83	0.1745	0.4071	1655.69	2.345
84	0.1768	0.4214	1677.51	2.427
85	0.1792	0.4361	1700.29	2.512
86	0.1815	0.451	1722.11	2.598
87	0.1839	0.4674	1744.88	2.692
88	0.1863	0.4836	1767.65	2.786
89	0.1886	0.5007	1789.47	2.884
90	0.191	0.5178	1812.25	2.983
91	0.1934	0.5357	1835.02	3.086
92	0.1957	0.5546	1856.84	3.194
93	0.1981	0.5745	1879.61	3.309
94	0.2004	0.5957	1901.44	3.431
95	0.2027	0.6189	1923.26	3.565
96	0.2048	0.6432	1943.18	3.705
97	0.2071	0.671	1965.01	3.865
98	0.2095	0.7031	1987.78	4.050
99	0.2118	0.7376	2009.60	4.249
100	0.2143	0.775	2033.32	4.464
101	0.2165	0.8191	2054.20	4.718
102	0.219	0.8717	2077.92	5.021
103	0.2207	0.9233	2094.05	5.318
104	0.2236	0.9837	2121.56	5.666
105	0.2261	1.0444	2145.28	6.016
106	0.2277	1.106	2160.46	6.371
107	0.2298	1.1776	2180.39	6.783
108	0.232	1.2642	2201.26	7.282
109	0.2351	1.3688	2230.68	7.884
110	0.2358	1.4488	2237.32	8.345
111	0.239	1.5572	2267.68	8.969
112	0.2414	1.6654	2290.45	9.593
113	0.2467	1.8085	2340.74	10.417
114	0.2495	1.9254	2367.31	11.090
115	0.2529	2.0395	2399.57	11.748
116	0.2556	2.1594	2425.18	12.438
117	0.2581	2.2784	2448.90	13.124
118	0.2606	2.3974	2472.62	13.809
119	0.2631	2.5166	2496.35	14.496

Note: 1 kip = 4.448 kN, 1 in. = 25.4 mm

Table 3-9 - Floor Drifts for the Modal Loading Case

	First Floor		Second Floor		Third Floor		Fourth Floor	
Step No.	Floor Drift (inches)	Drift Ratio (%)	Floor Drift (inches)	Drift Ratio (%)	Floor Drift (inches)	Drift Ratio (%)	Floor Drift (inches)	Drift Ratio (%)
1	0.002	0.001	0.003	0.002	0.004	0.003	0.004	0.003
2	0.003	0.002	0.007	0.005	0.008	0.006	0.008	0.006
3	0.005	0.004	0.010	0.007	0.012	0.009	0.012	0.009
4	0.007	0.005	0.013	0.009	0.016	0.011	0.017	0.012
5	0.009	0.006	0.017	0.012	0.020	0.014	0.021	0.014
6	0.010	0.007	0.020	0.014	0.025	0.017	0.025	0.017
7	0.012	0.008	0.023	0.016	0.029	0.020	0.029	0.020
8	0.014	0.010	0.027	0.018	0.033	0.023	0.033	0.023
9	0.015	0.011	0.030	0.021	0.037	0.026	0.037	0.026
10	0.017	0.012	0.033	0.023	0.041	0.028	0.042	0.029
11	0.019	0.013	0.037	0.025	0.045	0.031	0.046	0.032
12	0.021	0.014	0.040	0.028	0.049	0.034	0.050	0.035
13	0.022	0.016	0.043	0.030	0.053	0.037	0.054	0.038
14	0.024	0.017	0.047	0.032	0.057	0.040	0.058	0.040
15	0.026	0.018	0.050	0.035	0.061	0.043	0.062	0.043
16	0.028	0.019	0.053	0.037	0.065	0.045	0.067	0.046
17	0.029	0.020	0.057	0.039	0.069	0.048	0.071	0.049
18	0.031	0.022	0.060	0.042	0.074	0.051	0.075	0.052
19	0.033	0.023	0.063	0.044	0.078	0.054	0.079	0.055
20	0.034	0.024	0.067	0.046	0.082	0.057	0.083	0.058
21	0.036	0.025	0.070	0.049	0.086	0.060	0.087	0.061
22	0.038	0.026	0.073	0.051	0.090	0.062	0.092	0.064
23	0.040	0.027	0.077	0.053	0.094	0.065	0.096	0.067
24	0.041	0.029	0.080	0.055	0.098	0.068	0.100	0.069
25	0.043	0.030	0.083	0.058	0.102	0.071	0.104	0.072
26	0.045	0.031	0.087	0.060	0.106	0.074	0.108	0.075
27	0.047	0.032	0.090	0.062	0.110	0.077	0.113	0.078
28	0.048	0.034	0.093	0.065	0.115	0.080	0.117	0.081
29	0.050	0.035	0.097	0.067	0.119	0.082	0.121	0.084
30	0.052	0.036	0.100	0.069	0.123	0.085	0.125	0.087
31	0.054	0.037	0.103	0.072	0.127	0.088	0.129	0.090
32	0.055	0.038	0.107	0.074	0.131	0.091	0.134	0.093
33	0.057	0.040	0.110	0.077	0.135	0.094	0.138	0.096
34	0.059	0.041	0.114	0.079	0.139	0.097	0.142	0.099
35	0.061	0.042	0.117	0.081	0.143	0.100	0.146	0.102
36	0.062	0.043	0.120	0.084	0.148	0.102	0.150	0.104

Table 3-9 - Floor Drifts for the Modal Loading Case
(Continued)

	First Floor		Second Floor		Third Floor		Fourth Floor	
Step No.	Floor Drift (inches)	Drift Ratio (%)	Floor Drift (inches)	Drift Ratio (%)	Floor Drift (inches)	Drift Ratio (%)	Floor Drift (inches)	Drift Ratio (%)
37	0.064	0.044	0.124	0.086	0.152	0.105	0.155	0.107
38	0.066	0.046	0.127	0.088	0.156	0.108	0.159	0.110
39	0.068	0.047	0.131	0.091	0.161	0.111	0.163	0.114
40	0.071	0.049	0.135	0.094	0.165	0.115	0.168	0.117
41	0.074	0.052	0.140	0.097	0.171	0.118	0.173	0.120
42	0.078	0.054	0.145	0.100	0.176	0.122	0.179	0.124
43	0.081	0.056	0.150	0.104	0.181	0.126	0.184	0.128
44	0.085	0.059	0.155	0.107	0.187	0.130	0.190	0.132
45	0.089	0.062	0.160	0.111	0.193	0.134	0.195	0.136
46	0.093	0.064	0.165	0.115	0.198	0.138	0.201	0.140
47	0.097	0.067	0.171	0.119	0.204	0.142	0.207	0.144
48	0.101	0.070	0.176	0.122	0.210	0.146	0.213	0.148
49	0.105	0.073	0.182	0.126	0.216	0.150	0.219	0.152
50	0.109	0.076	0.188	0.130	0.223	0.155	0.225	0.156
51	0.114	0.079	0.194	0.134	0.229	0.159	0.231	0.160
52	0.118	0.082	0.200	0.139	0.235	0.163	0.237	0.165
53	0.123	0.085	0.206	0.143	0.242	0.168	0.244	0.169
54	0.127	0.088	0.212	0.147	0.248	0.173	0.250	0.174
55	0.132	0.092	0.218	0.152	0.255	0.177	0.257	0.178
56	0.137	0.095	0.225	0.156	0.262	0.182	0.264	0.183
57	0.142	0.098	0.231	0.161	0.269	0.187	0.270	0.188
58	0.147	0.102	0.238	0.165	0.276	0.192	0.277	0.193
59	0.155	0.108	0.248	0.173	0.286	0.199	0.287	0.199
60	0.164	0.114	0.259	0.180	0.297	0.206	0.297	0.207
61	0.174	0.121	0.270	0.188	0.308	0.214	0.308	0.214
62	0.183	0.127	0.282	0.196	0.319	0.222	0.319	0.221
63	0.193	0.134	0.293	0.204	0.331	0.230	0.330	0.229
64	0.202	0.141	0.305	0.212	0.342	0.238	0.341	0.237
65	0.212	0.147	0.317	0.220	0.354	0.246	0.352	0.245
66	0.223	0.155	0.330	0.229	0.366	0.254	0.364	0.253
67	0.233	0.162	0.342	0.238	0.379	0.263	0.376	0.261
68	0.243	0.169	0.355	0.246	0.391	0.272	0.389	0.270
69	0.254	0.176	0.368	0.256	0.404	0.281	0.401	0.279
70	0.265	0.184	0.382	0.265	0.418	0.290	0.414	0.288
71	0.277	0.193	0.396	0.275	0.432	0.300	0.428	0.297
72	0.289	0.201	0.410	0.285	0.446	0.310	0.442	0.307

Table 3-9 - Floor Drifts for the Modal Loading Case
(Continued)

	First Floor		Second Floor		Third Floor		Fourth Floor	
Step No.	Floor Drift (inches)	Drift Ratio (%)	Floor Drift (inches)	Drift Ratio (%)	Floor Drift (inches)	Drift Ratio (%)	Floor Drift (inches)	Drift Ratio (%)
73	0.301	0.209	0.425	0.295	0.460	0.320	0.456	0.316
74	0.313	0.218	0.439	0.305	0.475	0.330	0.470	0.326
75	0.326	0.227	0.456	0.316	0.491	0.341	0.485	0.337
76	0.340	0.236	0.473	0.328	0.508	0.353	0.502	0.349
77	0.355	0.246	0.490	0.340	0.525	0.365	0.519	0.360
78	0.370	0.257	0.508	0.353	0.544	0.377	0.537	0.373
79	0.386	0.268	0.528	0.367	0.563	0.391	0.556	0.386
80	0.403	0.280	0.548	0.381	0.583	0.405	0.575	0.399
81	0.420	0.291	0.569	0.395	0.603	0.419	0.595	0.413
82	0.437	0.303	0.590	0.409	0.623	0.433	0.615	0.427
83	0.454	0.316	0.611	0.424	0.645	0.448	0.635	0.441
84	0.472	0.328	0.633	0.439	0.666	0.463	0.656	0.456
85	0.491	0.341	0.655	0.455	0.688	0.478	0.678	0.471
86	0.510	0.354	0.678	0.471	0.711	0.494	0.700	0.486
87	0.530	0.368	0.703	0.488	0.735	0.511	0.724	0.503
88	0.550	0.382	0.727	0.505	0.760	0.528	0.749	0.520
89	0.571	0.397	0.753	0.523	0.786	0.546	0.774	0.538
90	0.592	0.411	0.779	0.541	0.812	0.564	0.800	0.555
91	0.614	0.426	0.806	0.560	0.839	0.582	0.827	0.574
92	0.637	0.442	0.835	0.580	0.867	0.602	0.855	0.594
93	0.661	0.459	0.865	0.601	0.898	0.624	0.886	0.615
94	0.686	0.477	0.897	0.623	0.930	0.646	0.918	0.637
95	0.714	0.496	0.933	0.648	0.966	0.671	0.953	0.662
96	0.742	0.515	0.970	0.673	1.003	0.696	0.990	0.688
97	0.775	0.538	1.012	0.703	1.045	0.726	1.033	0.717
98	0.813	0.565	1.061	0.737	1.094	0.760	1.082	0.751
99	0.855	0.593	1.113	0.773	1.147	0.796	1.134	0.788
100	0.899	0.625	1.170	0.813	1.204	0.836	1.191	0.827
101	0.951	0.661	1.237	0.859	1.271	0.883	1.259	0.874
102	1.013	0.704	1.318	0.915	1.351	0.938	1.339	0.930
103	1.072	0.745	1.397	0.970	1.431	0.993	1.419	0.985
104	1.143	0.794	1.489	1.034	1.523	1.057	1.512	1.050
105	1.214	0.843	1.582	1.098	1.615	1.122	1.605	1.114
106	1.284	0.892	1.676	1.164	1.710	1.188	1.700	1.181
107	1.366	0.948	1.786	1.240	1.821	1.264	1.811	1.257
108	1.463	1.016	1.919	1.333	1.955	1.358	1.945	1.351

Table 3-9 - Floor Drifts for the Modal Loading Case
(Continued)

	First Floor		Second Floor		Third Floor		Fourth Floor	
Step No.	Floor Drift (inches)	Drift Ratio (%)	Floor Drift (inches)	Drift Ratio (%)	Floor Drift (inches)	Drift Ratio (%)	Floor Drift (inches)	Drift Ratio (%)
109	1.581	1.098	2.080	1.444	2.117	1.470	2.107	1.463
110	1.667	1.158	2.204	1.530	2.242	1.557	2.233	1.550
111	1.788	1.242	2.370	1.646	2.410	1.674	2.401	1.667
112	1.924	1.336	2.532	1.758	2.573	1.787	2.564	1.781
113	2.127	1.477	2.738	1.901	2.780	1.931	2.771	1.925
114	2.280	1.583	2.911	2.021	2.955	2.052	2.946	2.046
115	2.426	1.684	3.080	2.139	3.125	2.170	3.117	2.164
116	2.576	1.789	3.259	2.263	3.306	2.296	3.297	2.290
117	2.725	1.892	3.437	2.387	3.485	2.420	3.477	2.415
118	2.873	1.995	3.615	2.510	3.665	2.545	3.657	2.539
119	3.021	2.098	3.793	2.634	3.845	2.670	3.837	2.664

Note: 1 in. = 25.4 mm

Table 4-1 - Turbine Building Nonlinear Model Node Coordinates
(Table 2-1 of Ref. 4)

NODE NO.	X-COORDINATE (Ft.)	Y-COORDINATE (Ft.)
1	0.	0.
2	.19	0.
3	19.19	0.
4	19.38	0.
5	38.38	0.
6	38.55	0.
7	55.55	0.
8*	55.55	49.42
9*	55.55	-49.42
10	189.16	49.42
11	189.16	-49.42
12	189.16	0.
13**	322.77	49.42
14**	322.77	-49.42
15	244.16	0.
16	322.77	0.
17	343.77	0.
18	343.98	0.
19	355.98	0.
20	356.10	0.
21	378.10	0.
22	378.32	0.

* Slaved to Node 7
** Slaved to Node 16

Note: 1 ft. = .3048 m

Table 4-2 - Turbine Building Nonlinear Model Nodal Masses
(Table 2-2 of Ref. 4)

NODE NO.	WEIGHT (Kips)	COMMENT
3	1,573	WALL 19 AND FLOOR AT EL 104
5	832	WALL 19 AND FLOOR AT EL 123
7	4,219	WALL 19 AND OPERATING FLOOR
10	2,250	OPERATING FLOOR
11	2,250	OPERATING FLOOR
12	25,000	TURBINE PEDESTAL
16	6,331	WALL 31 AND OPERATING FLOOR*
18	2,130	WALL 31 AND FLOOR AT EL 119
20	2,460	WALL 31 AND FLOOR AT EL 107

Note: 1 kip = 4.448 kN

Table 4-3 - Effective Shear Wall Elastic Shear and Flexural Stiffness Used
(Table 2-3 of Ref. 4)

CONCRETE SHEAR WALL	EFFECTIVE SHEAR STIFFNESS (Kips/Ft.)	EFFECTIVE FLEXURAL STIFFNESS (Kips/Ft.)
WALL 19		
EL 140 - EL 123	1.14×10^6	6.13×10^7
EL 123 - EL 104	1.22×10^6	7.55×10^7
EL 104 - EL 85	2.25×10^6	5.05×10^7
WALL 31		
EL 140 - EL 119	1.71×10^6	24.2×10^7
EL 119 - EL 107	3.10×10^6	99.0×10^7
EL 107 - EL 85	1.60×10^6	16.0×10^7

Note: 1 kip/ft. = 14.59 kN/m

Table 4-4 - Median Capacities of Shear Wall Elements
(Table 2-3 of Ref. 4)

CONCRETE SHEAR WALL	SHEAR CAPACITIES		FLEXURAL CAPACITIES	
	CONCRETE ONLY V_C (Kips)	ULTIMATE V_U (Kips)	YIELD MOMENT M_U (Kip-Ft.)	EQUIVALENT YIELD SHEAR V_M (Kips)
WALL 19				
EL 140 - EL 123	10,600	12,800	0.23×10^6	13,700
EL 123 - EL 104	11,000	13,300	0.39×10^6	11,200
EL 104 - EL 85	9,200	13,500	0.71×10^6	14,100
WALL 31				
EL 140 - EL 119	13,200	16,600	0.64×10^6	30,700
EL 119 - EL 107	17,000	21,700	0.72×10^6	24,800
EL 107 - EL 85	15,000	19,200	1.05×10^6	22,300

Note: 1 kip = 4.448 kN, 1 kip - ft. = 1.356 kN - m

Table 4-5 Nonlinear Results for Median Structural Model at Sa = 3.0g
(Table 5-1 of Ref. 4)

Trial No.	Wall 19	Wall 31	Operating Floor	Turbine Pedestal
	Top Drift (in.)	Top Drift (in.)	Drift (in.)	Drift (in.)
1	0.580	0.600	3.060	3.220
2	1.010	1.300	5.150	2.470
3	0.360	0.610	2.290	1.860
4	0.240	0.290	1.580	2.200
5	0.520	0.830	3.540	2.350
6	0.790	0.790	4.570	2.400
7	0.220	0.430	1.980	1.580
8	0.200	0.240	1.810	2.120
9	0.890	1.180	4.000	2.700
10	0.640	0.700	2.710	2.450
11	0.540	0.740	1.700	1.370
12	0.360	0.520	2.840	2.240
13	0.590	0.580	3.780	2.810
14	0.280	0.250	3.180	3.430
15	1.390	1.810	7.030	4.800
16	1.030	1.100	3.710	2.280
17	0.650	0.890	5.390	3.500
18	1.690	2.360	5.770	2.480
19	0.240	0.250	2.570	3.470
20	1.620	2.110	5.370	3.120
21	0.250	0.480	1.660	1.860
22	0.410	0.620	3.470	3.070
23	0.650	0.970	4.180	3.760
24	1.130	0.900	2.950	1.880
25	0.230	0.620	3.840	3.880
Median of 25 trials	0.537	0.704	3.252	2.579
Std. Dev.	0.662	0.624	0.417	0.300

Note: 1 in. = 25.4 mm

Table 4-6 Nonlinear Results for Median Structural Model at Sa = 6.0g
(Table 5-2 of Ref. 4)

Trial No.	Wall 19	Wall 31	Operating Floor	Turbine Pedestal
	Top Drift (in.)	Top Drift (in.)	Drift (in.)	Drift (in.)
1	4.800	5.900	8.800	6.100
2	6.400	7.700	14.000	10.600
3	2.100	4.200	7.400	4.000
4	2.400	3.100	7.300	4.600
5	3.200	5.800	8.600	5.200
6	4.600	6.300	11.500	8.100
7	1.500	2.000	4.400	3.100
8	1.300	1.900	3.600	3.500
9	7.200	9.100	13.100	9.700
10	2.800	4.000	7.300	5.400
11	1.500	1.800	3.900	2.800
12	3.600	5.900	9.300	5.900
13	3.800	5.600	10.700	7.300
14	3.000	4.200	8.800	6.300
15	6.600	9.400	11.800	9.900
16	6.600	8.200	11.800	8.400
17	6.100	8.100	10.300	8.300
18	10.100	12.200	18.500	15.100
19	1.600	2.800	5.600	5.300
20	7.700	8.800	14.200	10.800
21	1.700	2.000	4.900	4.000
22	4.300	5.300	10.000	6.600
23	3.800	5.200	9.600	6.200
24	4.200	5.200	7.900	5.000
25	2.200	5.000	8.000	6.800
Median of 25 trials	3.522	4.922	8.574	6.227
Std. Dev.	0.587	0.541	0.412	0.415

Note: 1 in. = 25.4 mm

Table 4-7
Inertial Load Distribution on Model
(% of Total Base Shear)

Node	Uniform Inertial Force (%)	Modal Inertial Force (%)
3	3.3	0.7
5	1.8	1
7	9	5
10	4.8	8.3
11	4.8	8.3
12	53.1	62.4
16	13.5	8.6
18	4.5	3.1
20	5.2	2.6

Table 4-8 Load Deflection Data for the Uniform Loading Case for Model A

		Node11	Node10	Node12	Node7	Node16
G	Force (Kips)	Disp (ft)	Disp (ft)	Disp (ft)	Disp (ft)	Disp (ft)
0	0	0	0	0	0	0
0.1	4,705	0.006	0.006	0.009	0.002	0.002
0.2	9,409	0.012	0.012	0.017	0.003	0.003
0.3	14,114	0.018	0.018	0.026	0.005	0.005
0.4	18,818	0.024	0.024	0.035	0.006	0.007
0.5	23,523	0.031	0.031	0.043	0.008	0.008
0.6	28,227	0.037	0.037	0.052	0.010	0.010
0.7	32,932	0.043	0.043	0.061	0.011	0.012
0.8	37,636	0.049	0.049	0.069	0.013	0.013
0.9	42,341	0.055	0.055	0.078	0.014	0.015
1	47,045	0.061	0.061	0.087	0.016	0.017
1.1	51,750	0.078	0.078	0.095	0.025	0.019
1.2	56,454	0.126	0.126	0.104	0.040	0.037
1.3	61,159	0.179	0.179	0.113	0.055	0.064
1.4	65,863	0.232	0.232	0.122	0.070	0.091
1.5	70,568	0.286	0.286	0.130	0.087	0.119
1.6	75,272	0.353	0.353	0.139	0.121	0.155
1.7	79,977	0.429	0.436	0.148	0.169	0.208
1.8	84,681	0.439	0.509	0.158	0.206	0.252
1.9	89,386	0.449	0.581	0.168	0.244	0.295
2	94,090	0.460	0.654	0.178	0.282	0.339
2.1	98,795	0.470	0.727	0.189	0.320	0.382
2.2	103,499	0.480	0.799	0.199	0.358	0.426
2.3	108,204	0.491	0.865	0.210	0.394	0.457
2.4	112,908	0.503	0.930	0.221	0.431	0.486
2.5	117,613	0.514	0.994	0.232	0.467	0.514
2.6	122,317	0.849	1.147	0.568	0.573	0.651
2.7	127,022	1.300	1.315	1.597	0.701	0.765
2.8	131,726	1.458	1.807	2.089	0.833	0.883
2.9	136,431	1.615	2.300	2.581	0.966	1.002
3	141,135	1.773	2.792	3.074	1.099	1.120
3.1	145,840	1.930	3.284	3.567	1.231	1.239
3.2	150,545	2.088	3.777	4.059	1.364	1.357
3.3	155,249	2.245	4.269	4.552	1.497	1.476
3.4	159,954	2.403	4.761	5.044	1.629	1.594
3.5	164,658	2.560	5.254	5.537	1.762	1.713
4	188,181	3.348	7.716	8.000	2.425	2.305
4.5	211,703	4.136	10.177	10.463	3.089	2.897
5	235,226	4.923	12.639	12.926	3.752	3.490

Note: 1 kip = 4.448 kN, 1 ft. = .3048 m

Table 4-9 Load Deflection Data for the Modal Loading Case for Model A

		Node11	Node10	Node12	Node7	Node16
G	Force (Kips)	Disp (ft)	Disp (ft)	Disp (ft)	Disp (ft)	Disp (ft)
0	0	0	0	0	0	0
0.1	4,705	0.009	0.009	0.010	0.001	0.001
0.2	9,409	0.018	0.018	0.020	0.003	0.003
0.3	14,114	0.028	0.028	0.031	0.004	0.004
0.4	18,818	0.037	0.037	0.041	0.006	0.006
0.5	23,523	0.046	0.046	0.051	0.007	0.007
0.6	28,227	0.055	0.055	0.061	0.009	0.009
0.7	32,932	0.103	0.103	0.071	0.010	0.010
0.8	37,636	0.160	0.160	0.082	0.012	0.012
0.9	42,341	0.217	0.217	0.092	0.013	0.013
1	47,045	0.274	0.274	0.102	0.014	0.014
1.1	51,750	0.331	0.331	0.112	0.016	0.016
1.2	56,454	0.388	0.388	0.122	0.017	0.017
1.3	61,159	0.415	0.445	0.133	0.019	0.019
1.4	65,863	0.426	0.504	0.145	0.025	0.020
1.5	70,568	0.437	0.570	0.156	0.034	0.031
1.6	75,272	0.449	0.638	0.168	0.043	0.048
1.7	79,977	0.461	0.707	0.179	0.052	0.066
1.8	84,681	0.472	0.778	0.191	0.063	0.084
1.9	89,386	0.484	0.857	0.203	0.085	0.111
2	94,090	0.496	0.942	0.215	0.114	0.140
2.1	98,795	0.508	1.029	0.227	0.144	0.173
2.2	103,499	0.813	1.168	0.532	0.231	0.252
2.3	108,204	1.394	1.355	1.112	0.372	0.374
2.4	112,908	1.537	1.947	2.229	0.508	0.492
2.5	117,613	1.724	2.527	2.809	0.649	0.614
2.6	122,317	1.911	3.108	3.390	0.791	0.736
2.7	127,022	2.098	3.688	3.970	0.932	0.858
2.8	131,726	2.285	4.268	4.551	1.073	0.980
2.9	136,431	2.473	4.848	5.131	1.214	1.101
3	141,135	2.660	5.429	5.712	1.355	1.223
3.1	145,840	2.847	6.009	6.292	1.497	1.345
3.2	150,545	3.034	6.589	6.873	1.638	1.467
3.3	155,249	3.221	7.169	7.453	1.779	1.589
3.4	159,954	3.408	7.749	8.034	1.920	1.711
3.5	164,658	3.595	8.330	8.614	2.061	1.833
4	188,181	4.530	11.231	11.517	2.768	2.442
4.5	211,703	5.466	14.132	14.419	3.474	3.052
5	235,226	6.401	17.033	17.322	4.180	3.661

Note: 1 kip = 4.448 kN, 1 ft. = .3048 m

Table 4-10 Load Deflection Data for the Modal Loading Case for Model B

	Reaction	Node8	Node7	Node16	Node12
G	Force (Kips)	Disp (ft)	Disp (ft)	Disp (ft)	Disp (ft)
0	0	0.000	0.000	0.000	0.000
0.1	4,705	0.009	0.001	0.001	0.010
0.2	9,409	0.018	0.003	0.003	0.020
0.3	14,114	0.028	0.004	0.004	0.031
0.4	18,818	0.037	0.006	0.006	0.041
0.5	23,523	0.046	0.007	0.007	0.051
0.6	28,227	0.055	0.009	0.009	0.061
0.7	32,932	0.103	0.010	0.010	0.071
0.8	37,636	0.160	0.012	0.012	0.082
0.9	42,341	0.217	0.013	0.013	0.092
1	47,045	0.274	0.014	0.014	0.102
1.1	51,750	0.331	0.016	0.016	0.112
1.2	56,454	0.388	0.017	0.017	0.122
1.3	61,159	0.415	0.018	0.018	0.134
1.4	65,863	0.428	0.022	0.019	0.146
1.5	70,568	0.440	0.027	0.022	0.159
1.6	75,272	0.453	0.033	0.036	0.172
1.7	79,977	0.466	0.039	0.051	0.184
1.8	84,681	0.479	0.045	0.065	0.197
1.9	89,386	0.492	0.051	0.079	0.210
2	94,090	0.505	0.057	0.093	0.223
2.1	98,795	0.595	0.085	0.128	0.314
2.2	103,499	0.984	0.229	0.251	0.703
2.3	108,204	1.358	0.367	0.370	1.639
2.4	112,908	1.747	0.510	0.493	2.028
2.5	117,613	2.136	0.653	0.617	2.418
2.6	122,317	2.525	0.796	0.740	2.808
2.7	127,022	2.915	0.939	0.863	3.197
2.8	131,726	3.304	1.082	0.987	3.587
2.9	136,431	3.693	1.225	1.110	3.976
3	141,135	4.082	1.368	1.233	4.366
3.1	145,840	4.471	1.511	1.357	4.755
3.2	150,545	4.861	1.654	1.480	5.145
3.3	155,249	5.250	1.797	1.604	5.535
3.4	159,954	5.639	1.940	1.727	5.924
3.5	164,658	6.028	2.084	1.850	6.314
4	188,181	7.975	2.799	2.467	8.262
4.5	211,703	9.921	3.514	3.084	10.209
5	235,226	11.867	4.230	3.701	12.157

Note: 1 kip = 4.448 kN, 1 ft. = .3048 m

Table 4-11 Predicted Displacements Based on FEMA Methodology

Node	Model A - 3g	Model B - 3g	Model A - 6g	Model B - 6g
7	0.444"	0.900"	2.88"	3.26"
16	0.432"	1.392"	3.08"	3.46"
10-11/8	7.08"	6.60"	14.16"	13.20"
12	1.92"	2.77"	6.77"	11.90"

Note: 1 in. = 25.4 mm

Table 4-12 Differences Between Forced Based and Displacement Based Analyses for 3 g Input

Location	Top of Wall 19	Top of Wall 31	Operating Floor	Turbine
Dm	0.537"	0.704"	3.252"	2.579"
Bd	0.662	0.624	0.417	0.3
Model A Dfema	0.44"	0.432"	7.08"	1.92"
Model A - E	0.3	0.78	1.87	0.98
Model B Dfema	0.90"	1.39"	6.60"	2.77"
Model B - E	0.78	1.09	1.7	0.24

Note: 1 in. = 25.4 mm

Table 4-13 Differences Between Forced Based and Displacement Based Analyses for 6 g Input

Location	Top of Wall 19	Top of Wall 31	Operating Floor	Turbine
Dm	3.522"	4.922"	8.574"	6.227"
Bd	0.587	0.541	0.412	0.415
Model A Dfema	2.88"	3.08"	14.16"	6.77"
Model A - E	0.34	0.87	1.28	0.2
Model B Dfema	3.26"	3.46"	13.20"	11.91"
Model B - E	0.13	0.65	1.05	1.56

Note: 1 in. = 25.4 mm

Appendix A

LITERATURE SURVEY

OF

DISPLACEMENT BASED SEISMIC

DESIGN METHODS

By:

Y.J. Park

Brookhaven National Laboratory
Upton, New York 11973

September 1998
(revised March 2001)

NOTICE

The following figures and tables were reproduced with the permission of the respective publishers. The complete reference is included in Section A6. The publishers assume no responsibility for the accuracy or the completion of the information provided in this report.

1. Figures A7 and A8 (Ref. 19) - International Conference of Building Officials (ICBO)
2. Figure A9 (Ref. 32) - Structural Engineers Association of California (SEAOC)
3. Figure A10 (Ref. 30) - Structural Engineers Association of Southern California (SEAOSC)
4. Figures A13-A14 and Table A10-A11 (Ref. 20) - Applied Technology Council (ATC)
5. Figures A15-A17 (Ref. 35) - SEAOC
6. Figure A18 (Ref. 42) - SEAOC
7. Figure 19a and 19b (Ref. 45) - Sigmund A. Freeman (author)
8. Figure A20 (Ref. 55) - John Wiley and Sons Limited
9. Figure A21 (Ref. 15) - ATC
10. Table A15 (Ref. 53) - American Society of Civil Engineers

A1. INTRODUCTION

As part of the initial phase of this study, a literature survey was conducted on the recent changes in seismic design codes/standards, on-going activities of code-writing organizations/communities, and published documents on the displacement-based design methods. This Appendix provides summaries of the reviewed documents, together with a brief overview of the current seismic design practice and design criteria for the nuclear power plant facilities. The following topics are covered in this report.

- Current seismic design practice and design criteria for nuclear plant facilities
  - Seismic design criteria in SRP
  - Seismic margin studies
- Recent changes in building codes
  - 1997 NEHRP Guidelines for Rehabilitation
  - 1997 UBC
  - 1997 NEHRP Provisions for New Buildings
  - ATC32 for Bridge Design
- On-going Activities for Future Codes
  - 2000 IBC
  - VISION 2000
  - Recent Studies by Researchers
- Technical Issues for Further Consideration

A2. CURRENT SEISMIC DESIGN PRACTICE AND DESIGN CRITERIA FOR NPP FACILITIES

A2.1 Design Criteria for Category I Structures, Systems and Components (SSC)

According to the SRP Section 3.7.2, "The SRP criteria generally deal with linear elastic analysis coupled with allowable stresses near elastic limits of the structures. However, for certain special cases (e.g., evaluation of as-built structures), the staff has accepted the concept of limited inelastic/nonlinear behavior when appropriate" (Ref. 1). In comparison with non-nuclear building codes, the SRP criteria are considered to be significantly more conservative.

The basic load combination for seismic design of Category I SSC is typically given by,

$$D + L + (LOCA) + (SSE)$$

Typical allowable stresses are listed in Table A1.

Table A1. Allowable Stresses for Level D Limit

ITEM	ALLOWABLE
Reactor Vessel	$3.6\ S_m,\ S_u$
Class 1 Piping	$3.0\ S_m,\ 2\ S_y$
Containment, Concrete	$0.75 f_c'$
Containment, Rebars	$0.9 f_y$

The determination of an SSE ground motion spectra is described in detail in Ref. 2. The ground motion intensity is determined based on the mean reference probability of 1.0×1.0^{-4}/year (return period of 10,000 years), which is considerably more conservative than a typical postulated return period of 475 years in non-nuclear building codes.

A2.2 Seismic Margin Studies

The seismic margin of existing NPP facilities is evaluated using the PRA method or the SMA method. Recent major industrial activities in this area include the IPEEE project (Ref. 3) and SMA analyses of advanced reactors (e.g., Ref. 4).

Based on past PRA/SMA studies (e.g. Refs. 5 through 10), components and failure modes that are considered to be "displacement sensitive" are identified and listed in Table A2. A limited number of studies have been performed regarding the displacement failure criteria (e.g. Ref. 11 for squatty shear walls). Structural analysis procedures in a typical fragility analysis of an NPP may be characterized as follows (in light of displacement-based design criteria):

1. The ground motion input is defined by an acceleration response spectrum.
2. The displacement responses, when needed, are usually estimated from acceleration responses.
3. A nonlinear analysis is very rarely performed. The nonlinear effects are considered by an F_μ factor.
4. Due to the conservative nature of the analysis procedure, the ductility for certain components is not taken into account. Flat-bottom tanks may be a typical example (see Ref. 12 for post-buckling hysteretic responses of flat- bottom tanks).

Table A2. Displacement Sensitive Components/Failure Modes

COMPONENTS	FAILURE MODES
Category II Structures (e.g. Turbine Building)	• Excessive inelastic deformation
Adjacent Buildings (e.g. Reactor & Turbine Buildings)	• Pounding between buildings
Masonry Walls	• Out-of-plane bending
Seismic Interaction	• Flexible distribution systems impacting equipment • Category II structures over Category I Equipment
Piping	• Differential anchor motions • Relative motion between buildings (Buried pipes)
Core Assembly	• Bending of cores • Deflection of guide tubes
Rotating Equipment	• Deflection of pump shaft • Deflection of fan blade
Non-Structural Components (partitions, doors, glasses, hang ceilings)	• Adverse affects on operators
Ductile Components (in general)	• Excessive inelastic deformation

A3. RECENT CHANGES IN BUILDING CODES

The historical evolvement of seismic design codes, prior to the 1994 Northridge and the 1995 Kobe earthquakes , are described in detail in the SEAOC publications (e.g. Refs. 13 and 14) and the ATC publications (e.g. Ref. 15). A comprehensive review of design codes/standards was also conducted by an NRC subcontractor in 1995 in conjunction with the proposed design of advanced reactors (Ref. 16).

This report summarizes more recent code changes after the Northridge and Kobe events including the1997 NEHRP Guidelines for Rehabilitation of Building (FEMA 273, 274, Refs. 17 and 18), the 1997 UBC (Ref. 19), the 1997 NEHRP Provisions for New Buildings (FEMA 302, 303, Refs. 21 and 22), and ATC-32 (Bridge design, Ref. 20). The two other building codes, i.e., the NBC code and the SBC code, as well as ASCE 7 (Ref. 23), are not described below because they are consistent with the NEHRP Provisions. Similarly, the so-called SEAOC "Blue Book," (Ref. 24) is not independently addressed here since their recommendations were incorporated in the 1997 UBC.

A3.1 1997 NEHRP Guidelines for the Seismic Rehabilitation of Buildings (FEMA-273, 274)

The guidelines are the first performance based seismic criteria adopted at the "national level." The evaluation criteria are displacement based. The main concepts are described in some detail in this report. A brief summary (Ref. 25) as well as application to various existing buildings (Ref. 26) of the guidelines are also available in open publications.

Performance Criteria

The building performance levels, which represent the post-earthquake condition of a building, are summarized in Table A3. They are expressed as a combination of the structural performance levels (S1, S3 and S5) and ranges (S2 and S4), and the nonstructural performance levels (NA through NE).

A total of four (4) performance levels, i.e., 4 combinations of structural and nonstructural performance levels, are recommended for possible performance objectives.

(S-1 + N-A).....Operational Level; very little damage
(S-1 + N-B).....Immediate Occupancy Level; green tag
(S-3 + N-C).....Life Safety Level; significant reserve strength
(S-5 + N-E).....Collapse Prevention Level; remain standing

Table A3. Building Performance Levels (BPL)

(Structural Performance)	(Nonstructural Performance)
• S-1: Immediate Occupancy Performance Range	• N-A: Operational Performance Level
• S-2: Damage Control Performance (extends between Life Safety and Immediate Occupancy Performance Levels)	• N-B: Immediate Occupancy Performance Level
• S-3: Life Safety Performance Level	• N-C: Life Safety Performance
• S-4: Limited Safety Performance Range (extends between Life Safety and Collapse Prevention Performance Levels)	• N-D: Hazards Reduced Performance Level
• S-5: Collapse Prevention Performance Level	• N-E: No Evaluation is performed

The structural performance levels are illustrated in Fig. A1, in which the Life Safety Level would be able to experience at least 33% greater lateral deformation before the building failure. The recommended story drifts corresponding to the structural performance levels are listed in Table A4.

Table A4. Typical Drift Ratio in Vertical Elements (Ref. 18)

Building Type	Collapse Prevention	Life Safety	Immediate Occupancy
RC frame	4% transient or permanent	2% transient 1% permanent	1% transient negligible permanent
Steel frame	5% transient or permanent	2.5% transient 1% permanent	0.7% transient negligible permanent
Braced steel frame	2% transient or permanent	1.5% transient or 0.5% permanent	0.5% transient negligible permanent
R.C. Wall	2% transient or permanent	1% transient or 0.5% permanent	0.5% transient negligible permanent

Seismic Hazard and Ground Motions

In the early 1990's, the USGS developed a new series of ground motion maps, utilizing the latest seismological knowledge. In their hazard analysis, the variabilities in the magnitude-recurrence relationship, rupture mechanism and attenuation relationship were considered directly in the probabilistic calculations. Other uncertainties, e.g. seismic source zoning and estimation of seismicity parameters, were not accounted for. Studies by USGS concluded that the mapped values represent a high degree of confidence about the mean plus one standard deviation. A committee of the BSSC decided to adopt a 2%/50 year exceedence level definition for the Maximum Considered Earthquake (MCE) in most regions. In regions at coastal California however, smaller ground motion intensities were adopted so that the MCE does not exceed 150% of the design motions determined in the 1994 NEHRP Provisions. The following two levels of basic safety earthquakes (BSE) are recommended for evaluation of existing building:

BSE	Exceedence Probability	Return Period	Note
BSE-1 BSE-2	10% in 50 years 2% in 50 years	474 (500) years 2,475 (2500) years	< ⅔ BSE-2 MCE

The rehabilitation objectives are shown in Fig. A2 as combinations of the building performance levels and the above earthquake hazard levels. The following two combinations are recommended as the basic safety objectives (BSO):

1. Life Safety for BSE-1
2. Collapse Prevention for BSE-2

The recommended ground motion acceleration spectrum is illustrated in Fig. A3. The effective peak acceleration, A_a, and the velocity-related peak acceleration, A_v, have been used until the 1994 version of NEHRP Provisions/Guidelines. In the 1997 version, the ground motions are defined by two spectral acceleration values, i.e., the long period (1 sec.) and short period (approx. 0.2 sec.) spectral accelerations, S_1 and S_s.

Linear Analysis Procedure

Although the Guidelines strongly recommend the use of nonlinear analysis procedures for the evaluation of existing building, linear analysis procedures (linear static, LSP, and linear dynamic, LDP) are still acceptable given the following restrictions:

- the demand-capacity ratios (DCRs) in primary components are less than 2.0.
- when the maximum DCRs are larger than 2.0, linear analysis procedures can still be used if
  - no significant in-plane discontinuity
  - no significant out-of-plane offset
  - ratios of DCRs between adjacent stories less than 1.25 (no soft story)
  - no significant torsional problem

To determine the stiffnesses of components, the use of secant stiffnesses at yielding is recommended (see Table A5 for R.C. structures).

Table A5. Effective Stiffness Values, R.C. Structures for Linear Analysis (Ref. 17)

Component	Flexural Rigidity	Shear Rigidity	Axial Rigidity
Beams - nonprestressed	$0.5E_cI_g$	$0.4E_cA_w$	—
Beams - prestressed	E_cI_g	$0.4E_cA_w$	—
Columns in compression	$0.7E_cI_g$	$0.4E_cA_w$	E_cA_g
Columns in tension	$0.5E_cI_g$	$0.4E_cA_w$	E_sA_s
Walls - uncracked (on inspection)	$0.8E_cI_g$	$0.4E_cA_w$	E_cA_g
Walls - cracked	$0.5E_cI_g$	$0.4E_cA_w$	E_cA_g
Flat Slabs - nonprestressed	See Section 6.5.4.2	$0.4E_cA_g$	—
Flat Slabs - prestressed	See Section 6.5.4.2	$0.4E_cA_g$	—

Note: I_g for T-beams may be taken as twice the value of I_g of the web alone, or may be based on the effective width as defined in Section 6.4.1.3. For shear stiffness, the quantity $0.4E_c$ has been used to represent the shear modulus G.

The definition of the pseudo lateral forces in LSP, illustrated in Fig. A4, is significantly different from the traditional design formulations in which the lateral forces are reduced by R (or R_w) factors. It is intended to produce calculated lateral displacements approximately equal to those that are expected in the real (nonlinear) structure during the design event.

$$V = C_1 C_2 C_3 S_a W \quad (1)$$

C_1 is the ratio of (nonlinear response disp.) to (linear response disp.)

$$C_1 = 1.5 \text{ for } T < 0.10$$
$$= 1.0 \text{ for } T \geq T_o \quad (2)$$

Or, a more detailed formulation:

$$C_1 = 1.0 \quad \text{for } T \geq T_o$$
$$= [1 + (R-1)\, T_o/T]/R \quad \text{for } T < T_o \quad (3)$$

in which, T is the fundamental period of building, T_0 is characteristic period of design spectrum (see Fig. A3), R is the ratio of elastic strength demand to yield strength.

C_2 is the factor to account for the effects of pinching and strength deterioration (see Table A6).

Table A6. Factor C_2 (Ref. 17)

Performance Level	T = 0.1 sec.	$T > T_o$
Immediate Occupancy	C_2 = 1.0	C_2 = 1.0
Life Safety	1.3	1.1
Collapse Prevention	1.5	1.2

C_3 is a factor to account for a negative post-yield stiffness due to P-Δ effects. The equations for C_3, which are not reiterated herein, are considered to be a significant simplification of analysis results which typically show a large scatter.

The acceptance criteria for components are displacement based, and expressed as

$$mk\, Q_{CE} \geq Q_{UD} \quad (4)$$

in which,

Q_{CE}	=	medium (best estimate, strain hardening is included) component strength.
Q_{UD}	=	member forces calculated by LSP.
m	=	μ (ductility ratio, defined in FEMA 273.)
	=	1.0 for nonductile comp.
K	=	knowledge factor (=0.75 when only minimum information is available for the component.)

Nonlinear Analysis Procedure

A nonlinear static analysis procedure (NSP) is recommended for the evaluation of most buildings given that the contribution from higher modes is not significant, i.e., the story shear from higher modes contributes less than 30% of that of the fundamental mode. Fig. A5 illustrates the load-deformation curves and acceptance

criteria for pushover analyses (NSP). All the necessary parameters are tabulated in FEMA 273.

Two types of pushover analyses are recommended.

Method 1: Conventional tangential stiffness method. The target roof displacement is defined as,

$$S_t = C_o C_1 C_2 C_3 S_a \frac{T^2 \cdot g}{4\pi^2} \qquad (5)$$

In which, C_1, C_2 and C_3 are the same as in Eq. (1), C_o is the ratio of roof displacement to the equivalent SDOF displacement (1.0 ~ 1.5).

Method 2: An equivalent linearization (secant stiffness) approach using only the 1st mode (see Ref. 27 for details), which is very similar to the capacity spectrum method (e.g. Ref. 28).

Besides general limitations in the pushover analysis in comparison with a direct time history analysis, the determination of a "realistic" lateral load pattern is always a problem. Recognizing this, the Guidelines mandate the use of at least two lateral load distribution patterns:

- Uniform distribution .... to see failure of lower stories
- Design (linear) codes basis distribution .... to see the effects of higher modes.

Summary of Deformation Limits

The displacement limits of beams, columns and shear walls are defined in terms of the chord rotation in radian as illustrated in Fig. A6.

For steel frames, the tabulated displacement limits depend on:

- whether fully restrained (connection deformation contributes no more than 5%) or partially restrained
- flange plate thickness ratio, b_f / t_f
- axial stress (for columns)
- size effect (multiply $18/d_b$, d_b = beam depth, in)

For R.C. components, the deformation limits are given by a function of failure mode (flexure or shear), shear stress, axial stress and reinforcements. Typical deformation limit values are listed in Table A7 for the collapse prevention case.

The acceptable drift ratios for non-structural components are summarized in Table A8.

Table A7. Deformation Limits of R.C. Components (Ref. 17)

Components	Deformation Limits (Radian) for CP	
	Flexural Failure	Shear Failure
Beam	$\theta = 0.01 \sim 0.05$	$\theta = 0.0 \sim 0.02$
Column	$0 \sim 0.03$	$0.0 \sim 0.015$
Shear Wall	$0.002 \sim 0.02$	$0.0075 \sim 0.015$

Table A8. Drift Ratios for Nonstructural Components (Ref. 17)

Components	Drift Ratio	
	Immediate Occupancy	Life Safety
Adhered Veneer	0.01	0.03
Anchored Veneer	0.01	0.02
Glass Blocks	0.01	0.02
Prefabricated Panels	0.01	0.02
Glazing	0.01	0.02
Heavy Partitions	0.005	0.01

A3.2 1997 UBC

The UBC Seismic Provisions have been updated based on the revised recommendations of the SEAOC Blue Book, on a 3 year cycle, through the 1980's and 1990's. The 1997 version, which is considered to be the last one since it will be replaced by the first "National Building Code" IBC in the year 2000, contains many significant changes. The main purposes of the new changes were:

- To reflect lessons learned from the Northridge and Kobe earthquakes.
- To be more consistent with the NEHRP Provisions for a smooth transition to the 2000 IBC.

A large number of publications and articles are available for understanding the technical basis for the new changes (e.g. Refs. 29 through 34). The major changes in the 1997 UBC, which are considered to be directly or indirectly related to the displacement based design, are discussed in some detail below.

Design Forces

The design response spectrum and basic seismic coefficients of the 1997 UBC are shown in Figs. A7 and A8.

As indicated in Table A9, the constant velocity portion of the design spectrum is defined by 1/T, instead of $1/T^{2/3}$, to be consistent with the 1997 NEHRP Provisions. The newly introduced near-source factors, N_a and N_v (see Fig. A8), came from a recognition that the ground motions near earthquake rupture could be larger than previously assumed. This phenomenon was very evident in the Kobe earthquake (Ref. 33).

Another significant change is the adoption of the strength design (SD) approach over allowable stress design (ASD) approach. Accordingly, the basic load combination has been changed as follows to be consistent with ASCE-7 (Ref.23) and the 1997 NEHRP:

$$\text{1994 UBC} \quad Q = 0.9D \pm 1.4E \tag{6}$$

$$\text{1997 UBC} \quad Q = 0.9D \pm 1.0E \tag{7}$$

Table A9. Comparison of 1994 and 1997 UBC's

1994 UBC Equation	1997 UBC Equation
$V = \frac{ZIC}{R_w} W$	$V = \frac{C_v I}{RT} W$
$C = \frac{1.2S}{T^{2/3}}$	$C_v = 0.8ZN_v$ to $3.2ZN_v$
$R_w = 3$ to 12	$R = 2$ to 8.5
$I = 1$ to 1.25	$I = 1$ to 1.25
$S = 1$ to 2	$N_a = 1$ to 1.5
	$N_v = 1$ to 2.0
$V_{max} = \frac{2.75I}{R_w}$	$C_a = 0.9ZN_a$ to $1.2ZN_a$

In order to avoid a significant reduction in the design forces due to the above change in the load combination rule, the R-factors were adjusted as,

$$R \text{ (1997 UBC)} \approx R_w \text{ (1994 UBC)} / 1.4 \tag{8}$$

Consideration of "Real" Responses

The current versions of seismic design codes, including the 1997 UBC and the 1997 NEHRP Provisions, are still not considered to be performance based. These design codes, however, are becoming increasingly more explicit regarding the "real" response of buildings during a design earthquake event.

In an early draft version of the 1997 UBC, the R-factor was defined as follows (Ref. 24):

$$R = R_i R_o \frac{R_\mu}{I} \tag{9}$$

in which

R_i = factor to account for response reduction in nonlinear system (1.0 ~ 1.4)
R_o = overstrength factor (2.0 ~ 2.8 according to 1997 UBC)
R_μ = inelastic energy absorbing factor due to ductility (2~ 4)
I = occupancy importance factor (1 ~ 1.25)

The above R-factors are further explained in a capacity spectra format in Fig. A9 (Ref. 32). Although the above equation (9) was not adopted in the final version, the basic concepts were utilized in defining the expected maximum displacement, Δ_m, and forces in brittle component, V_m, as (see Fig. A10),

$$\Delta_m = 0.7 R \cdot \Delta_s \left(= \frac{R\Delta_s}{R_i} \right) \tag{10}$$

$$V_m = \Omega_o \cdot V_E (= R_o \cdot V_E) \tag{11}$$

in which, Δ_s is the elastic drift under design forces, Ω_o is the overstrength factor and V_E is the elastic design forces. In the above eq. (10), the R_i factor is assumed to be 1.4 regardless of the frequency of structures (Ref. 32).

Drift Limits

The drift limits are given as follows:

1994 UBC: $\Delta_s < \min (0.04/R_w, 0.005H)$....less than 65ft.
$\Delta_s < \min (0.03/R_w, 0.004H)$....higher than 65ft.

1997 UBC: $\Delta_M < 0.025$ H...T < 0.7 sec.
$\Delta_M < 0.02$ H...T > 0.7 sec.

For a low-rise R.C. shear wall structure, (R= 4.5, R_w = 6.0), a comparison on Δ_s is made as below,

1994 UBC: $\Delta_s < 0.005$ H
1997 UBC: $\Delta_s < 0.025$ H /(0.7 x 4.5) = 0.008 H

(1997 UBC) / (1994 UBC) = 1.6

The above change in the drift limits was intended to be consistent with the NEHRP Provisions.

The technical basis for other changes, including the newly introduced redundancy/reliability parameters (ρ) and the soil classification, are described in Refs. 29 through 34.

A3.3 1997 NEHRP Provisions for New Buildings (FEMA 302, 303)

The seismic provisions of the first national building code, IBC 2000, will be based largely on the 1997 NEHRP Provisions. The changes made in the NEHRP Provisions from the 1994 version are relatively minor, and in parallel with the changes in UBC, except that the near-source factors were not adopted in the NEHRP Provisions. The major changes are,

- Response spectral values are used to define the design spectrum, instead of the effective peak acceleration, A_a, and velocity-related acceleration, A_v (Similar to UBC).
- The velocity constant portion of design spectrum is defined by $1/T$ instead of $1/T^{2/3}$ (same as UBC).
- Adoption of redundancy/reliability parameter, ρ (same as UBC).

Design Forces

The design earthquake for new buildings is defined 2/3 of the Maximum Considered Earthquake (MCE) (see Section A3.1). The design response spectrum, is shown in Fig. A11, in which,

$$S_{DS} = 2/3\ F_a\ S_s$$
$$S_{D1} = 2/3\ F_v\ S_1 \qquad (12)$$

The above S_s and S_1 are mapped response spectral values for MCE at T = 0.2 sec and 1.0 sec. The soil factors, F_a and F_v, are tabulated in Fig. A11, which indicate significantly lower soil amplifications at higher ground intensity for soft soil conditions.

Expected Building Performance

The provisions specify progressively more conservative strength, drift control, system selection and detail requirements according to the "Seismic Use Group."

Seismic Use Group III..... fire, rescue, police, hospital, hazardous, etc.
Seismic Use Group II.....public assembly, schools, power generation, water treatment
Seismic Use Group I.....none of the above

The importance factor, I (to increase design forces), expected building performance, and drift limits for each Seismic Use Group are shown in Fig. A12.

The drift is checked by the following equation:

$$\delta_x = C_d\ \delta_e / I < \Delta_a \qquad (13)$$

in which, C_d = deflection amplification factor for framing systems, δ_e = elastic drift under design forces, and Δ_a is given in Fig. A12. The importance factor, I, in eq. (13) is needed to offset the same factor used in

calculating the design lateral forces.

A3.4 ATC-32, Bridge Design

Although the bridge design codes are not directly related to the seismic design of NPP's, recent developments in this area are briefly outlined, based on ATC-32 (Ref. 20), herein, since some interesting developments in performance based design can be found.

The performance criteria and the type of analyses depend on whether or not the bridge is classified as Important (access to an emergency facility/major economic impact), and on the complexity of the structural configuration (Type I = simple, responses can be approximated by a single mode; and Type II = complex). The performance criteria are summarized in Table A10.

Table A10. Seismic Performance Criteria (Ref. 20)
[Reproduced with permission]

Ground Motion at Site	Ordinary Bridges	Important Bridges
Functional-Evaluation Ground Motion	Service Level - Immediate Repairable Damage	Service Level - Immediate Minimal Damage
Safety-Evaluation Ground Motion	Service Level-Limited Significant Damage	Service Level-Intermediate Repairable Damage

The two-level ground motions at a site are,

- Functional-evaluation ground motion.....a probabilistically assessed ground motion that has a 60% non-exceedence probability during the life of the bridge.
- Safety-evaluation ground motion.....maximum credible earthquake with a return period of 1000-2000 years,

The damage levels are described only quantitatively,

- Minimum damage..... essentially elastic performance.
- Repairable damage....yielding and minor spalling of concrete occurs, but no need for replacement of any component.
- Significant damage.....a minimum risk of collapse, but require closure to repair.

The minimum requirements for the structural analysis are also summarized in Table A11.

The ATC-32 recommends the use of inelastic static analysis (pushover analysis) for all bridges. Also, Caltrans, the main user of the Recommendations, intends to use both nonlinear static and dynamic analyses as a routine design procedure.

Table A11. Minimum Required Analysis (Ref. 20)
[Reproduced with permission]

	Functional Evaluation	Safety Evaluation
Ordinary Bridge Type I	None Required	A or B
Ordinary Bridge Type II	None Required	B
Important Bridge Type I	A or B	A or B
Important Bridge Type II	B	B or C

Note: A = Equivalent Static Analysis
B = Elastic Dynamic Analysis
C = Inelastic Static Analysis (Substitution of Inelastic Dynamic Analysis is Acceptable)

For the ground motion, sets of both acceleration and displacement spectra are defined for:

- different magnitudes - 6, 7 and 8;
- different soil types (same soil classifications as FEMA 302); and
- different peak acceleration levels.

The explicit definition of the displacement spectra can be useful in generating time histories with proper displacement contents. A typical example of the ground motion spectra is shown in Figure A13.

Unlike the building design codes, the definition of the force-reduction coefficients, Z (same as R-factor), is fairly straightforward as shown in Fig. A14. The same simplified formulation for R_μ-factor of Eq. (9) is directly used. Other R-factors in Eq. (9), R_i and R_o, are obviously not needed for bridge design. This relationship is also directly used to estimate the nonlinear displacement responses from the linear analysis as,

$$R_d = \left(1 - \frac{1}{Z}\right)\frac{T^*}{T} + \frac{1}{Z} \geq 1.0 \qquad (14)$$

A4. ONGOING ACTIVITIES FOR FUTURE BUILDING CODES

A4.1 Vision 2000 (Ref.35)

A committee was formed by SEAOC, named theVision 2000 Committee, to outline the conceptual framework for the next generation seismic codes based on performance based engineering. The Committee's report (Ref. 35) consists of the recommendations of performance criteria, overview of current (before 1995) building codes, and discussions on prospective performance based design approaches for future development.

Performance Criteria

The recommended performance criteria are summarized in Fig. A15, which are combinations of performance level (damage level), earthquake design level, and the occupancy importance of the building.

A detailed description of the proposed performance (damage) levels is given in Fig. A16. The proposed criteria are summarized in Table A12 in comparison with the foregoing FEMA 273 Guidelines.

Table A12. Performance Levels and Drift Limits

Vision 2000 (1995)			NEHRP Guidelines (1997)		
Performance Level	Description of Damage	Drift Limits	Performance Level	Drift Limits	
				Steel Frame	RC Wall
Fully Operational	No damage, all equipment operational	0.2%	Operational	—	—
Operational	Light structural damage, moderate damage to non-structures (green tag)	0.5%	Immediate Occupancy	0.7%	0.5%
Life Safety	Moderate structural damage	1.5%	Life Safety	2.5%	1%
Near Collapse	(Red tag)	2.5%	Collapse Prevention	5%	2%

Next, the occupancy importance, which is called performance objective in the Vision 2000, is summarized in Table A13 in comparison with the NEHRP Provisions for New Design and the DOE Standard, DOE-ST-1020 (Ref.36).

Performance Based Design Approaches for Future Development

A total of 6 design approaches are discussed in the Vision 2000, as listed below in the decreasing order of sophistication:

- Comprehensive Design Approach
- Displacement Based Design Approach
- Energy Based Design Approach
- General Force/Strength Design Approach
- Simplified Force/Strength Design Approach
- Prescriptive Design Approach

Table A13. Occupancy Importance

Occupancy	Vision 2000	NEHRP Provisions	DOE-1020
Ordinary buildings	Basic Facilities	Seismic Use Group I	Category 1
Public assembly, school	——	Seismic Use Group II	——
Fire, police, hospitals, hazardous, etc	Essential/ Hazardous Facilities	Seismic Use Group III	Category 2
Safety Critical Facilities	Large quantities of toxins, explosives, radioactive materials	——	Category 3
Nuclear Reactor	——	——	Category 4

The main features of the suggested approaches are summarized in Table A14. Several concepts are recommended for the future design methods (regardless of the above classification of different approaches).

Smoothed inelastic spectra...Fig. A17 illustrates the proposed inelastic design spectra. These spectra are considered to be conceptual, and detailed discussion are not provided regarding actual development of design criteria.

Use of damage index.... The following damage index is recommended for both development of "damage-consistent" design spectra and evaluation of components (Ref. 37):

$$D = \frac{\delta}{\delta_u} + b\frac{E}{Q \cdot \delta_u} \qquad (15)$$

where, δ = maximum response, δ_u = deformation limit under monotonic load, Q = strength, E = dissipated total energy, and β = deterioration factor.

Use of energy balance equation...The energy equation is repeatedly suggested to characterize the damage potential of ground motions, as

$$E_I = E_K + E_s + E_{H\xi} + E_{H\mu} \qquad (16)$$

in which, E_I = input energy, E_K = kinematic energy, E_s = elastic strain energy, $E_{H\xi}$ = hysteretic damping, $E_{H\mu}$ = plastic deformation energy. Detailed design formulations, however, are not provided in the report.

Table A14. Proposed Seismic Design Approaches (Ref. 35)

APPROACH	FEATURES	RESEARCH NEEDS
Comprehensive Approach	• Used to calibrate simpler design approaches • Use of energy balance equation • Probabilistic limit states based on total cost over life-span • Use of "damage index" for RC and Miner rule for steel	• Better definition of damage potential of ground motions • Define tolerable damage of component at each performance level
Displacement Based Approach	• To control displacements or drift, rather than force • Use of "substitute elastic structures" • Use of approximately damped elastic displacement response spectra for ground motion	• More studies on MDOF systems • Approach to apply to RC shear, wall, wood frames • Calibration of methods
Energy Based Approach	• Based on energy balance equation; E_I (input)=E_k (kinematic) + E_s (strain) + $E_{H\xi}$ (hysteresis) + $E_{m\mu}$ (plastic deformation) • It is not clear how the above equation can be applied • Use of damage index suggested	• Quantification of energy demand of ground motions, and energy capabilities of components
General Force/Strength Approach	• Modify the current design methods, e.g. UBC and NEHRP, with the following enhancements: - design at multiple (at least 2) earthquake levels; - use nonlinear design spectra; - change R-factors at different damage levels - use Pushover Analysis	• Development of nonlinear design spectra • Decomposition/refinement of R-factors • Better definition of target displacement for Pushover Analysis
Simplified Force/Strength Approach	• Same as the above method, except it is intended for Life Safety criterion only	• Refinements of current design format for more explicit definition of performance
Prescriptive Approach	• Current design approach (not performance based)	

A4.2 2000 IBC

The 2000 International Building Code (IBC) (Ref. 38) was published in March 2000 and was not reviewed as part of this literature survey. The technical content of the latest model codes prepared by Building Officials and Code Administrators International (BOCA), International Conference of Building Officials (ICBO) and Southern Building Code Congress International (SBCCI) was utilized for the development of the 2000 IBC. Reports issued by the Board for the Coordination of Model Codes (BCMC) were also used as the basis of the development of this new code.

A4.3 Recent Studies by Researchers

A4.3.1 Substitute Structure Approach

A displacement-based design method is proposed by N. Priestley for R.C. structures with flexural failure mode (Refs. 39 through 42). According to Priestley, the traditional force-based design approach has the following disadvantages:

- does not directly address the inelastic nature of a structural system;
- requires the use of somewhat arbitrary force-reduction factors;
- provides little insights into actual structural behavior; and
- does not provide a consistent level of protection against reaching a specified limit state.

The proposed method is based largely on the substitute structure approach developed by Gulkan and Sozen (Ref. 43) and Shibata and Sozen (Ref. 44). The design objective is to achieve the target drift, Δ_m, which in turn is expressed as a function of the target strains of concrete (ϵ_c) and reinforcement (ϵ_s) as,

- $\Delta_m = f(\epsilon_c, \epsilon_s, \phi_y)$, target drift
- $\Delta_y = f'(\phi_y)$, yield drift
- $\mu = \Delta_m / \Delta_y$ (17)

The above functions, $f(\,)$ and $f'(\,)$, were developed based on the flexural behavior of components (Ref.42), and it appears other types of deformations, e.g. shear deformation, were not directly accounted for. In addition, the selection of the target strains are based on engineering judgement. The proposed design procedure for a single mode structure is outlined below (Ref.42).

Step 1. Select target drift, e.g. $\Delta_m = 0.03H$, $\Delta_y = 0.005H \therefore \mu = \Delta_m/\Delta_y = 6$.
Step 2. Estimate effective damping, ζ, $\zeta = f(\mu)$, (see Fig. A18a)
Step 3. Estimate effective vibration period, T_e, from displacement spectra, (see Fig. A18b)
Step 4. Calculate effective stiffness (see Fig. A18c),

$$K_{eff} = \frac{4\pi^2 M}{T_e^2}$$

and effective design forces, F_m

$$F_m = K_{eff}\,\Delta_m$$

Step 5. Design components
Step 6. Revise the maximum disp.

$$\Delta_m = f(\epsilon_c\,,\ \epsilon_s\,,\ \phi_y)\,,\ \Delta_y = f(\phi_y)$$

A4.3.2 Capacity Spectrum Method

The capacity spectrum method was originally developed by S.A. Freeman as a rapid evaluation method for the U.S. Navy, and later has been incorporated in the TriService Seismic Design Guidelines (Ref. 45).

Fig. A19a shows a graphical illustration of the method, in which the ground motion demand is expressed by acceleration-displacement response spectrum format (ADRS), together with the results of a building pushover analysis. In this figure, the point D represents the "response" of the equivalent SDOF system. Fig. A19b shows an example of ADRS calculated from a recorded ground motion.

The results of a building pushover analysis is converted to the ADRS format using the following equations (Ref.28):

$$A = (V/W) / \alpha_1 \qquad (18)$$

$$D = \delta_{Roof} / \alpha_2$$

$$\alpha_1 = \left[\sum_{i=1}^{N} w_i\phi_i\right]^2 \Big/ W\sum_{i=1}^{N} w_i\phi_i^2$$

$$\alpha_2 = \phi_{Roof}\left[\sum_{i=1}^{N} w_i\phi_i \Big/ \sum_{i=1}^{N} w_i\phi_i^2\right]$$

where:

	A	=	spectral acceleration, in g's, at D,
	D	=	spectral displacement, in inches
	V	=	pushover base shear in kips, at δ_{Roof}
	δ_{Roof}	=	pushover curve displacement, in inches,
	α_1	=	fraction of mass in pushover mode,
	α_2	=	ratio: roof/pushover mode displacement,
	ϕ_i	=	pushover mode shape, at location i,
	ϕ_{Roof}	=	pushover modes shape, at roof,
	w_i	=	tributary weight, in kips, at location i,
	W	=	total weight of structure, in kips,
	N	=	number of discrete weight/pushover mode shape locations.

It should be noted that the following assumption is made on the lateral seismic force distribution:

$$Q_i \propto w_i \cdot \phi_i \tag{19}$$

The method requires the determination of the effective damping values, β_{eff}. According to ATC-40 (Ref. 26), which recommends the capacity spectrum method for evaluation of existing buildings, the effective damping value is estimated as,

$$\beta_{eff} = k \cdot \beta_o + 0.05 \tag{20}$$

where, β_o = damping value calculated assuming a bilinear modal; k = factor for deterioration, takes a value of 1.0, ⅔ or ⅓ depending on structure type. For further improving the accuracy of the method, the use of nonlinear spectra (instead of liner spectra for effective damping) was suggested in Ref. 35.

A4.3.3 Nonlinear Displacement Spectrum Method

The studies performed at the UC at Berkeley (Ref. 46) and the Univ. of Illinois (Ref. 47), which are based on similar concepts, are summarized here. The method used is referred to in this report as the "nonlinear displacement spectrum method." As the starting point, both studies cited the earlier study by Shimazaki and Sozen (Refs. 48 and 49). Based on comparisons of linear and nonlinear responses of a large number of SDOF systems, Shimazaki and Sozen observed that inelastic displacements were always bounded by the elastic responses for the elastic period T longer than T_g. Where, T_g is the characteristic period of ground motions determined on an energy spectrum. For the elastic period T shorter than T_g, the inelastic displacements were still bounded by the elastic responses if the sum, $T/T_g + C_y/S_a$, exceeds unity, where, C_y is the base shear coefficient in g, and S_a is the elastic acceleration in g. By using three-ratios, DR, SR and TR, the "bounding rule" is simply stated as,

$$\begin{aligned} &\text{if } TR + SR \geq 1 \\ &\quad DR < 1 \end{aligned} \tag{21}$$

DR = Nonlinear-Response Displacement/Linear-Response Displacement
SR = Base Shear Strength/Base Shear for Linear-Response
TR = Characteristic Period/Characteristic Period for Ground Motion

According to Ref. 46, the formulation was modified as,

$$\begin{aligned} DR &= (TR)^{1.6y} \quad TR < 1 \\ &= 1 \qquad\quad TR \geq 1 \end{aligned} \tag{22}$$

where, y = the ratio of the seismic strength coefficient to the peak ground acceleration. Reference 47 proposed the following bounding rule:

$$DR = \frac{1 - SR}{TR} + SR \qquad TR < 1 \tag{23}$$

$$= 1 \qquad TR \geq 1$$

Both Equations 22 and 23 seem to provide conservative estimates of inelastic displacement responses. Applications to MDOF RC frames were also demonstrated through the use of equivalent SDOF systems.

A4.3.4 Drift Demand Spectrum

To characterize the high drift demands due to velocity pulses from near-source earthquake, the drift spectrum was developed by W.D. Iwan (Ref. 50-53). Simple uniform shear beam models, defined either by the fundamental periods, T, or the height of the model, are used as the structural model, and the maximum shear stress (radian) is calculated through a time history analysis to represent the drift demand of the ground motion.

Table A15 lists the calculated peak values of drift spectrum in percent (for typical steel frame buildings). Significantly large drift values are found in the near-source motions of Takatori Station (Kobe earthquake) and Sylmar Station (Northridge earthquake) in comparison with El Centro N–S record. Use of the drift spectra is suggested in the displacement based building design (Ref. 52).

Table A15. Peak Values of Drift Spectrum of Selected Ground Motions, 2% damping (Ref. 53).
[Reproduced with permission]

Record	Max DS %	Period (S)	PGV (cm/s)	PGA (g)
Takatori (TAK) Station, Kobe: maximum velocity direction	7.8	1.2	155	0.73
Sylmar Convention Station (SCS): N–S	5.4	0.8	134	0.78
JMA-KOBE (JMA-K) Station: N-S	4.6	0.7	92	0.82
Rinaldi Receiving Station (RRS): N-S	4.5	1.3	159	0.82
Sylmar County Hospital (SCH), Free Field: N-S	3.3	1.5	136	0.88
Lucerne (LUC) Station: Landers maximum velocity direction	2.1	4.1	147	0.73
El Centro (ELC): N-S	1.4	1.0	33	0.35

A4.3.5 Reliability-Based Design Method

The reliability based and displacement based design methodology was proposed by W.K. Wen, et al (Refs. 54, 55) to directly account for the uncertainties in the seismic hazard, soil effects, and structural analysis. As part of the development of design procedures, uniform hazard spectra and the following strength reduction factor were evaluated:

$$R(p, T, \mu, \alpha) = \frac{C_e(T)}{C_p(T, \mu, \alpha)} \qquad (24)$$

in which, p = target probability, T = period, μ = target duplicity ratio, α = post-yield stiffness ratio, C_e = elastic force coefficient, and C_p = inelastic force coefficient. Comparison with other simpler formulation for the R-factor indicated that above R-factor was not significantly affected by the target probability, p (Ref.55).

A dual-level design procedure, i.e., serviceability limit and ultimate limit, is proposed. Fig. A20 shows the proposed design procedure for the ultimate limit, which is based on pushover analysis and the use of approximate SDOF responses. The reliability-based design criterion is,

$$P(\mu_{MDOF} > \mu_{Code}) \leq P_t \qquad (25)$$

in which, μ_{MDOF} is the calculated maximum ductility ratio, μ_{Code} is the code-defined ductility limit, and P_t is the target probability. No specific values for P_t were suggested in the reviewed documents.

A4.3.6 Other Reviewed Papers

Several other publications, which proposed displacement based design methodologies, were reviewed (e.g. Refs. 56, 57, 58). The use of pushover analysis, approximate SDOF nonlinear responses, and drift limits are the common major ingredients of the proposed design methodologies.

A5. TECHNICAL ISSUES FOR FURTHER CONSIDERATION

A5.1 Is Nonlinear Analysis Warranted for Seismic Design of NPPs?

The implementation of a displacement based design would require consideration of some type of nonlinear response analysis. The reasons for "no" to the above question may be:

- The current criteria for seismic design of Category I SSC's are considered to be significantly more conservative than conventional building codes because the strength reduction factor, R-factor, is not used. The SSC's designed under such conservative criteria are not expected to develop a significant nonlinearity during a design earthquake event.

- The design of some components, particularly pressure boundaries such as pressure vessels, piping and containments, may not be controlled by the seismic loads. A high overstrength factor is expected for such components.

The possible reasons for "yes" may be,

- There seems to exist a large discrepancy in seismic margins between rigid brittle components and flexible ductile components. To make the design criteria more risk-consistent, some type of nonlinear analysis should be allowed for flexible ductile components (e.g. Ref. 59).

- In the US, a large number of old NPPs exist which were designed mostly in the 1960's and 1970's. Problems associated with age-related degradation were also reported (e.g. Ref. 60). Nonlinear analyses and displacement based criteria may be used for re-evaluation of the seismic margins for such plants.

Future studies for possible resolutions may include,

- Evaluation of overstrength factors for typical structures and components based on previous studies on seismic margins.

- Comparison of seismic margins between linear analysis/force-based and nonlinear analysis/displacement-based for components, such as those listed in Table A2.

A5.2 Technical Bases for Displacement /Drift Limit Values

Statistical studies on the displacement capacities have been performed before for reinforced concrete components (e.g. Ref. 11, 37, 46) and steel structures (e.g. Ref. 61). The deformation limits in the 1997 NEHRP Guidelines (Ref. 17 and 18) are considered to be the most comprehensive so far. For the design of NPPs, additional considerations are required for safe shutdown and maintaining hot/cold shutdown states. Possible studies in this area should include:

- Tabulation and comparison of various recommended displacements limits.
- Statistical analysis of existing test data.
- Development of displacement/drift limits related to safe shutdown and maintaining hot/cold shutdown states.

A5.3 Approximation of Nonlinear Responses

In the implementation of the displacement-based criteria to either new plant design or seismic margin evaluation, an approximation of nonlinear responses may be required except when the direct nonlinear time history analysis is used. The approximate equations, e.g. Eqs. (2), (3), (14), (22), (23), and (24) in the above sections, are not considered to be accurate in the high frequency range (e.g. Ref. 15 and 61). Fig. A21 shows the calculation made by Miranda for bilinear models, which indicate a large deviation in the high frequency range from the so-called "equal displacement rule." In the design of NPP's, equipment housed inside the buildings is subjected to highly narrow-banded floor motions. Most of the existing approximate equations, however, are based on responses of ground motions with a broad-banded spectrum. Possible future tasks in this area may include,

- Review/refinement of existing equations for building analysis, particularly in the high frequency range.
- Additional considerations for narrow-banded floor motions.

A5.4 Structural Analysis Methods

It appears that the pushover analysis is increasingly a popular analysis tool in the displacement based design. This analysis method, however, is not applicable to genuinely 3-D structures such as nuclear piping. The issues that need to be resolved in this area include:

- Is pushover analysis recommended for the design of NPP's structures/components? If so, for what types of structures/components?
- Can some type of combination (for different loading directions, X, Y and Z) rule be used to

apply to nonlinear 3-D structures such as nuclear piping?

- Is direct time integration approach or MDOF equivalent linearization approach considered to be a practical design tool?
- Is the conventional linear analysis with a combination of some type of response modification factor good enough?

A5.5 Application to Fragility Analysis

In the past fragility analysis of NPP's (including IPEEE), very conservative failure criteria were used for certain classes of components due partly to the lack of available test data. As an example, the fragility evaluation of storage tanks is mentioned herein. Some of the recent Japanese papers on the hysteretic behavior of storage tanks are attached to this report for review. It appears that Japanese engineers have already adopted the energy-based seismic design of tank structures based on a large number of failure tests (e.g. Ref. 12). As the overall volume of seismic test data is increasing, more realistic displacement based criteria may be applied to various components, which have been analyzed using highly conservative criteria. The issues related to this area include:

- What types of components are best suitable for the consideration of displacement based criteria?
- Are enough test data available to confidently apply the displacement based criteria?
- What is the significance of the application of the displacement criteria in terms of the calculated fragility values?

A6. REFERENCES

[1] USNRC Standard Review Plan, NUREG-0800, Rev. 2-October 1990.

[2] Murphy, A.J., Chokshi, N.C., McMullen, R., Shao, L.C., Rothman, R., "Revision of Seismic and Geological Siting Criteria," 16th SMIRT, Lyon, France, August 1997, pp. K1-K12.

[3] Chen, J.J., Chokshi, N.C., Kenneally, R.M., Kelly, G.B., Beckner, W.D., McCracken, C., Murphy, A.J., Reiter, L., Jeng, D., "Procedural and Submittal Guidance for the Individual Plant Examination of External Events (IPEEE) for Severe Accident Vulnerabilities," NUREG-1407, June 1991.

[4] Westinghouse AP6000 PRA, Chapter 55, "Seismic Margin Analysis," Revision 10, June 30, 1997.

[5] EPRI, "A Methodology for Assessment of Nuclear Power Plant Seismic Margin," EPRI NP-6041, October 1988.

[6] Kennedy, R.P., et al, "Dominant Contributors to Seismic Risk - An Appraisal," Proceedings: EPRI/NRC Workshop on Nuclear Power Plant Reevaluations to Quantify Seismic Margins, NP-4101-SR, October 1984.

[7] SQUG, "Generic Implementation Procedure (GIP) for Seismic Verification of Nuclear Plant Equipment," February 14, 1992.

[8] Budnitz, R.J., Amico, P.J., Cornell, C.A., Hall W.J., Kennedy, R.P., Reed, J.W., Shinozuka, M., "An Approach to the Qualification of Seismic Margins in Nuclear Power Plants," NUREG/CR-4334, July 1985.

[9] Reed, J.W., Kennedy, R.P., "Methodology for Developing Seismic Fragilities," EPRI TR-103959, EPRI, June 1994.

[10] Park, Y.J., Hofmayer, C.H., Chokshi, N.C., "Survey of Seismic Fragilities Used in PRA Studies of Nuclear Power Plants," Reliability Engineering and Systems Safety, 1998.

[11] Duffey, T.A., Goldman, A., Farrar, C.R., "Shear Wall Ultimate Drift Limits," Los Alamos National Laboratory, NUREG/CR-6104, April 1994.

[12] Central Research Institute of Electric Power Industry, "Seismic Buckling Design Guideline of FBR Main Vessels - A Draft," March 1994.

[13] SEAOC, "Evolvement of Earthquake Codes Since San Fernando," Papers from 1974, 1975, 1981, 1985, SEAONC Seminars, NC #85-1.

[14] SEAOC, "Changes to the Building Code: Preview of 1994 UBC," October 1993.

[15] ATC-34, "A Critical Review of Current Approaches to Earthquake-Resistant Design," ATC, 1995.

[16] Adams, T.M., Stevenson, J.D., "Assessment of United States Industry Structural Codes and Standards for Application to Advanced Nuclear Power reactors," NUREG/CR-6358, October 1995.

[17] BSSA, "NEHRP Guidelines for the Seismic Rehabilitation of Buildings," FEMA-273, October 1997.

[18] BSSA, "NEHRP Commentary on the Guidelines for the Seismic Rehabilitation of Buildings," FEMA-274, October 1997.

[19] ICBO, 1997 edition of the "Uniform Building Code," Copyright©1997, International Conference of Building Officials.

[20] ATC, "Improved Seismic Design Criteria for California Bridges: Provisional Recommendations," ATC-32, 1996.

[21] BSSA, "NEHRP Recommended Provisions for Seismic Regulations for New Buildings and Other Structures," FEMA 302, February 1998.

[22] BSSA, "NEHRP Recommended Provisions for Seismic Regulations for New Buildings and Other Structures, Part 2 - Commentary," FEMA 303, February 1998.

[23] ASCE, "Minimum Design Loads for Buildings and Other Structures," ANSI/ASCE 7-95, Approved June 6, 1996.

[24] SEAOC, "Recommended Lateral Force Requirements and Commentary," 6th Edition, 1996.

[25] Cagley, J.R., Hooper, J.D., "Performance Based Engineering Concepts," Structure, SEAOC, Summer 1997.

[26] ATC, "Seismic Evaluation and Retrofit of Concrete Buildings," ATC-40, November 1996.

[27] Krawinkler, H., "Pushover Analysis: Why, How, When, and When Not to Use It," 65th Annual Convention of SEAOC, October 1996, pp. 17-36.

[28] Kircher, C.A., "Capacity Spectrum Pushover Method: Seeing is Believing," 65th Annual Convention of SEAOC, October 1996, pp. 5-15.

[29] SEAOC, "Overview of 1997 Uniform Building Code (UBC)," November 22, 1997.

[30] SEAOSC, "New Methodology in Structural Design," September 21, 1996.

[31] Kircher, C.A., "1997 UBC: New Ground Shaking Criteria," 66th Annual Convention of SEAOC, September 1997, pp. 235-241.

[32] Hamburger, R.O., "General Design Requirements of the 1997 Uniform Building Code," 66th Annual Convention of SEAOC, September 1997, pp. 243-261.

[33] Low, M., et al, "Development of New Los Angeles Seismic Analysis Criteria for Tall Buildings - Site-Specific Considerations," The Structural Design of Tall Buildings, Vol. 5, 1996, pp. 235-264.

[34] "Seismic Design According to the 1997 Uniform Building Code," Concrete Structures, PCA, Vol. 11, No. 1, April 1998.

[35] SEAOC, "Vision 2000, Performance Based Seismic Engineering of Buildings," April 3, 1995.

[36] DOE Standard, "Natural Phenomena Hazards Design and Evaluation Criteria for Department of Energy Facilities," U.S. Department of Energy, DOE-STD-1020-94, January 1996.

[37] Park, Y.J., Ang, A. H-S., "Mechanistic Seismic Damage Model for Reinforced Concrete," Journal of Structural Engineering, ASCE, Vol. 111, No. 4, April 1985, pp. 722-739.

[38] International Code Council, Inc., "2000 International Building Code," March 2000.

[39] Priestley, M.J.N., "Seismic Design Philosophy for Precast Concrete Frames," Structural Engineering International, Vol. 6, No. 1, February 1996, pp. 25-31.

[40] Priestley, M.J.N., "Displacement-Based Seismic Assessment of Existing Reinforced Concrete Buildings," Bulletin of the New Zealand National Society for Earthquake Engineering, Vol. 29, No. 4, December 1996, pp. 256-272.

[41] Priestley, M.J.N., "Displacement-Based Seismic Assessment of Reinforced Concrete Buildings, Journal of Earthquake Engineering, Vol. 1, No. 1, January 1997, pp. 157-192.

[42] Priestley, M.J.N., et al, "Preliminary Development of Direct Displacement-Based Designation Multi-Degree of Freedom Systems," 65th Annual Convention of SEAOC, October 1996, pp. 47-66.

[43] Gulkan, P., Sozen, M., "Inelastic Response of Reinforced Concrete Structures to Earthquake Motions," ACI Journal, December 1974.

[44] Shibata, A., Sozen, M., "Substitute Structure Method for Seismic Design in R/C," Journal of the Structural Division, ASCE, January 1976.

[45] Freeman, S.A., "The Capacity Spectrum Method for Determining the Demand Displacement," ACI 1994 Spring Convention, March 1994.

[46] Qi, X., Moohle, J.P., "Displacement Design Approach for Reinforced Concrete Structures Subjected to Earthquakes," University of California at Berkeley, UCB/EERC-91/02, January 1991.

[47] Lepage, A., "A Method for Drift-Control in Earthquake-Resistant Design of RC Building Structures," Ph.D. Thesis, University of Illinois at Urbana-Champaign, 1997.

[48] Shimazaki, K., Sozen, M.A., "Seismic Drift of Reinforced Concrete Structures," Technical Research Reports of Hazama-Gumi Ltd., Tokyo, Japan, 1984, pp. 145-166.

[49] Sozen, M.A., "Drift-Driven Design for Earthquake Resistance of Reinforced Concrete," The EERC-COREe Symposium in Honor of Vitetmo V. Berlero, UCB/EERC-97-05, 1997.

[50] Iwan, W.M., "Implication of Measured Near-Field Motion on Structural Response," Proceedings of Structures Congress XIV, Chicago, IL, ASCE, 1996, pp. 1213-1220.

[51] Iwan, W.D., Huang, C.T., "The Shear-Drift Demand Spectrum: Implications for Earthquake Resistant Design," 6th NCEE, 1998.

[52] Iwan, W.D., "The Drift Demand Spectrum and its Application to Structural Design and Analysis," 11th WCEE, 1996, Paper No. 1116.

[53] Iwan, W.D., "Drift Spectrum: Measure of Demand for Earthquake Ground Motions," Journal of Structural Engineering, Vol. 123, No. 4, April 1997, ©ASCE, pp. 397-404.

[54] Wen, Y.K., et al, "Dual-Level Design of Buildings Under Seismic Loads," Structural Safety, Vol. 18, No. 2, 1996, pp. 195-224.

[55] Collins, K.R., Wen, Y.K., Foutch, D.A., "Dual-Level Seismic Deisgn: A Reliability-Based Methodology," Earthquake Engineering and Structural Dynamics, Vol. 25, Copyright ©1996, John Wiley and Sons Limited, pp. 1433-1467.

[56] Chaollal, O., Guizani, L., Malenfant, P., "Drift-Based Methodology for Seismic Proportioning of Coupled Shear Walls," Canadian Journal of Civil Engineering, Vol. 23, 1996, pp. 1030-1040.

[57] Garcia, L.E., "Economic Considerations of Displacement-Based Seismic Design of Structural Concrete Buildings," Structural Engineering International, SABSE, April 1998, pp. 243-248.

[58] Itano, A., Gaspersic, P., Saiidi, M., "Response Modification Factors for Seismic Design of Circular Reinforced Concrete Bridge Columns," ACI Structural Journal, Vol. 94, No. 1, February 1997, pp. 23-38.

[59] Kennedy, R.P., "Establishing Seismic Design Criteria Margin," 14th SMIRT, Plenary Lectures, Vol. 0, 1997, pp. 89-112.

[60] Shao, L.C., Murphy, A.J., Chokshi, N., Kua, P.T., Chang, T.Y., "Seismic Response and Resistance of Age Degraded Structures and Components," Current Issues Related to Nuclear Power Plant Structures, Equipment and Piping, 1996.

[61] Roeder, C.W., Foutch, D.A., "Experimental Results for Seismic Resistant Steel Moment Frame Connections," Journal of Structural Engineering, ASCE, Vol. 122, No. 6, 1996, pp. 581-588.

[62] Wallace, J.W., "Evaluation of UBC-94 Provisions for Seismic Design of RC Structural Walls," Earthquake Spectra, Vol. 12, No. 2, May 1996, pp. 327-348.

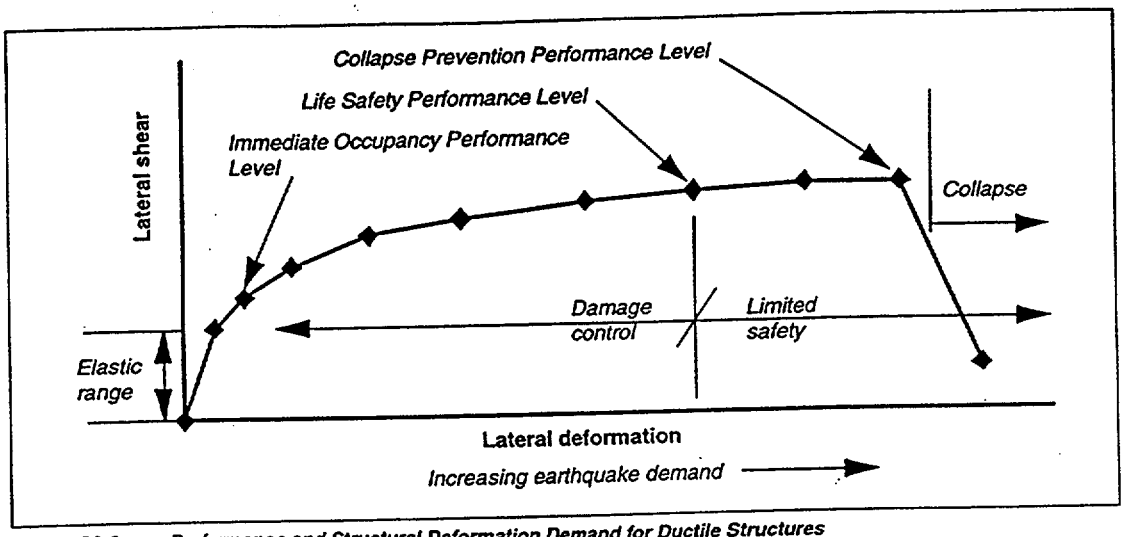

Figure C2-3 ***Performance and Structural Deformation Demand for Ductile Structures***

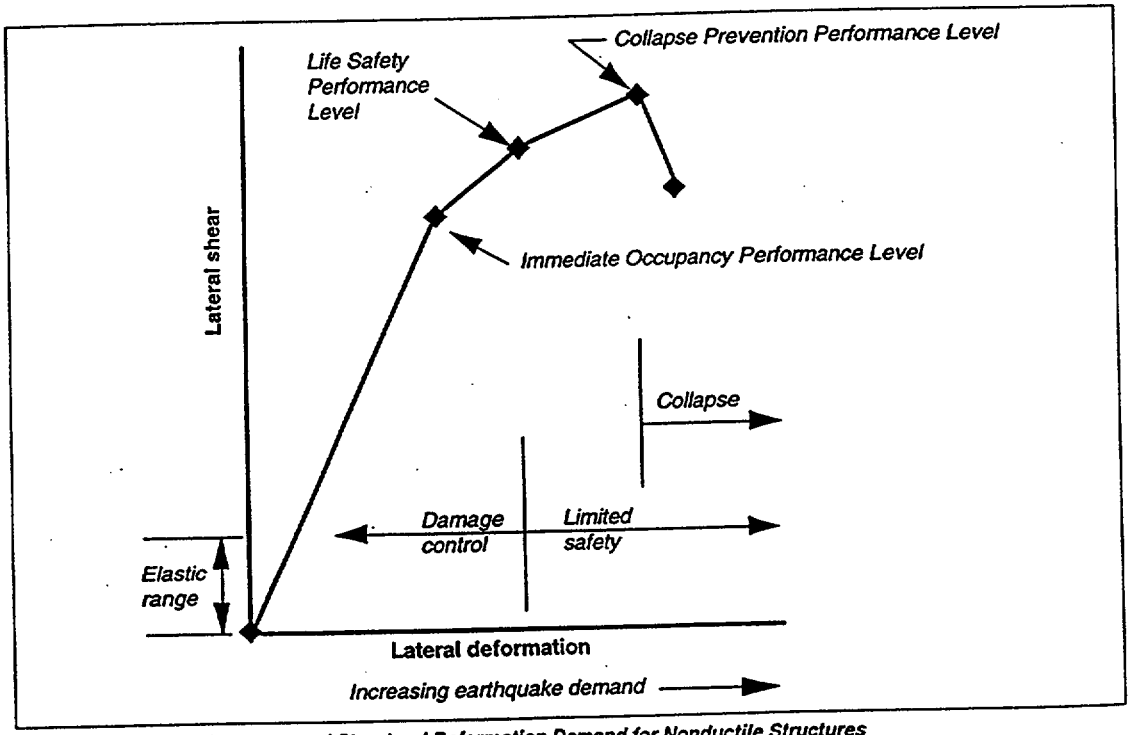

Figure C2-4 ***Performance and Structural Deformation Demand for Nonductile Structures***

Fig. A1: Structural Deformation Demands for Ductile and Nonductile Structure (Ref. 18)

Earthquake Hazard Level	Building Performance Levels			
	Operational Performance Level (1-A)	Immediate Occupancy Performance Level (1-B)	Life Safety Performance Level (3-C)	Collapse Prevention Performance Level (5-E)
50%/50 year	a	b	c	d
20%/50 year	e	f	g	h
BSE-1 (~10%/50 year)	i	j	k	l
BSE-2 (~2%/50 year)	m	n	o	p

k + p = BSO
k + p + any of a, e, i, m; or b, f, j, or n = Enhanced Objectives
o = Enhanced Objective
k alone or p alone = Limited Objectives
c, g, d, h = Limited Objectives

Fig. A2: Rehabilitation Objectives (Ref. 17)

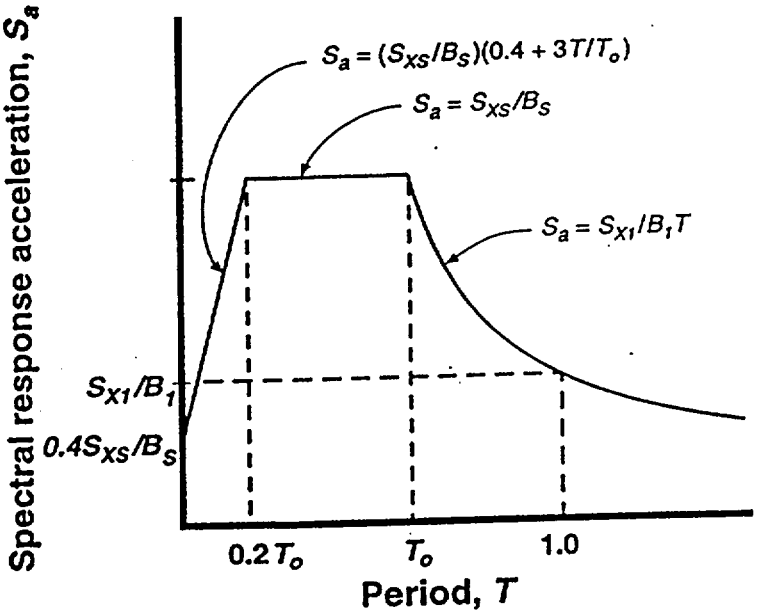

Fig. A3: Ground Motion Response Spectrum (Ref. 17)

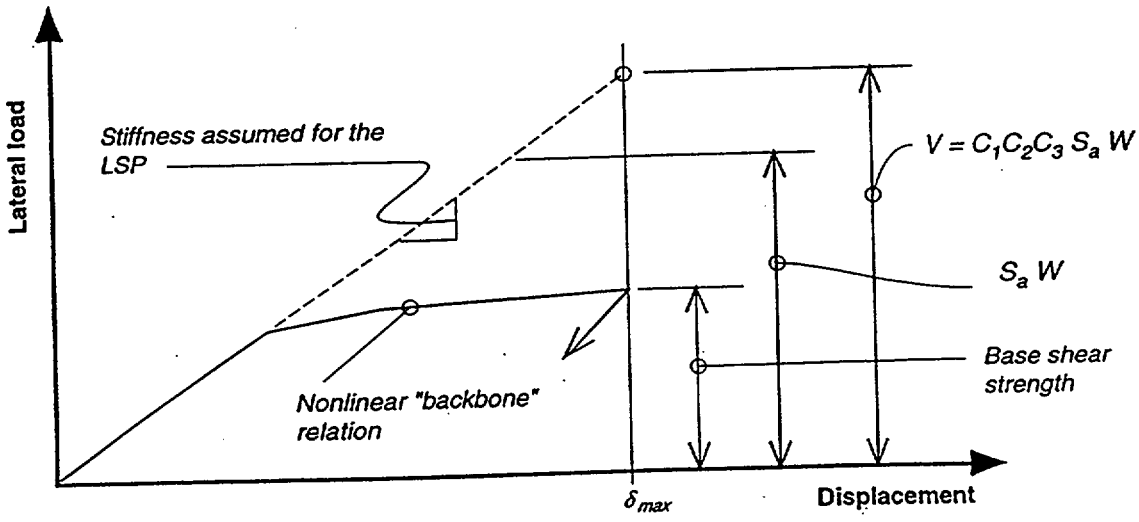

Fig. A4: Pseudo Lateral Forces in LSP (Ref. 18)

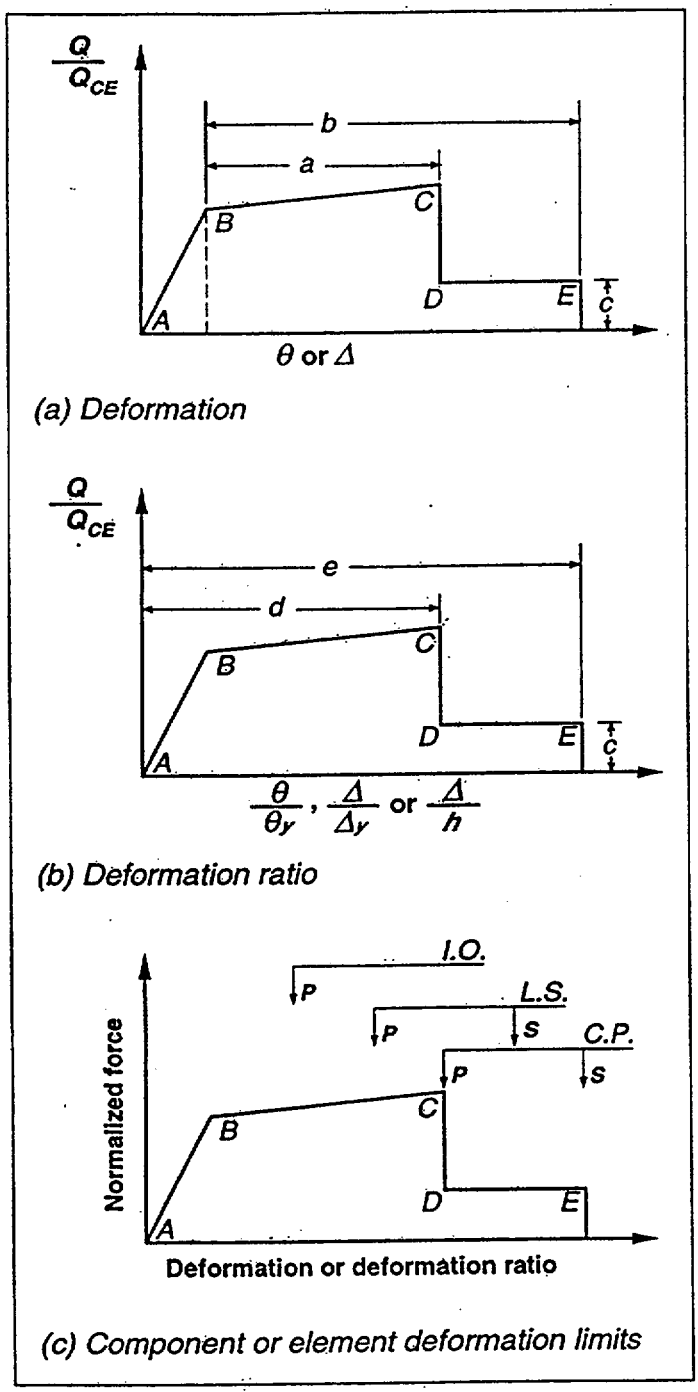

Fig. A5: Idealized Component Load Versus Deformation Curves for Depicting Component Modeling and Acceptability (Ref. 17)

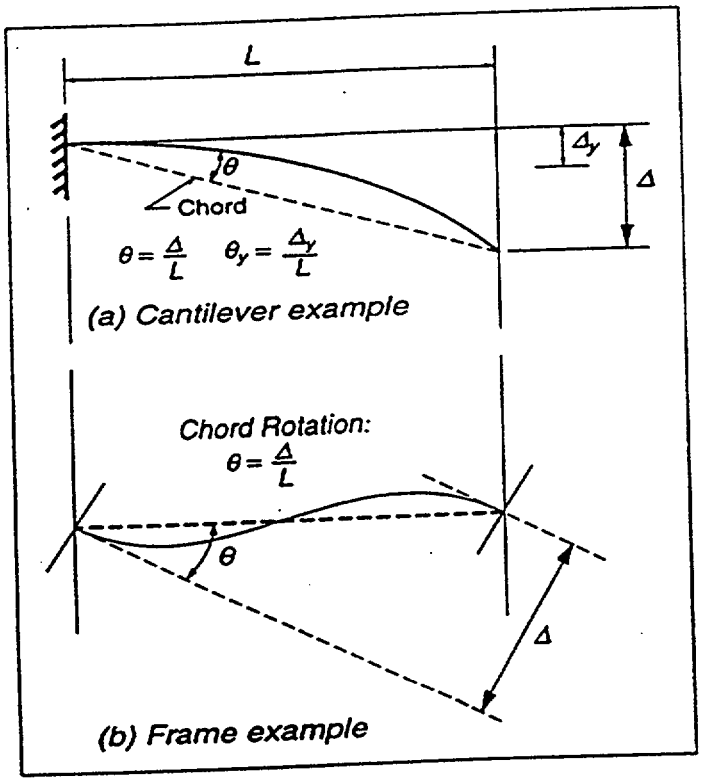

Fig. A6: Definition of Chord Rotation (Ref. 17)

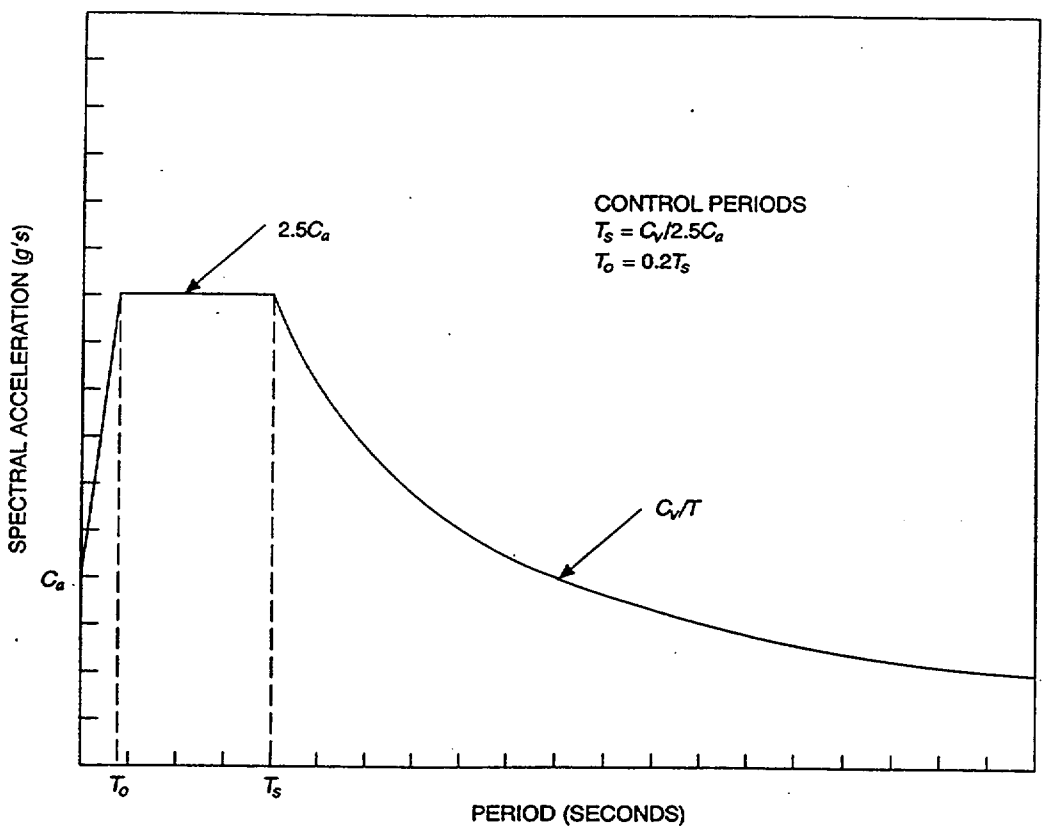

Fig. A7: 1997 UBC Spectrum (Ref. 19)
[Reproduced with permission]

TABLE 16-R—SEISMIC COEFFICIENT C_v

SOIL PROFILE TYPE	SEISMIC ZONE FACTOR, Z				
	Z = 0.075	Z = 0.15	Z = 0.2	Z = 0.3	Z = 0.4
S_A	0.06	0.12	0.16	0.24	$0.32N_v$
S_B	0.08	0.15	0.20	0.30	$0.40N_v$
S_C	0.13	0.25	0.32	0.45	$0.56N_v$
S_D	0.18	0.32	0.40	0.54	$0.64N_v$
S_E	0.26	0.50	0.64	0.84	$0.96N_v$
S_F	See Footnote 1				

[1]Site-specific geotechnical investigation and dynamic site response analysis shall be performed to determine seismic coefficients for Soil Profile Type S_F.

TABLE 16-S—NEAR-SOURCE FACTOR N_a[1]

SEISMIC SOURCE TYPE	CLOSEST DISTANCE TO KNOWN SEISMIC SOURCE[2,3]		
	≤ 2 km	5 km	≥ 10 km
A	1.5	1.2	1.0
B	1.3	1.0	1.0
C	1.0	1.0	1.0

[1]The Near-Source Factor may be based on the linear interpolation of values for distances other than those shown in the table.

[2]The location and type of seismic sources to be used for design shall be established based on approved geotechnical data (e.g., most recent mapping of active faults by the United States Geological Survey or the California Division of Mines and Geology).

[3]The closest distance to seismic source shall be taken as the minimum distance between the site and the area described by the vertical projection of the source on the surface (i.e., surface projection of fault plane). The surface projection need not include portions of the source at depths of 10 km or greater. The largest value of the Near-Source Factor considering all sources shall be used for design.

TABLE 16-T—NEAR-SOURCE FACTOR N_v[1]

SEISMIC SOURCE TYPE	CLOSEST DISTANCE TO KNOWN SEISMIC SOURCE[2,3]			
	≤ 2 km	5 km	10 km	≥ 15 km
A	2.0	1.6	1.2	1.0
B	1.6	1.2	1.0	1.0
C	1.0	1.0	1.0	1.0

[1]The Near-Source Factor may be based on the linear interpolation of values for distances other than those shown in the table.

[2]The location and type of seismic sources to be used for design shall be established based on approved geotechnical data (e.g., most recent mapping of active faults by the United States Geological Survey or the California Division of Mines and Geology).

[3]The closest distance to seismic source shall be taken as the minimum distance between the site and the area described by the vertical projection of the source on the surface (i.e., surface projection of fault plane). The surface projection need not include portions of the source at depths of 10 km or greater. The largest value of the Near-Source Factor considering all sources shall be used for design.

TABLE 16-U—SEISMIC SOURCE TYPE[1]

SEISMIC SOURCE TYPE	SEISMIC SOURCE DESCRIPTION	SEISMIC SOURCE DEFINITION[2]	
		Maximum Moment Magnitude, M	Slip Rate, SR (mm/year)
A	Faults that are capable of producing large magnitude events and that have a high rate of seismic activity	$M \geq 7.0$	$SR \geq 5$
B	All faults other than Types A and C	$M \geq 7.0$ $M < 7.0$ $M \geq 6.5$	$SR < 5$ $SR > 2$ $SR < 2$
C	Faults that are not capable of producing large magnitude earthquakes and that have a relatively low rate of seismic activity	$M < 6.5$	$SR \leq 2$

[1]Subduction sources shall be evaluated on a site-specific basis.

[2]Both maximum moment magnitude and slip rate conditions must be satisfied concurrently when determining the seismic source type.

Fig. A8: 1997 UBC Seismic Coefficients (Ref. 19)

[Reproduced with permission]

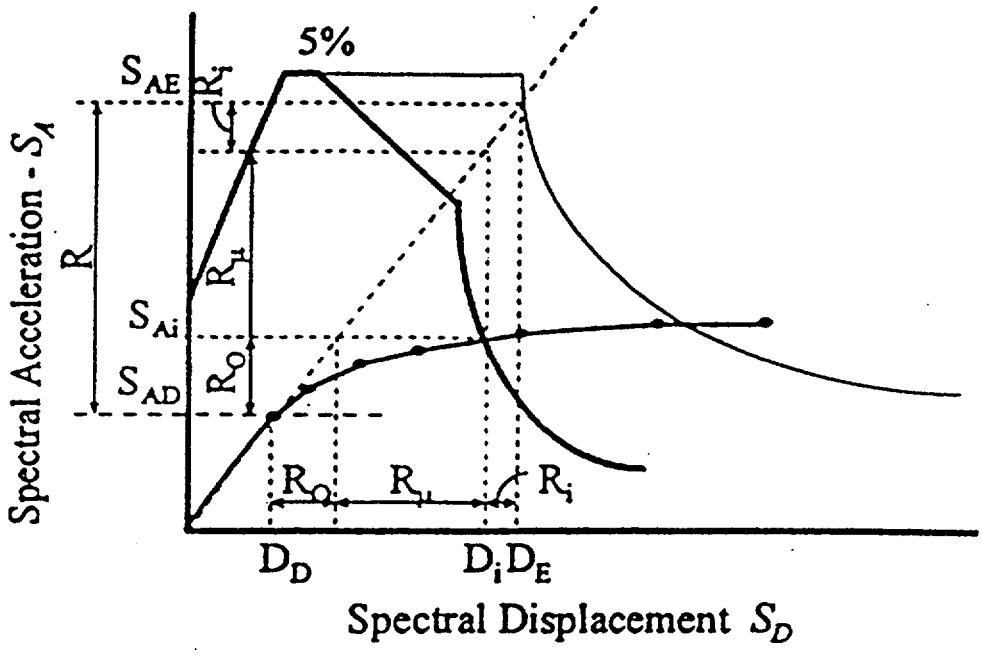

Fig. A9: R-factors in Capacity Spectra (Ref. 32)
[Reproduced with permission]

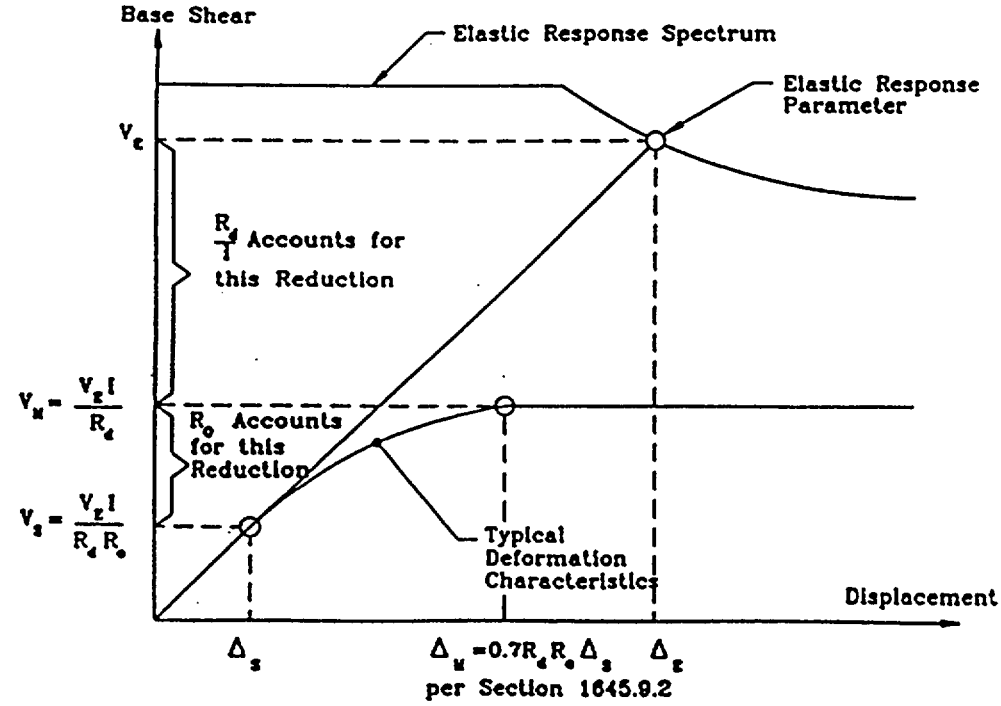

Fig. A10: Definitions of Drift, Δ_m, and Component Force, V_M, in 1997 UBC (Ref. 30)
[Reproduced with permission]

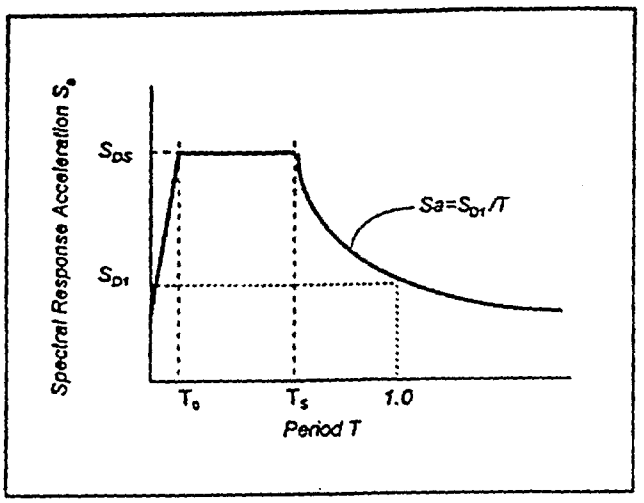

Site Class	Mapped Maximum Considered Earthquake Spectral Response Acceleration at Short Periods				
	$S_s \le 0.25$	$S_s = 0.50$	$S_s = 0.75$	$S_s = 1.00$	$S_s \ge 1.25$
A	0.8	0.8	0.8	0.8	0.8
B	1.0	1.0	1.0	1.0	1.0
C	1.2	1.2	1.1	1.0	1.0
D	1.6	1.4	1.2	1.1	1.0
E	2.5	1.7	1.2	0.9	*a*
F	*a*	*a*	*a*	*a*	*a*

NOTE: Use straight line interpolation for intermediate values of S_s.
* Site-specific geotechnical investigation and dynamic site response analyses shall be performed.

Site Class	Mapped Maximum Considered Earthquake Spectral Response Acceleration at 1 Second Periods				
	$S_1 \le 0.1$	$S_1 = 0.2$	$S_1 = 0.3$	$S_1 = 0.4$	$S_1 \ge 0.5$
A	0.8	0.8	0.8	0.8	0.8
B	1.0	1.0	1.0	1.0	1.0
C	1.7	1.6	1.5	1.4	1.3
D	2.4	2.0	1.8	1.6	1.5
E	3.5	3.2	2.8	2.4	*a*
F	*a*	*a*	*a*	*a*	*a*

NOTE: Use straight line interpolation for intermediate values of S_1.
* Site-specific geotechnical investigation and dynamic site response analyses shall be performed.

Fig. A11: NEHRP Design Response Spectrum (Refs. 21 and 22)

Seismic Use Group	*I*
I	1.0
II	1.25
III	1.5

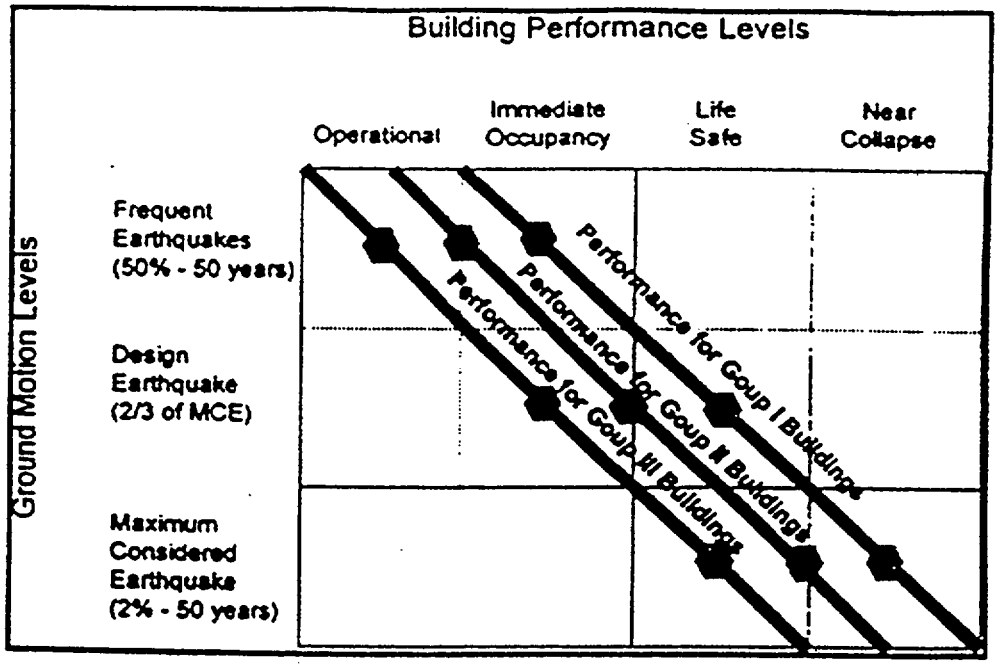

Structure	Seismic Use Group		
	I	II	III
Structures, other than masonry *shear wall* or masonry *wall* frame *structures*, four stories or less in height with interior *walls*, *partitions*, ceilings, and exterior *wall* systems that have been designed to accommodate the *story* drifts	0.025 h_{sx} [b]	0.020 h_{sx}	0.015 h_{sx}
Masonry cantilever *shear wall structures* [c]	0.010 h_{sx}	0.010 h_{sx}	0.010 h_{sx}
Other masonry *shear wall structures*	0.007 h_{sx}	0.007 h_{sx}	0.007 h_{sx}
Masonry *wall* frame *structures*	0.013 h_{sx}	0.013 h_{sx}	0.010 h_{sx}
All other *structures*	0.020 h_{sx}	0.015 h_{sx}	0.010 h_{sx}

Fig. A12: Seismic Use Group and Expected Performance (Refs. 21 and 22)

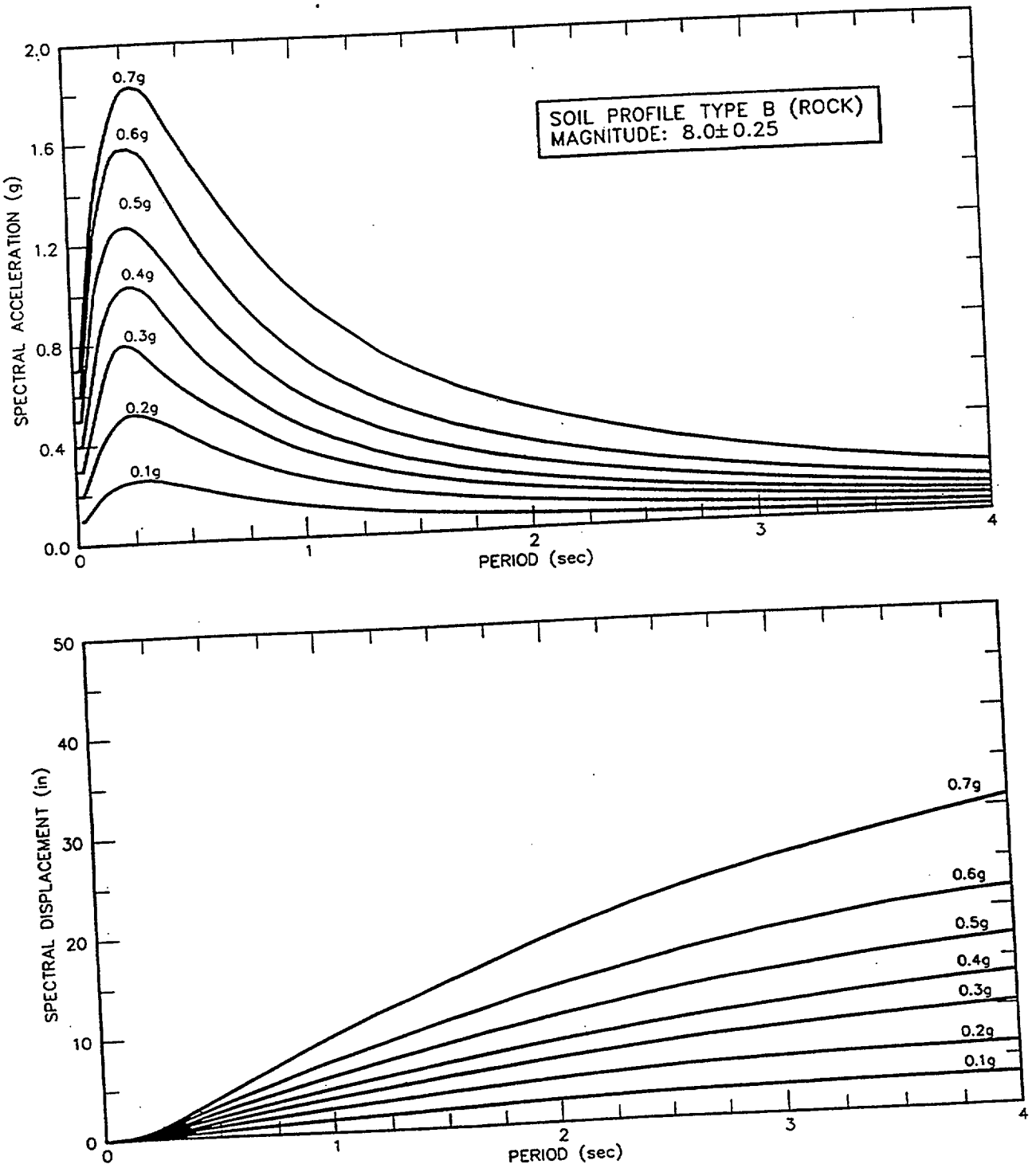

Fig. A13: Example of Ground Motion Spectra for Bridge Design. (Ref. 20)

[Reproduced with permission]

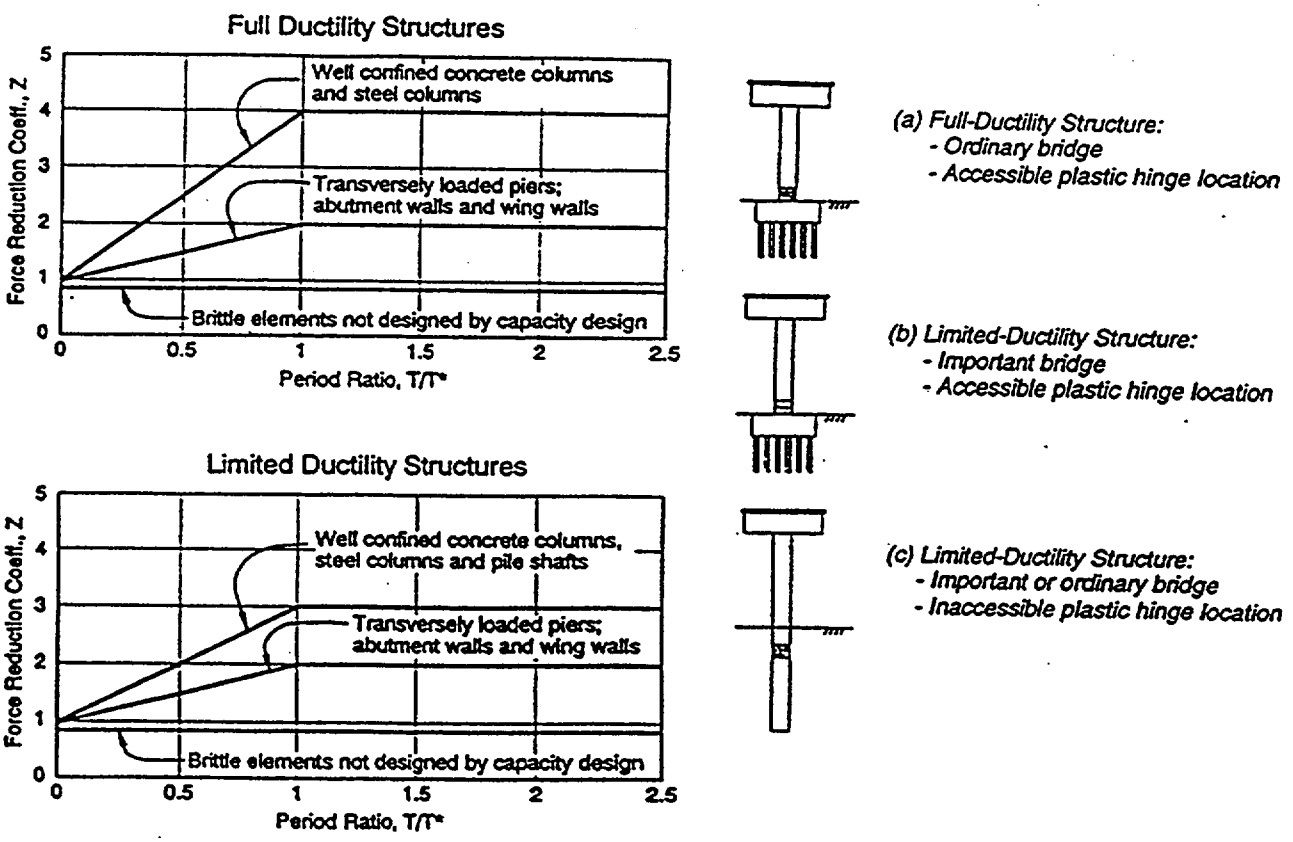

Fig. A14: Force-reduction Coefficients, Z for Bridge Design (Ref. 20)
[Reproduced with permission]

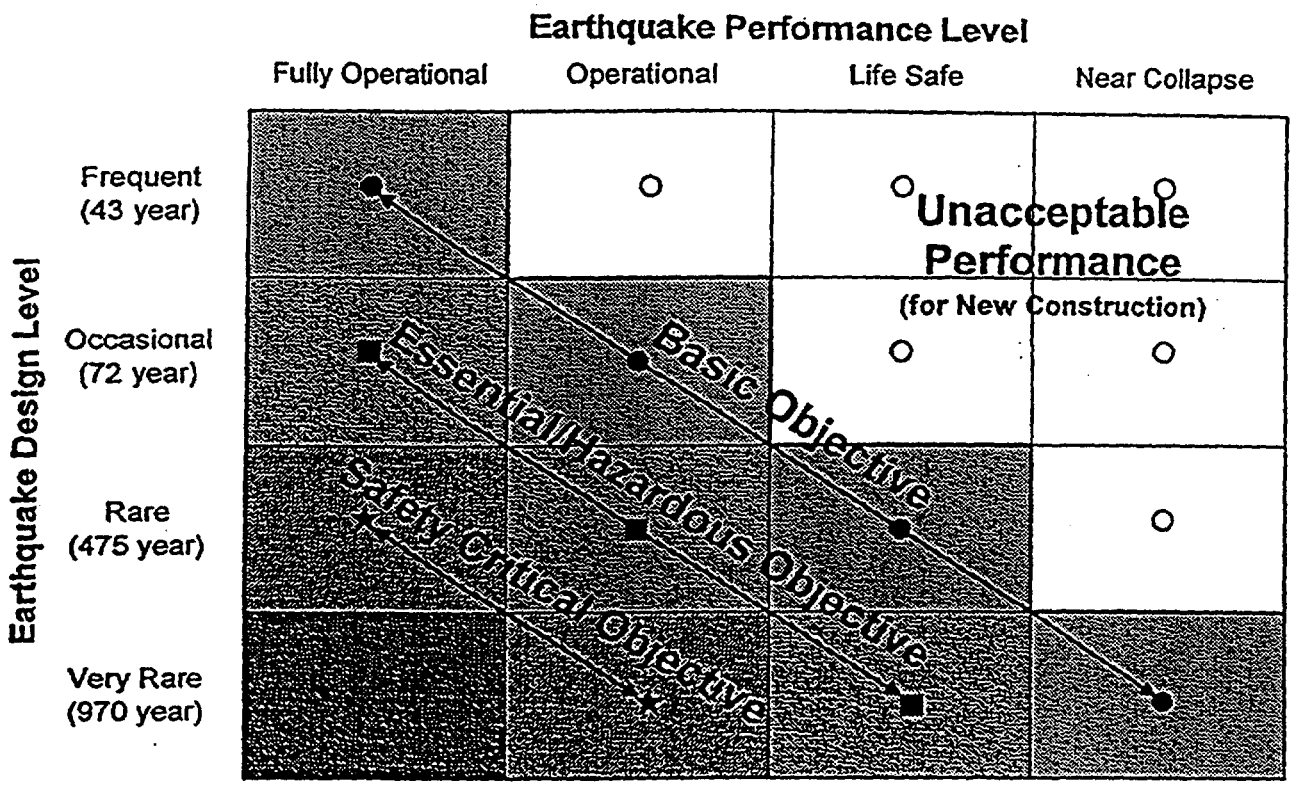

Fig. A15: Performance Objectives for Buildings Recommended by Vision 2000 (Ref. 35)
[Reproduced with permission]

System Description	Performance Level				
	10 Fully Operational 9	8 Operational 7	6 Life Safe 5	4 Near Collapse 3	2 Collapse 1
Overall building damage	Negligible	Light	Moderate	Severe	Complete
Permissible transient drift	< 0.2%+/-	< 0.5%+/-	< 1.5%+/-	< 2.5%+/-	> 2.5%+/-
Permissible permanent drift	Negligible.	Negligible.	< 0.5%+/-	< 2.5%+/-	> 2.5%+/-
Vertical load carrying element damage	Negligible.	Negligible.	Light to moderate, but substantial capacity remains to carry gravity loads.	Moderate to heavy, but elements continue to support gravity loads.	Partial to total loss of gravity load support.
Lateral Load Carrying Element damage	Negligible - generally elastic response; no significant loss of strength or stiffness.	Light - nearly elastic response; original strength and stiffness substantially retained. Minor cracking/yielding of structural elements; repair implemented at convenience.	Moderate - reduced residual strength and stiffness but lateral system remains functional.	Negligible residual strength and stiffness. No story collapse mechanisms but large permanent drifts. Secondary structural elements may completely fail.	Partial or total collapse. Primary elements may require demolition.
Damage to architectural systems	Negligible damage to cladding, glazing, partitions, ceilings, finishes, etc. Isolated elements may require repair at users convenience.	Light to moderate damage to architectural systems. Essential and select protected items undamaged. Hazardous materials contained.	Moderate to severe damage to architectural systems, but large falling hazards not created. Major spills of hazardous materials contained.	Severe damage to architectural systems. Some elements may dislodge and fall.	Highly dangerous falling hazards. Destruction of components.
Egress systems	Not impaired.	No major obstructions in exit corridors. Elevators can be restarted perhaps following minor servicing.	No major obstructions in exit corridors. Elevators may be out of service for an extended period.	Egress may be obstructed.	Egress may be highly or completely obstructed.

Fig. A16: Performance Levels by Vision 2000 (Ref. 35)
[Reproduced with permission]

System Description	Performance Level				
	10 Fully Operational 9	8 Operational 7	6 Life Safe 5	4 Near Collapse 3	2 Collapse 1
Mechanical/Electrical/ Plumbing/Utility Systems	Functional.	Equipment essential to function and fire/life safety systems operate. Other systems may require repair. Temporary utility service provided as required..	Some equipment dislodged or overturned. Many systems not functional. Piping, conduit ruptured.	Severe damage and permanent disruption of systems.	Partial or total destruction of systems. Permanent disruption of systems.
Damage to contents	Some light damage to contents may occur. Hazardous materials secured and undamaged.	Light to moderate damage. Critical contents and hazardous materials secured.	Moderate to severe damage to contents. Major spills of hazardous materials contained.	Severe damage to contents. Hazardous materials may not be contained.	Partial or total loss of contents.
Repair	Not required.	At owners/tenants convenience.	Possible - building may be closed.	Probably not practical.	Not possible.
Effect on occupancy	No effect.	Continuous occupancy possible.	Short term to indefinite loss of use.	Potential permanent loss of use.	Permanent loss of use.

Fig. A16: Performance Levels by Vision 2000 (Ref. 35) (Continued).

[Reproduced with permission]

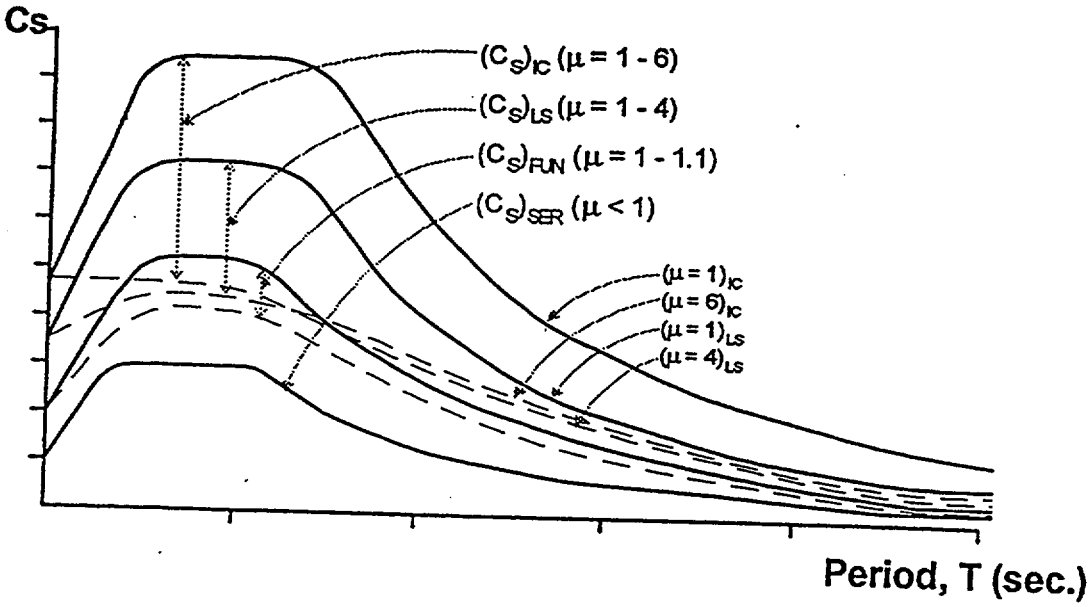

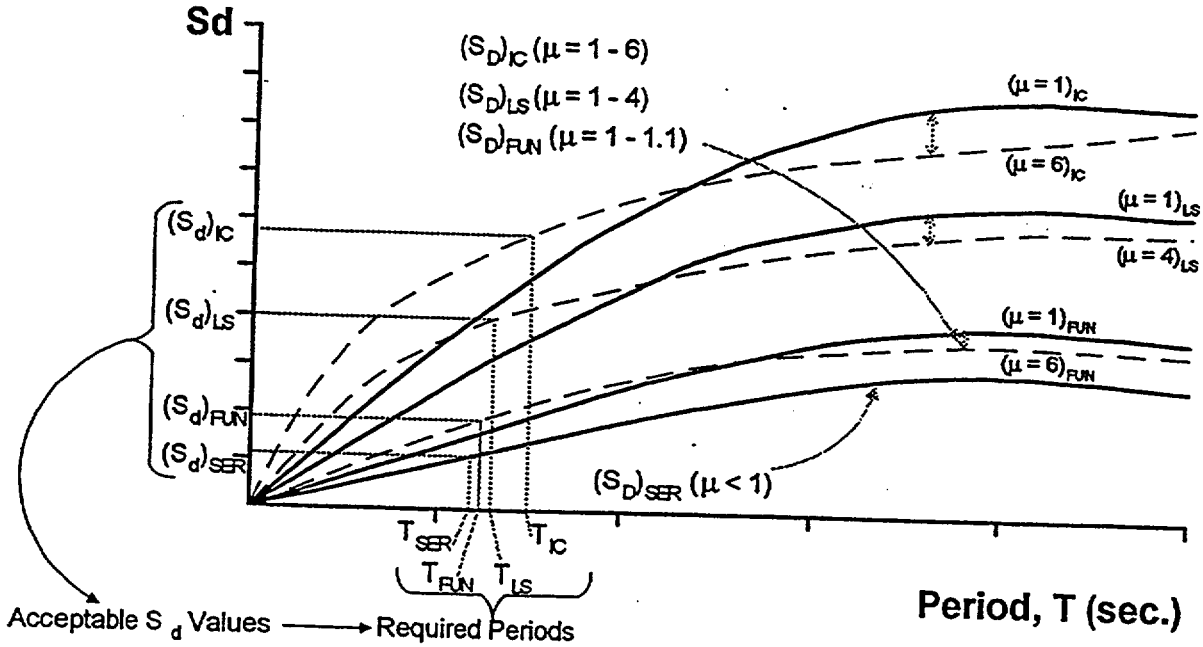

Fig. A17: Smoothed Elastic (Solid Lines) and Inelastic (Broken Lines) Design Spectra for Different Performance Levels (Ref. 35)
[Reproduced with permission]

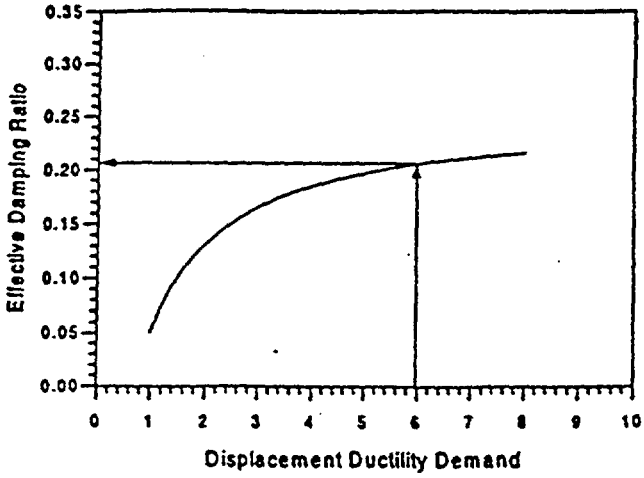

(a) Effective Damping based on Takeda Model

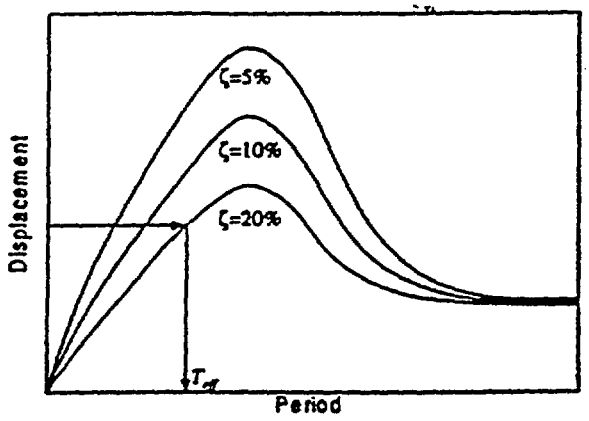

(b) Effective Period given Target Displacement and Effective Damping

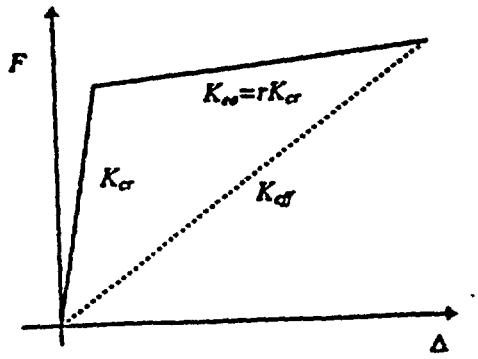

(c) Effective Stiffness

Fig. A18: Substitute Structure Approach (Ref. 42).
[Reproduced with permission]

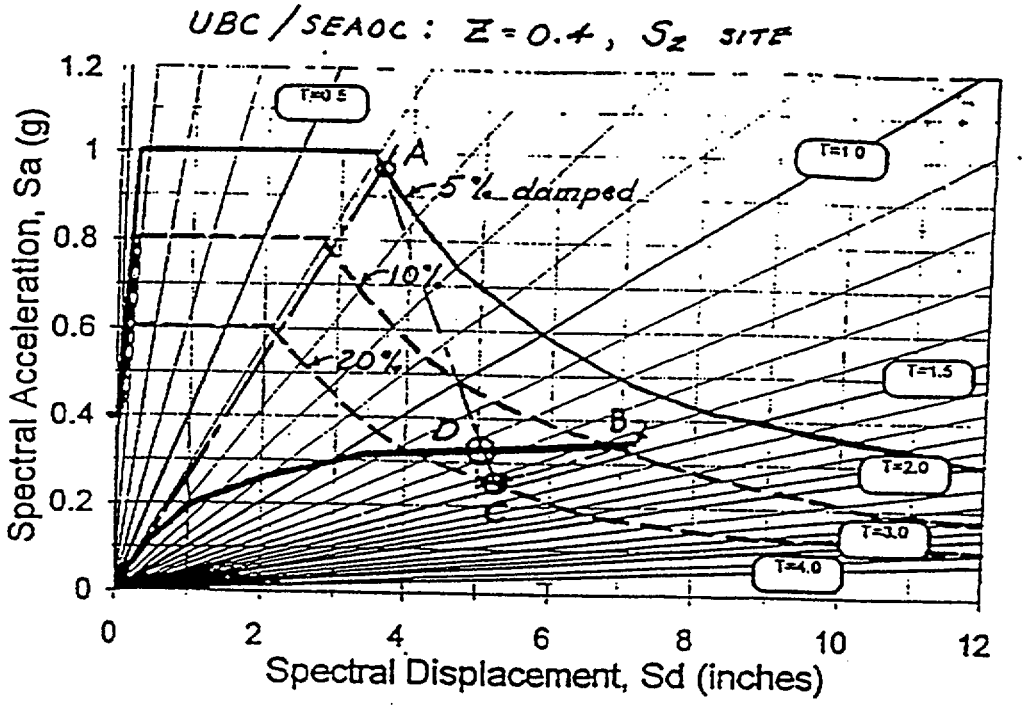

Fig. 19a: Capacity Spectrum Method - Acceleration-Displacement Response Spectrum (ADRS) Format (Ref. 45).
[Reproduced with permission]

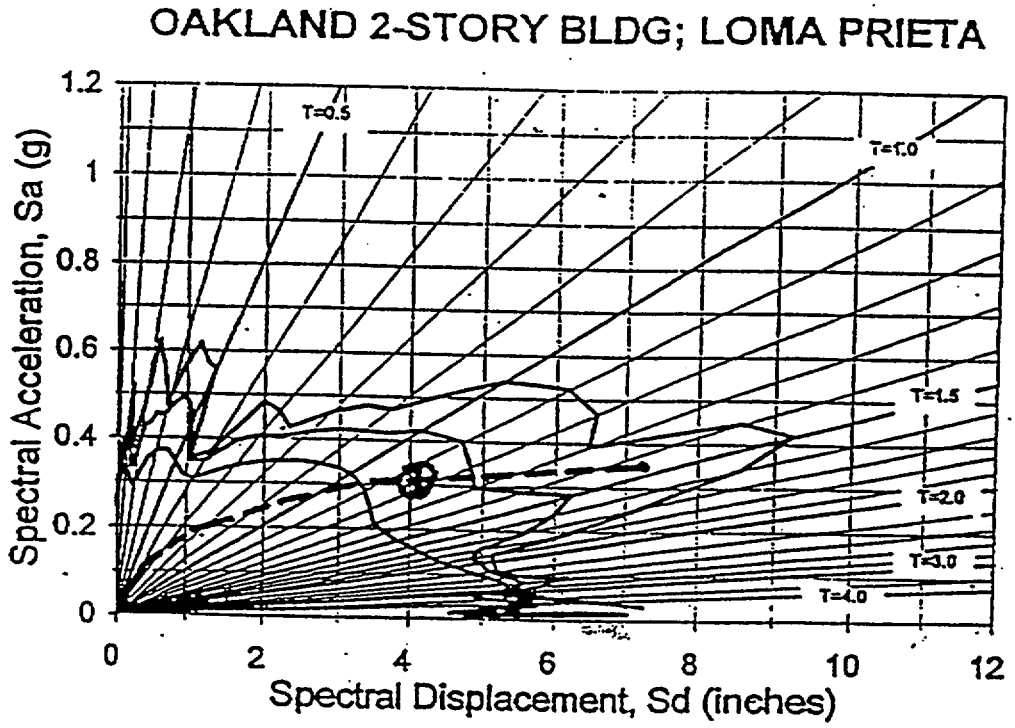

Fig. A19b: Capacity Spectrum Method - Oakland (Ref. 45)
[Reproduced with permission]

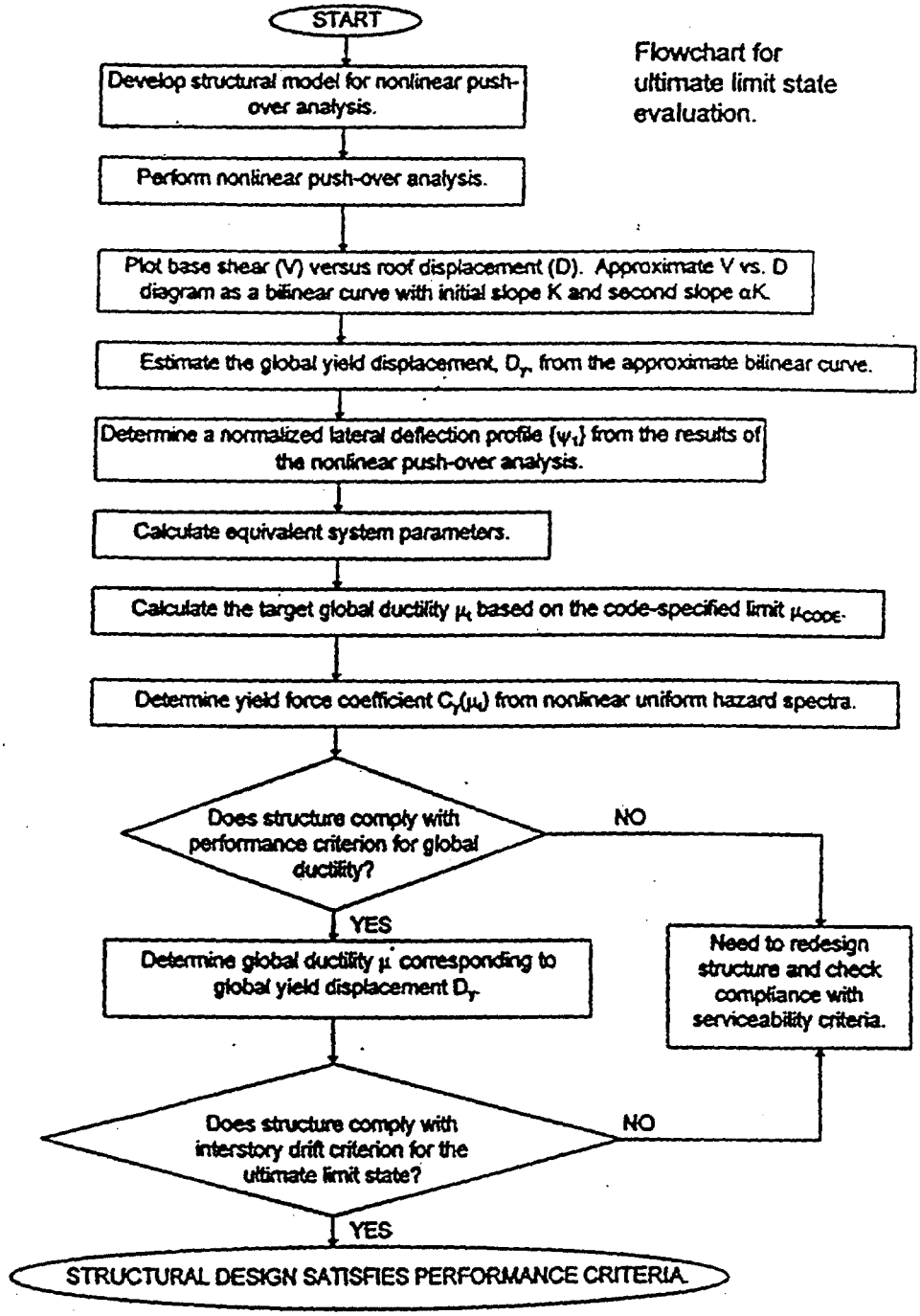

Flowchart for ultimate limit state evaluation.

Fig. A20: Flowchart Summarizing the Steps in the Ultimate Limit State Evaluation (Ref. 55)

[Reproduced with permission]

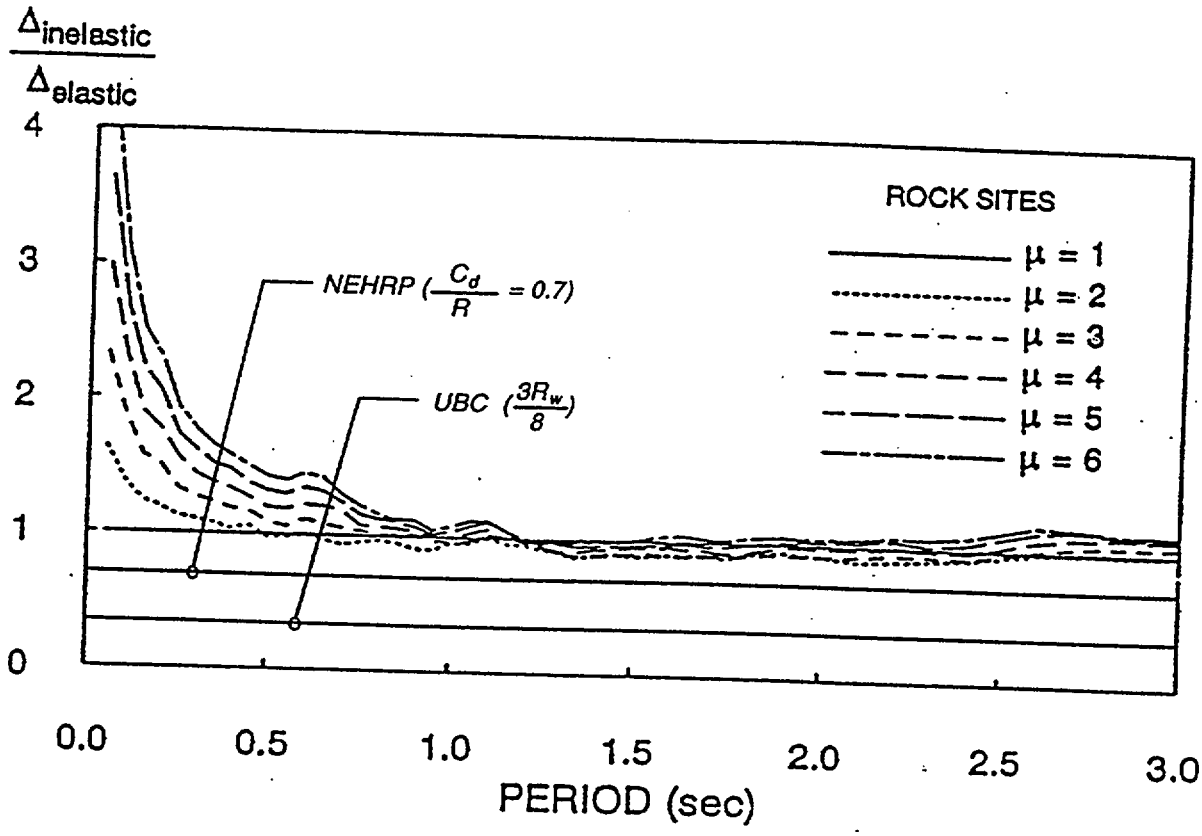

Fig. A21: Relationship Between Inelastic and Elastic Displacements
(Adapted from Miranda (1991)) (Ref. 15)
[Reproduced with permission]

NRC FORM 335
(2-89)
NRCM 1102,
3201, 3202

U.S. NUCLEAR REGULATORY COMMISSION

BIBLIOGRAPHIC DATA SHEET

(See instructions on the reverse)

1. REPORT NUMBER
(Assigned by NRC, Add Vol., Supp., Rev., and Addendum Numbers, if any.)

NUREG/CR- 6719
BNL-NUREG-52619

2. TITLE AND SUBTITLE

Assessment of the Relevance of Displacement Based Design Methods/Criteria To Nuclear Plant Structures

3.DATE REPORT PUBLISHED

MONTH	YEAR
July	2001

4. FIN OR GRANT NUMBER
W-6691

5. AUTHOR(S)

Wang, Y.K., Miller, C.A., Hofmayer, C.H.

6. TYPE OF REPORT

7. PERIOD COVERED *(Inclusive Dates)*

8. PERFORMING ORGANIZATION - NAME AND ADDRESS *(if NRC, provide Division, Office or Region, U.S. Nuclear Regulatory Commission, and mailing address; if contractor, provide name and mailing address.)*

Energy Science and Technology Department
Brookhaven National Laboratory/Bldg. 130/P.O. Box 5000
Upton, NY 11973-5000

9. SPONSORING ORGANIZATION - NAME AND ADDRESS *(if NRC, type "Same as above"; if contractor, provide NRC Division, Office or Region, U.S. Nuclear Regulatory Commission, and mailing address.)*

Division of Engineering Technology
Office of Nuclear Regulatory Research
U.S. Nuclear Regulatory Commission
Washington, DC 20555-0001

10. SUPPLEMENTARY NOTES

James F. Costello, Project Manager

11. ABSTRACT *(200 words or less)*

The objective of the work described in this report is to evaluate the extent to which displacement based methods may be useful to evaluate the seismic response of nuclear power station structures. A literature review of displacement based seismic design methods was completed during the first phase of the project. As a result of this review it was decided to investigate the displacement based method outlined in FEMA 273 by applying it to two structures.

The first structure considered was a four story reinforced concrete building with shear walls. FEMA 273 pushover analysis methods were compared with nonlinear time history analysis and response spectrum analysis including ductility factors. The comparisons show that the FEMA analysis results are comparable to those achieved with the current force based methods.

The second structure analyzed was the Diablo Canyon nuclear power station turbine building. The main portion of this building is a reinforced concrete shear wall building that contains the turbine. The turbine is mounted on a pedestal which is a reinforced concrete frame structure. It is separately founded from the building and separated from the building by gaps at the operating floor. These gaps close under large earthquakes resulting in geometric nonlinearities. The results predicted with the FEMA analysis are found to compare poorly with nonlinear time history analyses.

It was concluded that the displacement based approach is appropriate for those problems where the structure contains material nonlinearities but not when significant geometric nonlinearities occur.

12 KEY WORDS/DESCRIPTORS *(List words or phrases that will assist researchers in locating the report.)*

Displacement based; seismic response; nuclear power; structures; seismic design; reinforced concrete; shear walls; pushover analysis; nonlinear time history; response spectrum; ductility factors; force based; geometric nonlinearities; material nonlinearities; FEMA analysis.

13. AVAILABILITY STATEMENT

Unlimited

14. SECURITY CLASSIFICATION
(This Page)
Unclassified

(This Report)
Unclassified

15. NUMBER OF PAGES

16. PRICE

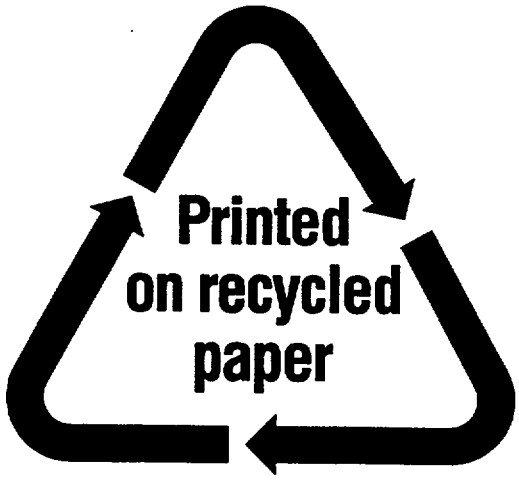

Federal Recycling Program

UNITED STATES
NUCLEAR REGULATORY COMMISSION
WASHINGTON, DC 20555-0001

OFFICIAL BUSINESS
PENALTY FOR PRIVATE USE, $300